ROYAUME DU MAROC
Université Mohammed V - RABAT -
جامعة محمد الخامس - الرباط -
Faculté des sciences
كلية العلوم

CENTRE D'ETUDES DOCTORALES - SCIENCES ET TECHNOLOGIES

N° d'ordre 3913

THESE

En vue de l'obtention du : ***DOCTORAT***

Structure de Recherche : Laboratoire de Matière Condensée et Sciences Interdisciplinaires « Unité de Recherche Labellisé CNRT »
Discipline : Physique Informatique
Spécialité : Physique Appliquée

Présentée et soutenue le : 07/05/2024 par :

Ayoub LAAREJ

Safety, Energy Efficiency, and Environmental Impact In Road Vehicular Traffic: A Statistical Physics and Cellular Automata Analysis

JURY

Abdallah EL KENZ	PES, Université Mohammed V, Faculté des Sciences, Rabat	Président
Abdelaziz MHIRECH	PES, Université Mohammed V, Faculté des Sciences, Rabat	Rapporteur/ Examinateur
Youssef EL AMRAOUI	PES, Université Mohammed V, Faculté des Sciences, Rabat	Rapporteur/ Examinateur
Ismail ESSAOUDI	PES, Université Moulay Ismail, Faculté des Sciences, Meknès	Rapporteur/ Examinateur
Abdelilah BENYOUSSEF	Expert, PES, Académie Hassan II des Sciences et Techniques, Rabat	Examinateur
Hamid EZ-ZAHRAOUY	PES, Université Mohammed V, Faculté des Sciences, Rabat	Directeur de thèse

Année Universitaire: 2023/2024

Dedication

I would like to express my heartfelt appreciation to my parents and my entire family. Their unwavering support and encouragement have been instrumental in my academic journey.

Additionally, I would like to express my sincere appreciation to **Noureddine LAKOUARI** Professor at National institute of Astrophysics, Optics and Electronics, Mexico, for his invaluable assistance throughout my thesis, his guidance, support, and expertise has been instrumental in shaping and improving my research.

Acknowledgements

This thesis has been performed at the laboratory of condensed matter and interdisciplinary sciences (LAMScI) Faculty of Sciences, Mohammed V University – Rabat, under the supervision of **Hamid EZ-ZAHRAOUY** Professor in higher education at University Mohammed V, faculty of science Rabat.

I would like here to express my gratitude to all the people who contributed, from near or far, to the realization of this thesis work.

First of all, I would like to express my sincere thanks to **Hamid EZ-ZAHRAOUY** Professor in higher education at University Mohammed V, faculty of Sciences Rabat, for his encouragement, his availability, giving me the opportunity to work in this laboratory and accompanying me during every step in my researcher career. I also thank him for his kindness and his human qualities.

I would also like to express my deep gratitude to **Abdallah EL KENZ,** Professor in higher education at University Mohammed V, faculty of Sciences Rabat, for agreeing to chair my thesis jury.

I would like to thank **Abdelaziz MHIRECH,** Professor in higher education at University Mohammed V, faculty of Sciences Rabat, for reporting and reviewing this thesis.

I would like to thank **Youssef EL AMRAOUI,** Professor in higher education at University Mohammed V, faculty of Sciences Rabat, for reporting and reviewing this thesis.

I would like to thank **Ismail ESSAOUDI,** Professor in higher education at University Moulay Ismail, faculty of Sciences Meknés, for reporting and reviewing this thesis.

I would like to thank **Abdelilah BENYOUSSEF,** Expert, Professor, Hassan II Academy of Sciences and Technology, faculty of Sciences Rabat, for reviewing this thesis.

Finally, I would like to thank all the members of the **LAMScI** for the interest that everyone could bring to my work, for all their advices and all their ideas that allowed me to progress in my research, and for their contribution to the good atmosphere in the laboratory.

Abstract

Seriously, traffic congestion is one of the biggest challenges in our societies, where we see different categories of vehicles that differ by their length and maximal speed. Despite the growing prevalence of highways, two-lane roads dominate national networks. Therefore, traffic modeling has emerged as a solution to comprehend complex traffic phenomena, which are often simulated using diverse models. The Cellular Automaton (CA) model, as a good tool for studying traffic dynamics because it's simple, powerful, and fast reliability. This thesis delves into a two-lane cellular automaton model, focusing on energy dissipation and satisfaction rates in mixed traffic flows. It is founded that the slow vehicles in the same lane as fast vehicles hinder the flow of faster vehicles, especially in the intermediate density. Examining initial configurations, the study reveals that an inhomogeneous configuration leads to more unsatisfied fast vehicles, increased lane-changing frequency, and higher the energy dissipation. The model also explores the impact of slow vehicles on carbon dioxide emissions, introducing their significant effect at low and intermediate densities. The study concludes by considering both moving and fixed bottlenecks, emphasizing the influence of slow-moving vehicles on traffic patterns and accident probabilities. The analysis revealed that as the length of the fixed bottlenecks increases, the probabilities of rear-end collisions and lane-changing collisions decrease.
Keywords: Two-lane, Satisfaction rate, Energy dissipation, carbon dioxide emissions, fixed bottleneck, moving bottlenecks.

Résumé

Sérieusement, la congestion routière est l'un des plus grands défis dans nos sociétés, où l'on observe différentes catégories de véhicules qui diffèrent par leur longueur et leur vitesse maximale. Malgré la prévalence croissante des autoroutes, les routes à deux voies dominent les réseaux nationaux. Par conséquent, la modélisation du trafic a émergé comme une solution pour comprendre les phénomènes de trafic complexes, qui sont souvent simulés à l'aide de différents modèles. Le modèle de l'Automate Cellulaire (AC) est largement accepté et bien accueilli comme un bon outil pour étudier la dynamique du trafic en raison de sa fiabilité simple, puissante et rapide lors de son utilisation. Cette thèse aborde un modèle d'automates cellulaires à deux voies, en se concentrant sur la dissipation d'énergie et les taux de satisfaction dans les flux de circulation mixtes. On constate que la présence de véhicules lents dans la même voie avec des véhicules rapides gêne la circulation des véhicules plus rapides, surtout en densité intermédiaire. En examinant les configurations initiales, l'étude a révélé que la configuration inhomogène conduit à plus de véhicules rapides insatisfaits, par conséquente une dissipation d'énergie plus élevée. Le modèle explore également l'impact des véhicules lents sur les émissions de dioxyde de carbone, introduisant leur effet significatif à faible et à densité intermédiaire. L'étude intègre aussi les goulots d'étranglement mobiles et fixes. L'analyse a montré que si la longueur des goulots d'étranglement fixes augmente, les probabilités de collisions arrière et de collisions par changement de voie diminuent.

Mots-clefs: Deux voies, taux de satisfaction, dissipation d'énergie, goulot d'étranglement fixe, goulots d'étranglement mobiles, dioxyde de carbone.

Contents

General introduction

Traffic follow is an important aspect of transportation and plays a significant role in the functioning of modern societies. It affects various aspects of our lives such as economy, social interactions, and the environment. Moreover, Transportation systems are a significant consumer of energy and a major source of emissions. The burning of fossil fuels by cars, buses, trucks, and trains releases pollutants such as carbon monoxide, nitrogen oxides, and particulate matter into the air. Additionally, transportation systems can also lead to energy dissipation, which is the amount of energy that is lost or wasted during the transportation process. This can occur in several ways, such as through friction and air resistance while vehicles are in motion, or through idling and braking while vehicles are stopped. Hence, we can say that traffic flow, energy dissipation, and emission are closely related concepts that refer to the movement and distribution of vehicles on roads and highways, the amount of energy required to maintain that movement, and the release of pollutants and greenhouse gases into the atmosphere because of vehicle use. As traffic increases, the amount of energy required to maintain that movement also increases, which can lead to higher emissions of pollutants and greenhouse gases. These emissions can have negative impacts on human health as air pollution from vehicles is linked to respiratory and cardiovascular disease, as well as other health problems and the environment, where the carbon dioxide emissions contribute to global warming and climate change, as CO_2 is a potent greenhouse gas. Higher levels of CO_2 in the atmosphere can lead to changes in the Earth's temperature, precipitation patterns, and sea level.

However, traffic modelling has become a multidisciplinary field. Road network managers (engineers, urban planners, computer scientists, physicists and mathematicians) have studied traffic and have contributed their expertise to better operate the infrastructure and to find appropriate control tools. Computer scientists and physicists have approached the study of traffic from a modelling perspective by creating accurate simulations (i.e. model experiments) to analyze and predict a wide variety of problems that are difficult to study by other expensive or dangerous means.
A simulation model represents the traffic characteristics according to the level of detail considered. In the literature, three types of models are encountered: macroscopic, mesoscopic and microscopic. Macroscopic traffic modelling corresponds to a continuous view of the flow and gives a global description of the vehicle behavior. In the mesoscopic model, the vehicles are individual, but they have a global behavior (groups of entities). In the microscopic

model, the individual behavior of each vehicle and the level of detail are the focal points of the model, also it can be used to simulate a wide variety of traffic scenarios, including single-lane and multi-lane roads. Some examples of microscopic traffic flow models include:

1. Intelligent driver model (IDM): This model simulates the behavior of individual drivers based on their desired speed and the distance to the vehicle in front of them. IDM can be used to simulate traffic flow on a single-lane road.

2. Optimal Velocity (OV) model: This model is based on the ideal speed of each vehicle and considers the effects of both the traffic density and speed of the vehicle.

3. Cellular Automaton models (CA): These models simulate the movement of vehicles on a roadway using a grid of cells, each of which represents a small segment of the road. CA models can be extended to include additional features such as merging lanes, exits and entrances, and different types of vehicles.

4. Car-Following models: This models simulate the behavior of a vehicle following the vehicle in front of it, taking into account the distance, speed and acceleration of the leading vehicle, as well as the reaction time and maximum acceleration of the following vehicle.

In this thesis, we focus on the Nagel-Schreckenberg model; also well known as NaSch model, which is a type of cellular automata model that simulates the movement of vehicles on a highway. It was developed by Kai Nagel and Michael Schreckenberg in 1992 and is commonly used to study traffic flow in urban environments. In this model, each cell represents a vehicle on a one-dimensional road. The state of a cell can be one of several different states, such as "empty," "occupied by a slow-moving vehicle," or "occupied by a fast-moving vehicle." The rules of the model dictate how the state of a vehicle changes over time, based on the state of the vehicle in front of it, the speed of the vehicle, and other factors. In a single lane version of this model, the focus is on the movement of vehicles on a single lane. The model can simulate the formation of traffic jams and the emergence of traffic patterns, such as the formation of stop-and-go waves. It can also be used to study the effects of different traffic control strategies on traffic flow and emissions. In a two-lane version of this model, the focus is on the movement of vehicles on two lanes of a road. The model can simulate the interaction between vehicles on different lanes, such as lane changing and merging behavior. The lane changing can be symmetric or asymmetric. A symmetric model would assume that the number of vehicles travelling in the left lane is the same as the number of vehicles travelling in the right lane, while an asymmetric model would take into account differences in the flow of traffic between the two lanes. In addition, this model can be extended to include emission and energy dissipation calculations, by adding the vehicle's fuel consumption and emissions as a function of velocity, acceleration and other related parameters.

Finally, in a two lane traffic model, bottlenecks can increase the collision probability of vehicles on two-lane. When a bottleneck occurs, the available space for vehicles to travel through is reduced, causing vehicles to slow down or stop. This can lead to a chain reaction where vehicles behind the bottleneck are forced to slow down or stop suddenly, increasing the risk of rear-end collisions. Moreover, if the bottleneck occurs on a roadway where drivers are travelling at high speeds, such as a highway, the risk of collisions may be greater due to the reduced space available for vehicles to manoeuver and the increased stopping distances required at higher speeds.

Objectives of the thesis

Road traffic encompasses several factors, namely the geometry of the road infrastructure, the driver's behavior, the diversity of vehicle flows, etc. Among the major phenomena which are considered to be the most qualifiable and quantitative for road users. Heterogeneity of traffic is one of these phenomena, which consists of different types of vehicles (cars, trucks, etc.), The length of slow-moving vehicles can also have an impact on traffic flow, also large vehicles such as trucks, or buses, can take up more space on the road, making it difficult for other vehicles to pass them safely, they may also require more time and space to manoeuver, which can further slow down traffic. Consequently, this leads to a deterioration of traffic conditions, increased traffic density and contributes to the faster formation of congestion on roads.

The main purpose of this thesis is to study the energy dissipation and CO_2 emission in symmetric and asymmetric two-lane traffic follow model. Firstly, our interest will focus on the study of the energy dissipation and satisfaction rate in a closed boundary with a mixture of vehicles distinguished by their lengths and maximum speed, which leads us to raise several questions, such as: how does the heterogeneity of vehicles influence the traffic? What is the impact of slow vehicles on the flow of traffic? Can it be said that the slow vehicles give rise to a large number of unsatisfied fast vehicles and a high frequency of lane changing? Are slow vehicles obstructing the fast ones while driving continuously in the same lane? Does the initial configuration of slow vehicles affect the traffic flow? Does the satisfaction rate and the dissipation energy depend on the longitudinal interactions of vehicles? Can energy dissipation be considered a congestion index?.

Next, we will analyse the effect of slow vehicles on CO_2 emission. Hence, it prompts us to ask a number of questions: Does the distribution of the slow vehicles along the two- affect the CO_2 emission? Is the lane changing of fast provoke an increase or a decrease in CO_2 emission? Are slow vehicles have a great effect on carbon dioxide in all density regions?

Additionally, the implementation of a two-lane with bottlenecks can leads us to ask if the length of a bottleneck can have a substantial impact on both traffic flow and the probability of accidents or not?.// This thesis aims to answer the previous questions. So, this manuscript is structured as follows:

-The first and second chapters are devoted to a bibliographical study of road traffic where we describe the different approaches to modelling road traffic, as well as we will make a synthesis of the main empirical results.

-The third chapter investigates the energy dissipation And satisfaction rate for a two-lane traffic Model with two types of vehicles.

-The fourth chapter focuses on the study of the effects of slow vehicles on carbon dioxide emission in the two-lane cellular automata model.

-The fifth chapter dedicates to studying the effect of fixed and moving bottlenecks on traffic flow and car accidents in a two-lane cellular automaton model.

-Finally, the conclusion summarizes the main results obtained during this thesis work and some perspectives of our research work.

Chapter I

Bibliographical study of road traffic

I.1 History

Traffic theories have been developed to describe the interactions between vehicles as well as the overall movements on the road infrastructure. These theories use a number of flow variables and characteristic relationships.

Road traffic theories seek to describe in a precise mathematical manner the interactions between vehicles and their operators (the moving components) and the infrastructure (the stationary component). The first models proposed were mathematical models. However, given the complexity of the road traffic phenomenon, the analytical approaches proved to be unsatisfactory in terms of the results they provided.

The scientific study of traffic began in the 1930s with the application of probability theory to the description of road traffic (Adams 1936), Greenshields [1]was among the first to study traffic as he conducted tests to measure traffic flow, traffic density and speed using photographic measurement methods for the first time.

During the 1940s there was little theoretical development due to the interruption caused by the Second World War. After the Second World War, with the considerable increase in the use of automobiles and the expansion of the road network, there was also a strong increase in the study of traffic characteristics and the development of traffic flow theories.

New studies were carried out in the 1950s based on several theories such as the queue theory [2] and the traffic flow theory [3, 4]. In 1959, road traffic theory was developed to such an extent that an international colloquium was desirable. The first international colloquium on road traffic theory was held at the General Motors Research Laboratories in Warren, Michigan in December 1959 [5]. After this colloquium, several others were organised to deal with the various problems of road traffic. In the 1970s, a new approach was developed by Payne and Whitham [6, 7], based on the analogy with fluid mechanics, where it considers traffic as a continuous flow. In the 1990s another approach based on cellular automata was proposed. This approach was widely used because it has a simple structure and does not take much time during simulation. The first cellular automaton model to study road traffic was proposed by Cermer and Ludwi [8]. Currently, the NaSch model [9] is a very famous probabilistic model based on cellular automata.

A glance through the proceedings of these colloquia will give the reader a good indication of the considerable evolution in the understanding of traffic flows over the last 40 years. Since then, numerous colloquia and other specialisations have been held regulary basis, dealing with a variety of traffic-related topics.

I.2 Definition of road traffic

Road traffic is the set of phenomena due to the movement of users on road network. It is characterised by a supply consisting of a road infrastructure and by a demand from users who seek an individual optimum [10]. There are two types of traffic:

- Uninterrupted traffic: the flow of vehicles flows over long stretches of road, where vehicles are not required to stop by any cause outside the traffic flow.

- Interrupted traffic: vehicles must stop for any reason outside the traffic flow, such as traffic signs and traffic lights.

Road traffic always changes in situations that can be simple or difficult to manage. In addition, many incidents can occur on the road such as public works and accidents. These incidents disrupt the flow of vehicles and can block traffic. It is therefore essential to understand the impact of these incidents on road traffic at both macroscopic and microscopic levels in order to find solutions.

I.3 Why road traffic simulation

Simulation is a computer representation of a dynamic system from which conclusions can be drawn about the properties of the real system.
Simulation is an indispensable and effective tool for analysing a wide variety of dynamic problems that cannot be studied by other means. These problems are usually associated with

complex processes that cannot easily be described in analytical terms.
The objective of simulation in the field of road traffic is to ensure its fluidity by anticipating congestion and blockage situations, to have an explanatory role in the causes of certain events such as accidents and to determine the parameters that influence these events. On the other hand, it makes it possible to provide methodologies for estimating road traffic, determine the right conditions for traffic operation, to know its condition in the future and to determine the maximum capacities of roads when drawing up transport projects and road networks.

I.4 Usual traffic measurements

There are many types of sensors for the direct or indirect measurement of traffic variables. These sensors are generally transducers, sensitive to the physical quantity that we want to capture: presence, passage and speed of a vehicle [11].
The sensor can change the information into an elementary signal, transmitted to the detector. The received signal is transformed into a simple electrical information, significant of the flow parameter. In view of the rapid technological developments in the field of road metrology, only the main types of commonly used sensors are mentioned here [12], namely:

- Pneumatic sensors.
- Electromagnetic loops.
- Ultrasound.
- The video sensor.

I.4.1 Pneumatic sensors

They are used to carry out road counts and therefore measure flows. They consist of a rubber cable, stretched across the road and connected to a detector. The crushing of the cable during the passage of a vehicle causes an overpressure, detected by a pressure gauge activating a relay. It is then possible to count the number of axles passing over the sensor by accumulating the pulses in a counter. The counts are then expressed in $p.u.s.$ (special vehicle unit): $1 p.u.s. = 2 axles$. These sensors, which are still widely used for road counts, have a number of advantages, including:

- The ease of installation.
- The good portability of the sensor-detector assembly.
- The possibility of operating on battery providing an autonomy of several days.

On the other hand, the system has a high average cost. Moreover, the cable can be torn off when heavy vehicles pass by. In saturated conditions, the inaccuracy can sometimes exceed 20

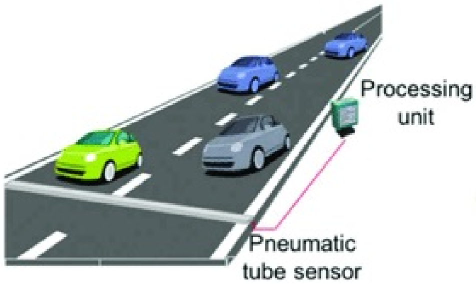

FIGURE I.1: Pneumatic sensor

Today, it is the most widely used device for measuring traffic parameters in many countries, both in cities and on urban expressways and highways.
The sensor consists of an inductive loop, embedded in the road surface. The passage of the metallic mass of a vehicle over the loop causes a variation in the electromagnetic field. This variation results in a voltage window whose length is linked to the length of the vehicle and its transit time.
With only one loop per channel, we measure not only the throughput but also the occupancy rate t ,defined by:

$$t = \frac{100 \sum_{i=1}^{N} t_i}{T} \tag{I.1}$$

Where t_i denotes the loop occupancy time at measurement period i , and T is the total mesure time.

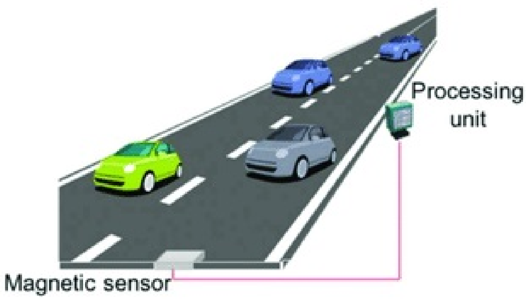

FIGURE I.2: Electromagnetic sensor

I.4.2 Acoustic detectors: Ultrasound

The acoustic sensor consists of a directional antenna fixed on a support. This antenna emits an ultrasound wave propagating with a known speed. When a vehicle passes, the ultrasound wave meets a reflecting surface. A fraction of this wave is reflected by the mobile, and is then captured by the receiver after a certain detection time. This detection time allows the calculation of the occupancy rate. The detector also allows the counting of the vehicles.
The sensor can often be mounted on a gantry above and in line with the traffic lane. The detection time is then variable according to the height of the vehicles. This feature allows for discrimination several categories.
With the right installation, no false echoes can be received. Under operating conditions, normal operation, the accuracy of the distance measurement is $0.5m$. The propagation speed of the ultrasonic waves is the function of the temperature and the humidity of the air.

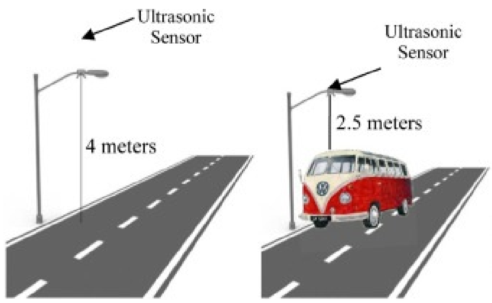

FIGURE I.3: Ultrasound sensor

I.4.3 The video sensor

This field is currently the subject of a great deal of research, particularly in the European context. The principle of this sensor consists in using a video camera and in automatically processing the images provided by this camera in order to deduce the traffic parameters.

FIGURE I.4: Video camera

I.5 Characteristics and representation of road traffic phenomena

Road traffic obeys laws of physics that explain most of the phenomena observed on our road networks. For several decades, these laws have been supported by observations of these phenomena thanks to counting devices: flow rate, speed, occupation, type of vehicle, etc. These counts have made it possible to measure these physical phenomena, understand them, explain them and make the link with theoretical knowledge on road flows.

In order to understand the functioning of a section or a road network, a first approach often consists in measuring the evolution of traffic speed as a function of flow ("flow-speed" relationship or "fundamental diagram") and deducing from this the operating parameters of the section, such as free speed or capacity. This part returns to the concept of the fundamental diagram by detailing its origins and mathematical properties, its interpretation, and its elaboration, and proposes a method for estimating its characteristic parameters that is simple to implement.

I.5.1 Traffic variables

A traffic flow on a road network has many similarities with the flow of a fluid. The first similarity concerns the definition of the network, which consists of pipes (road sections), junctions (crossroads), interchange areas, storage areas, etc. The similarities continue in the definition of the demand that irrigates the network: it flows from upstream to downstream. And when it flows on the network, overflows (congestion) are observed when the network capacity is not sufficient to handle the entire volume of demand. These overflows may remain local or disrupt the overall functioning of the network.
These similarities lead us to use the same microscopical and macroscopical variables from fluid mechanics to describe road traffic conditions. These variables are defined as follows:

I.5.1.1 Microscopic variables

Microscopic road traffic variables describe individual vehicle behavior and interactions.

A- Instantaneous speed :

It is the vehicle speed at a given moment t. The recording of the instantaneous speeds of a vehicle makes it possible to characterise the time profile of its speed.
The arithmetic mean of the instantaneous speeds is called the average instantaneous speed.

B- Inter-vehicle time:

Inter-vehicular time (h) is one of the most important microscopic variables. It describes the difference between the times at which two successive vehicles ($i+1$ followed by i) pass in front of each other at a given point on the road :

$$h(x) = t_i(x) - t_{i+1}(x) \tag{I.2}$$

C- Inter-vehicle space (headway):

Inter-vehicular spaces are instantaneous microscopic variables (measured at a given moment), measuring the distance separating at a given moment the front of successive vehicles (i and $i-1$) on the same traffic lane :

$$g_i(t) = x_{i+1}(t) - x_i(t) \tag{I.3}$$

We also note that inter-vehicular time and inter-vehicular spacing are linked by the following relationship:

$$g_i(t) = v_{i+1}(t) \times h_i \tag{I.4}$$

With v_{i+1} designates the speed of the vehicle ahead.

D- Length of vehicles :

It is related to the instantaneous speed of the vehicles and is calculated by the following relationship:

$$L_i = v_i(t) \times \Delta t_i \tag{I.5}$$

with Δt_i is the occupation time of the magnetic loop.

I.5.1.2 Macroscopic variables

Macroscopic variables describe traffic flows globally, by calculating the average values of microscopic variables.

A- Flow (flow or current)

The flow J represents the number of N vehicles passed during a period of time T, at a given point. And can be defined by the following ratio:

$$J = \frac{N}{T} = \frac{N}{\sum_i^N h_i} \tag{I.6}$$

With :
N: is the number of vehicles.
T: is the period of time.
h: is the inter-vehicle time.
This expression shows the relationship between flow and inter-vehicular time (h). In other words, it shows the relationship between a macroscopic variable (J) and another microscopic one (h). The capacity of a road is called the maximum possible flow of that road.

B- Density or concentration

This variable defines the distribution of vehicles in space. It refers to the number of vehicles (N) present on a section of road (L) at a given time. Density is expressed as the number of vehicles per unit length (veh/km or veh/m) and is given by :

$$\rho = \frac{N}{L} \tag{I.7}$$

The density ρ is also related to flow and speed by the following relationship:

$$\rho = \frac{J}{V} \tag{I.8}$$

C- Occupancy rate

It can be seen as an alternative to density [13], which is the time interval during which the sensor detects the vehicle. It is calculated by the following relationship:

$$\Delta t_i = \frac{(L_i + d)/v_i}{T} \tag{I.9}$$

with
v_i: the speed of the vehicle.
L_i: is the length of the vehicle.
d: is the length of the detector.
T: the time interval during which the calculation is made.
The Average Occupancy Rate is calculated by the following relationship:

$$\Delta t_m = \frac{1}{\Delta t_i} \sum_{i=1}^{N} \Delta t_i \tag{I.10}$$

From this value, we can deduce the density of vehicles ρ by the following relationship:

$$\Delta t_m = (l_m + d) \times \rho \tag{I.11}$$

With : l_m is the average length of the vehicles during the time interval Δt, and d is the length of the detector.

D- Vehicle speeds and average speeds :

- **Instantaneous speed of a vehicle**

For the same vehicle, the recording of the instantaneous speeds makes it possible to characterize the temporal profile of the speed. This recording is useful to obtain various parameters. It reveals the quality of the traffic on a route and is frequently used in calculations relating to the energy consumption of vehicles.
At a fixed point on the road, the collection of individual vehicle speeds defines an empirical distribution. For a given category of vehicles, this type of distribution can often be adjusted according to a theoretical law: normal law or Erlang law.
In cities, the distributions of instantaneous speed have a characteristic shape. The large peak at the origin reveals the preponderant part due to stops: more than 25% of the total travel time in French cities.

- **Average speed of a vehicle**

On a route of duration T, the average speed v_{moy} of a vehicle is defined by :

$$v_{moy} = \frac{\int_0^T v(t)dt}{T} \tag{I.12}$$

Where $v(t)$ is the instantaneous speed of the vehicle at time t.

- **Time average speed**

In the macroscopic approach, we are no longer interested in a single vehicle but in a set of vehicles. At a fixed point on the road, the temporal average speed u_t ,is the arithmetic average of the instantaneous speeds ui of the N vehicles, passing during an indefinite time interval:

$$u_t = \frac{\sum_{i=1}^{N} \frac{d_i}{t}}{N} \tag{I.13}$$

where d_i is the distance traveled by the $i-th$ vehicle during period t .

- **Mean space velocity**

The notion of the average speed of space, defined by [14], is more useful in practice. Thus, on a road section of fixed length, the arithmetic mean of the vehicle speeds at a given time is :

$$u_t = N.\frac{d}{\sum_{i=1}^{N} t_i} \tag{I.14}$$

Where t_i is the time required for the ith vehicle to travel the distance d. The two velocity concepts thus defined are different. For a stationary traffic flow, we establish the following relation:

$$u_t = u_s + \frac{\sigma^2 s}{u_s} \tag{I.15}$$

Where σ denotes the standard deviation of the velocity distribution in space. Therefore, we observe the inequality $u_t \geq u_s$. On the other hand, the mean space s, the mean time difference h, and the mean velocity u_s are related by:

$$h = \frac{s}{u_s} \tag{I.16}$$

The variables of flow, velocity and concentration are therefore linked together by the relation $J = \rho \times V$, the relation (called fundamental) that links them two by two constitutes **the fundamental diagram (DF)**.

I.6 Origin of the Fundamental Diagram

As early as the 1930s, similarities with fluid mechanics made it possible to lay the first theoretical foundations for road flows. The first of these analogies concerns the conservation of the number of vehicles along the sections.

I.6.1 The principle of conservation

Let us observe a road section, of length dx for a short period dt. On this road section there are vehicles whose number is described by the variable N (vehicles are indexed in ascending order of their entry on the road section). Assuming that no vehicles appear or disappear spontaneously from this section (a reasonable assumption), then the vehicle conservation equation is written:

$$\frac{d\rho}{dt} + \frac{dJ}{dx} = 0 \tag{I.17}$$

I.6.2 Existence of the fundamental diagram

To be solved, this equation can be transformed into a hyperbolic equation according to the concentration variable ρ :

$$\frac{d\rho}{dt} + \frac{dJ(\rho)}{dx} = 0 \tag{I.18}$$

Solving this equation assumes that there is a relationship between flow rate and concentration, $J = J(\rho)$: this is the fundamental relationship.

I.6.3 Mathematical properties

The fundamental diagram, therefore, has its origin in the principle of vehicle conservation. Without going into complex mathematical considerations, it should be remembered that this hyperbolic system confers mathematical properties to the fundamental diagram. Failure to respect these mathematical properties calls into question the very existence of the fundamental diagram and the solvency of the hyperbolic system at its origin.

These properties are as follows:

- Flow values are positive or zero.
- The fundamental diagram is continuous, over a bounded concentration range from zero concentration (when no vehicle is present) to maximum concentration (when all vehicles are stationary in a queue). Over this concentration range, each concentration value corresponds to a unique flow rate value.
- The fundamental diagram is concave.

Given these three properties, only the lower diagram respects the properties of continuity and concavity.

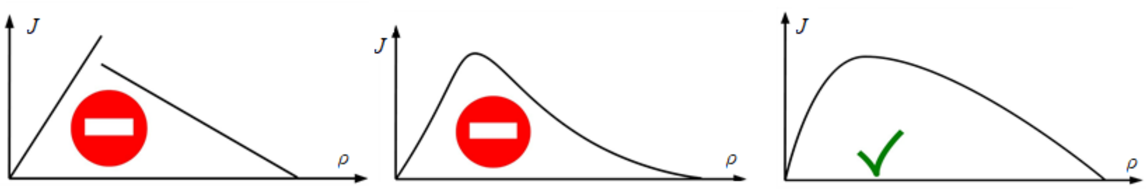

FIGURE I.5: Diagram which not respects (respects) the properties of continuity and concavity.

I.6.4 What shape for the fundamental diagram

In summary, all concave, continuous and positive functions over a bounded range of concentration are acceptable to define a basic diagram. In the literature, there are many possible forms for representing the fundamental diagram: piecewise linear, bilinear, semi-parabolic, parabolic, etc.
Nevertheless, it must represent observable phenomena, and a final constraint is therefore added to the mathematical requirements: its physical properties. The function chosen to represent the fundamental diagram must above all relate the values of flow, velocity and concentration faithfully to what is observed in the field.
As an example, consider an urban section composed of a traffic lane and on which vehicles are circulating in this way:

- When not obstructed, vehicles travel at a speed of $50 km/h$;
- In a queue at a standstill, vehicles are positioned every 7 metres, i.e. a maximum concentration of approximately 140 vehicles per kilometre.
- When the infrastructure is operating at capacity, the vehicles are spaced two seconds apart, corresponding to a capacity of $1,800$ vehicles per hour.

Based on this data, which is easily measurable in the field, it is possible to propose a fundamental diagram that respects each of these constraints. For the sake of simplicity, we consider here that the fundamental diagram is triangular: This diagram describes the fluid

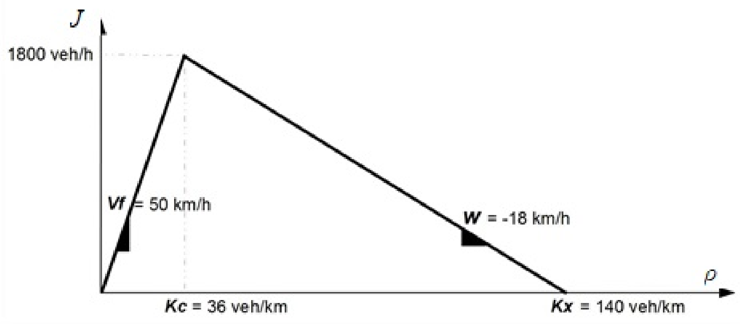

FIGURE I.6: Fundamental triangular diagram of a single-lane section in an urban area.

and congested traffic conditions that may exist in this single-lane urban section. Additional information can also be derived from it. For example that the critical concentration is of the order of 36 vehicles per kilometre. In other words, when vehicles are separated by a distance of less than about 30 metres (including vehicle length), the vehicles interfere with each other and adapt their distance to the speed of their predecessor: this is the pursuit behaviour.

I.6.5 Other representations

The relation $J = \rho \times V$. remains true. Therefore, all the representations below are strictly equivalent and correspond to a simple change of reference mark:

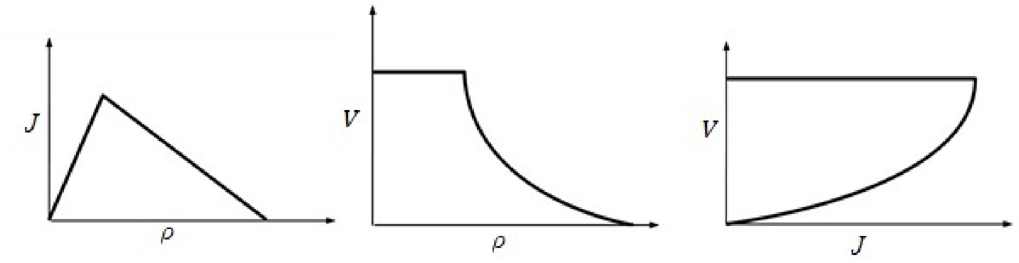

FIGURE I.7: Different representation planes of the fundamental diagram.

I.7 Scales of flow phenomena

Traffic flow is the result of a sum of individual behaviour. Each driver will interact with his environment, i.e., other drivers and the infrastructure on which he is driving. Observation of this flow shows that there are two types of phenomena: local phenomena and global phenomena. The aim of this section is not to make a catalogue of the phenomena at the origin of the flow but rather to give examples illustrating the diversity of scale that exists between these phenomena, and also to show that the boundary between local and global is relatively diffuse. Furthermore, we will see that this flow is characterized by a strong heterogeneity, and in some cases, it even presents certain properties that can be described as chaotic.

I.7.1 Definition of global and local scales

Before discussing the description of local and global phenomena, it is important to consider what is meant by local and global. In traffic, it is relatively difficult (if not impossible) to determine with precision the orders of magnitude characteristic of a local phenomenon or a global phenomenon, as these notions depend on the context in which they are placed. Suffice it to say that, as a first approximation, a phenomenon is local if it involves only a small number of vehicles, over a relatively small space and time span, of the order of a few meters and a few seconds. For a phenomenon to be considered global, the number of vehicles involved must be greater (at least several dozen vehicles) and occur over a space-time span of a few hundred meters (or even kilometres) and a minute. It seems difficult to us to give a more precise definition of the notion of global or local phenomenon given the diversity of the traffic conditions in which we can be interested (urban, interurban environment, etc.). It is mainly a question of seeing that the global phenomenon concerns a fairly large number of vehicles and can therefore be observed at an aggregate level, whereas a local phenomenon concerns only a limited number of vehicles and can therefore only be observed by taking a microscopic view of traffic.

I.7.2 Global and local phenomena

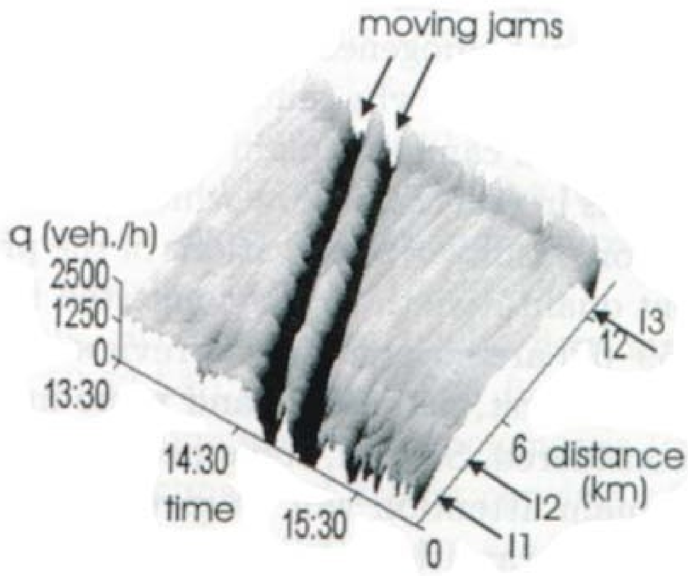

FIGURE I.8: Propagation of two congestions on the A5-North motorway in Germany, from [Kerner, 1999].

The notions of global and local phenomena have been defined, we will present an example of each of these phenomena, which will enable us to illustrate this difference in the scales of flow phenomena. The most illustrative example of what a global phenomenon can be is the propagation of congestion on motorways. Although the reasons for the appearance of such congestion are still poorly understood and are still being researched, numerous observations [15–17], have shown that when congestion has created, it propagates in the form of "waves" separating a fluid state from a congested state. These waves move upstream at a speed of between 10 and 20km/h.

Heavy congestion (such as can be observed on days when people go on holiday) spreads over tens of kilometres and for several hours. They are characterized by very low vehicle speeds and flows, close to zero. Figure I.8 illustrates this phenomenon. It represents the evolution in space and time of the flow (noted q on the figure and expressed in vehicles per hour) on a

motorway:
The darker the color, the lower the flow. We can clearly see the propagation in the form of waves of two congestions which propagate upstream. It can also be seen that these two waves have an identical propagation speed which remains constant. The study of these congestion phenomena [18] clearly shows that it is a global phenomenon involving a very large number of vehicles and over significant spatial and temporal expanses.

Conversely, the phenomenon of slot acceptance is a local traffic phenomenon. It can be defined as follows: let us take a vehicle that wishes to a move in a different lane from the one in which it is travelling. In order to manoeuvre, it needs to have a certain amount of time during which no vehicle will be present in the lane where it wishes to make its manoeuvre. If this time is not sufficient, the manoeuvre is impossible and the vehicle must wait for a sufficient window of opportunity (the time interval between the times when two vehicles pass in the lane in which it wishes to manoeuvre is called a window of opportunity). This phenomenon is clearly a local phenomenon because it involves only a few vehicles, over a very small space and time span.
There are various situations where such a mechanism exists. Let us take the classic example of a vehicle travelling on a secondary lane and wishing to cross a priority lane at an intersection (typically a yield sign). To cross, this vehicle will take a certain amount of time (of the order of a few seconds). This vehicle must wait for a slot in the priority flow that is longer than this crossing time to carry out its manoeuvre. This phenomenon is also found on motorway slip roads and in the process of overtaking between vehicles.

I.7.3 Link between local and global phenomena

While these two examples clearly show the existence of phenomena taking place at local and global scales, we will see that the boundary between these two scales is relatively blurred. Taking the two examples described above, we will see that there is a constant interaction between the local and global levels.
There are congestion situations where the global nature of the phenomenon may be less obvious than what we saw in I.7.2. Take the example of phantom traffic jams. Phantom traffic jams occur for no obvious reason (e.g. without an accident or capacity restriction). It can only be observed that when a disturbance (which has yet to be determined) occurs in an area where vehicles are fairly close to each other, this disturbance may be amplified and lead to congestion. This can be seen in Figure I.9 where the trajectory of vehicles is represented in space and time. One can clearly see the "spontaneous" appearance of congestion which spreads upstream.
According to Helbing [16], the origin of this congestion can be a rather small disturbance,

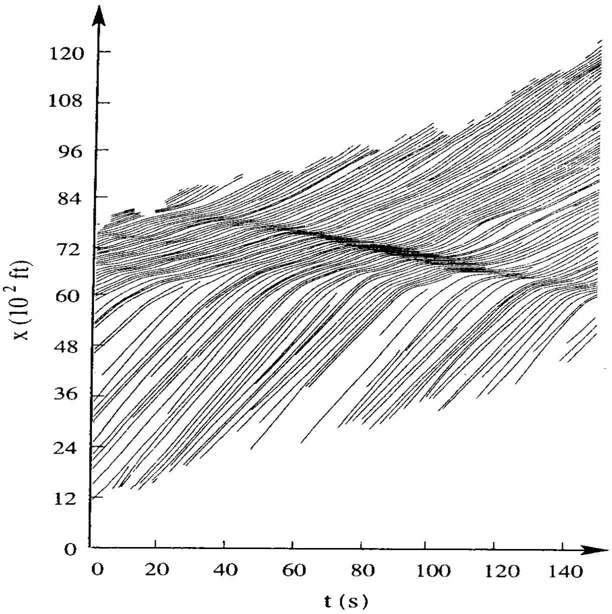

FIGURE I.9: Appearance of a phantom traffic jam, according to [16], based on aerial photographic data obtained by Treiterer and Myers in 1974.

e.g. a simple lane change of a vehicle. A typical example of this phenomenon (and one that every driver has experienced) is the case of a truck changing lanes to overtake another truck on a motorway. In this case, the appearance of a slow vehicle in the middle lane slows down the faster vehicles and creates congestion.

In the case of these phantom congestions, the propagation of the congestion remains a global phenomenon because it concerns a significant number of vehicles and has a spatial and temporal extent that remains of the order of several hundred metres and one minute. However, its origin is very local and concerns only a small number of vehicles. It is therefore a global phenomenon, but its origin is local. Similarly, the slot acceptance phenomenon can influence the aggregate level. For example, the capacity of an intersection (i.e. the maximum number of vehicles that can pass through it) is directly related to this slot acceptance phenomenon. Similarly, at motorway junctions, lane changing phenomena play a major role in the overall functioning of the infrastructure [19]. These examples illustrate that in traffic there is no real separation of scale (this point is also made by Helbing in [20]. While it is clear that there are global flow phenomena as such, it is also clear that there is no real separation of scale in traffic.

Therefore, in order to represent the dynamics of the flow, it is necessary to look at both local and global phenomena. It also appears that these phenomena cannot be entirely uncorrelated with certain local phenomena.

Chapter II

Models and methods of traffic analysis

II.1 Intorduction

Traffic models are indispensable tools in the realm of transportation planning and management. These models serve as intricate frameworks designed to unravel the complexities of vehicular movement, offering valuable insights into the dynamics of traffic flow within diverse infrastructures.

At their core, traffic models aim to explain and predict traffic flow in order to better reproduce reality and thus enable better optimization of infrastructures. Schematically, modeling can have three objectives: (i) describe (summarize) the data(ii) predict (simulate) (iii) explain (understand) empirical results.

Generally, road traffic models can be classified according to different criteria: type of variables (continuous, discrete), level of detail, representation of the process (deterministic, stochastic). Throughout this thesis, road traffic models will be classified according to the level of detail adopted: macroscopic, microscopic and mesoscopic.

In next section, we start with a description of existing flow models. Subsequently, we are mainly interested in models of cellular automata, more particularly the Nagel and Schreckenberg model [39].

II.2 Road traffic modelling

II.2.1 Road traffic patterns

For a long time, different approaches have been used and several tools and technologies have been exploited in the study and modelling of road traffic. Nowadays road traffic and transport systems play a crucial role in the development of countries and societies. Moreover, studies on road traffic are becoming very indispensable due to the increasing need for the movement of goods and people. Thus, a lot of work has been done on road traffic with the aim of optimisation, use of transport infrastructure, improvement of road safety and security, etc.

II.2.2 Classification of traffic patterns

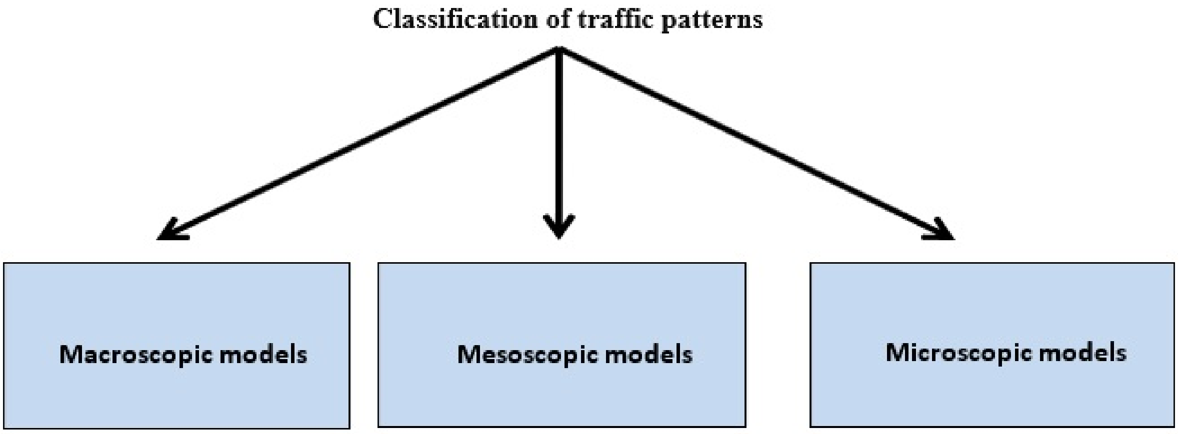

FIGURE II.1: Classification of traffic patterns.

The methods used include three different models:

- The type of model from a behavioural point of view.
- The level of detail.
- Type of variable.
- The type of model from the analysis point of view.

The first work on traffic modelling began with the rise of the automobile in the first half of the last century. Thus, today there are many models and it would probably be impossible to draw up a complete list of them. On the other hand, each model has its own modelling objectives and can therefore be grouped into categories. They are therefore classified according to their properties:

II.2.3 Macroscopic models

Macroscopic models describe traffic at a high level of aggregation, as a flow of vehicles, regardless of the component parts. These models are generally used for planning and control operations, covering large networks and long periods of time. Road traffic is represented in a compact method using a series of interdependent variables such as flow, density and speed. Typical vehicle manoeuvers, such as lane changes, cannot be represented.
There is an interesting analogy between the mathematical description of road traffic and the flow of a fluid, an analogy exploited by these models. However, there are traffic-specific

phenomena that do not correspond to fluid flow, such as instability, road congestion or stop-and-go traffic. However, macroscopic models are important tools for simulation, forecasting, estimation and design of control strategies. Three models are the most recognized today in the literature to represent traffic dynamics at the macroscopic level: the equilibrium model, the non-equilibrium model and the multi-class origin-destination model. In these models, the temporal evolution of macroscopic quantities such as density, velocity and flux are represented by systems of non-linear partial differential equations called conservation laws.
As far as traffic models are concerned, Lighthill, Whitham and Richards are the first to have proposed using a partial differential equation to model the evolution of traffic density along motorways. The only parameter of this model is the fundamental diagram [21] which gives an empirical (usually concave) relationship between density and flow, a relationship which is valid at all points. This model has been well mastered since the work of [22], even in the presence of boundary conditions and inhomogeneities in the parameters. Moreover, several numerical schemes are available for such equations, such as the Godunov scheme. It should be noted that the work on the analysis of the LWR model and its extensions has a long history in the transport community, particularly in the United States and France. Finally, Lebacque proposes in [23] a modification of the LWR model where vehicles have a bounded acceleration, which makes the model more realistic and provides an alternative to the treatment of discontinuities.

II.2.4 Mesoscopic models

A mesoscopic model does not differentiate and track vehicles as individual entities, but it does specify the behaviour of vehicles in probabilistic terms. Thus, traffic is represented by a small group of vehicles, for which activities and interactions are described in a low level of detail. For example, a lane-change manoeuver can be represented for a vehicle as an instantaneous event, where the decision to make a lane change is based on relative lane densities and speed differences. Some mesoscopic models are obtained by analogy with kinetic gas theory, describing the dynamics of speed distributions.
Mesoscopic models occupy an intermediate position between microscopic and macroscopic models. They can model large networks without a great deal of effort on coding and calibration, while providing a better representation of traffic dynamics and the individual behaviour of the participants, compared to macroscopic models.
Mesoscopic models are used for planning, but also for real-time operations. They are more flexible than macroscopic models in terms of modelling important elements such as travel behaviour (e.g. route selection). However, there are limitations in the ability to represent detailed traffic operations.

A few mesoscopic models, most often found in the literature, will be briefly presented in the following.

- ✓ Represents the road network by nodes and arcs, and the vehicles on the arcs are grouped into packets that travel from origin to destination (note that packets can be formed from a single vehicle) [24].
- ✓ Uses individual vehicles moving along the segments based on speed-density relationships and waiting queue patterns [25]. The lanes are shown in detail when network congestion occurs and queues begin to grow. The queues are specific to each lane. Operations at intersections are captured in terms of their capacity.
- ✓ Also uses the speed-density relationship, but adopts a more detailed representation for signalled intersections (at the level of the succession of traffic lights) to model delays at these positions [26].
- ✓ Works in a similar way to the previous model, but the vehicle dynamics in the links are captured by simplified vehicle-tracking relationships [27]. The lanes are represented explicitly, including lane-changing operations.
- ✓ Represents vehicles individually, responding to speed-density relationships, and uses stochastic queuing servers at nodes to justify delays due to traffic lights, as well as interactions with traffic flows from other directions [28].

II.2.5 Microscopic models

A microscopic model describes both the spatio-temporal behaviour of the system components (vehicles and drivers) and their interactions at a high level of detail (individually). For example, for each participating vehicle, the lane change is described as a chain of driver decisions.

Microscopic models are suitable for modelling vehicle interactions at the high level of detail needed to evaluate several Intelligent Transport Systems, but they are limited to small areas due to the large amount of data required.

In the same way as microscopic models, microscopic models describe the characteristics of each vehicle involved in traffic. However, in addition to the detailed description of traffic behavior, the vehicle's control behavior (e.g. gear shifting) is also modelled according to environmental conditions.

Furthermore, even the functioning of specific parts of the vehicle (subassemblies) is described. The two types of representative models for microscopic models are car-following models and cellular automaton-type models.

✓ Car-following models try to describe the process by which one vehicle follows another. In this category, we find three types of models: prevention models, stimulus-response models and psycho-spatial models.

✓ Cellular automaton type models are a rather recent development in road traffic modelling at the microscopic level and they use the adaptation of particle hopping models to represent traffic movement.

II.3 Cellular automaton

II.3.1 A brief review of particle hopping models of traffic flow

Cellular automata represent an efficient modelling tool to describe, finely and efficiently, the dynamic and complex behaviors of traffic, they use the adaptation of particle hopping models to represent traffic movement. However, there is a close similarity between cellular automata (CA) and the particle hopping models [29, 30]. Where The problem of traffic flow can be seen as the large-scale dynamics of interacting particle systems [31, 32]. all particle hopping models are shared by the following characteristics: a lane is investigated by a one-dimensional lattice divided into sites which can be empty or occupied by a "vehicle"; the lattice constant is defined as the nearest distance between two adjacent vehicles. The concentration of the vehicles on the lane is defined by the ratio of the number of vacated lattice sites to the total number of lattice sites. The vehicles proceed following certain rules. There is an "exclusion clause," which states that a vehicle will occupy the new location computed by these rules, only if it is not already occupied by another vehicle.
Cellular automata are an idealization of physical systems. This is due to the following properties: Cellular automatons can be used from several perspectives. One, which is oriented towards understanding the basic mechanisms of traffic rather than realistic simulation of flows, consists in taking oversimplified models, for which most of the characteristics can be calculated analytically, and studying the effect of a particular choice for the dynamics [33].

- The physical space is discreet. It is divided into a set of identical cells or sites. Each cell can have a discrete and finite set of states. Time is also discreet. This means that :

$$t_k = k * \Delta t \tag{II.1}$$

With k an integer and Δt the time step.

- Short-range interaction i.e., the state of a site i at time $t+1$, depends on its state as well as the state of its close neighbors at time t.

II.3.2 Asymmetric simple exclusion process and its generalizations

The totally asymmetric exclusion model was introduced in 1968 [34], it is a simple model that allows the study of interacting systems [35, 36]. In this model, updating is carried out in a random parallel or sequential method. A particle moves forward through a single site with a probability p if and only if the target site is empty. The ASEP model can be a special case of the NaSch model when: $v_{max} = 1$, in the NaSch model, and the update in the ASEP model is parallel. The generalization of the ASEP model was investigated by Nagatani [37] which describes the one-dimensional lattice with both closed and open boundaries. Recently a generalized ASEP, in which the hopping probabilities are independent has been considered [38].

II.3.2.1 The periodic boundary conditions

They are also called closed boundary conditions and are necessary to describe a system of infinite size. For closed boundary conditions when the vehicle reaches the end of the chain it then occupies an empty site at the beginning of the chain according to its maximum speed so we can say that the chain has neither beginning nor end.

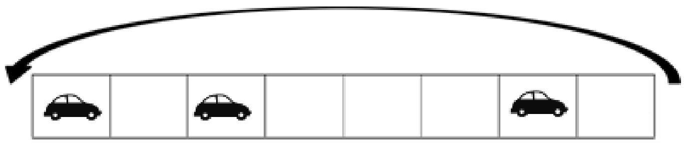

FIGURE II.2: Periodic boundary conditions.

II.3.2.2 Open boundary conditions

The open boundary conditions are implemented as follows: if the first cell on the left is empty, a vehicle with velocity 1 is injected with the probability α and extracted with the probability β regardless of their speed.

II.3.2.3 Nagel-Schreckenberg model (NaSch)

NS [39], described the simplest single-lane stochastic cellular automata (STCA), in this model, the road is considered as a lattice where this lattice is discretized into a set of sites

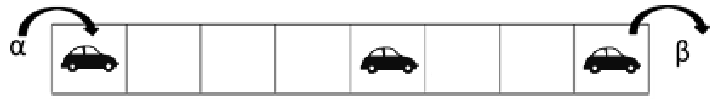

FIGURE II.3: Open boundary conditions.

(cells) of identical size which actually corresponds to $\Delta x = 7.5m$, the minimum space occupied by a vehicle. Time is also discretized, where the time step corresponds to $\Delta t = 1s$.
The vehicle speed can only take one discrete values $v = 0, 1, 2, ..., v_{max}$, is the number of sites that a vehicle can jump during a time step $\Delta t = 1s.$, where v_max shows the maximum speed that must not be exceeded. For example, a jump of 5 sites in an iteration has a speed of $135km/h$ in reality $(i.e., 5 \times 7.h/sec = 135km/h)$.
At each iteration, the vehicle i is characterized by the position $x_i(t)$ and the speed v_i, the free-space between vehicles is given by :

$$g_i(t) = x_{i+1}(t) - x_i(t) \tag{II.2}$$

The system status is updated at any time by applying the following rules.
Rule of motion :

✓ Step 1:

- Acceleration : If $v_i < v_{max}$, the speed of vehicle i is increased by one, but remains unchanged if $v_i = v_{max}$, (i.e. $v_i \longrightarrow min(v_i + 1, v_{max})$), here drivers wish to drive at the highest possible speed while respecting the maximum speed constraint v_{max}. This step reflects the general tendency of drivers to drive as fast as possible, if they are allowed to do it, without exceeding the maximum speed limit.

✓ Step 2:

- Deceleration: (due to other vehicles) The vehicle is not alone on the road, so ensures that there is no collision between the ith vehicle and the vehicle sited at position $(i+1)$. this condition must be added, $v_i \longrightarrow min(v_i + 1, g_i)$.

✓ Step 3:

- Randomization: If $v_i > 0$, the speed of the vehicle i is randomly decreased by the unit with probability p, but v_i does not change if $v_i = 0, i.e., v_i \longrightarrow max(v_i - 1, 0)$ with probability p. This probability quantifies on average the condition of the driver. When this probability is high, it refers to safe drivers. On the other hand, when p is low, drivers are aggressive in the sense that they do not hesitate to accelerate even if there is not enough space. This step is important for taking into account individual behaviours that differ from one driver to another.

✓ Step 4:

- Movement: The vehicle moves forward at the set speed:

$$x_i(t+1) \longrightarrow x_i(t) + v_i(t+1).$$

These rules must apply to all vehicles in the same iteration, so it is a parallel dynamic.
If $p = 0$ (p is the braking probability) then the dynamics are parallel deterministic. If $p > 0$ the dynamic becomes random parallel (non-deterministic), i.e., the movement of the vehicle is probabilistic.

The figure below illustrates the four previous steps:
For configuration at time t :

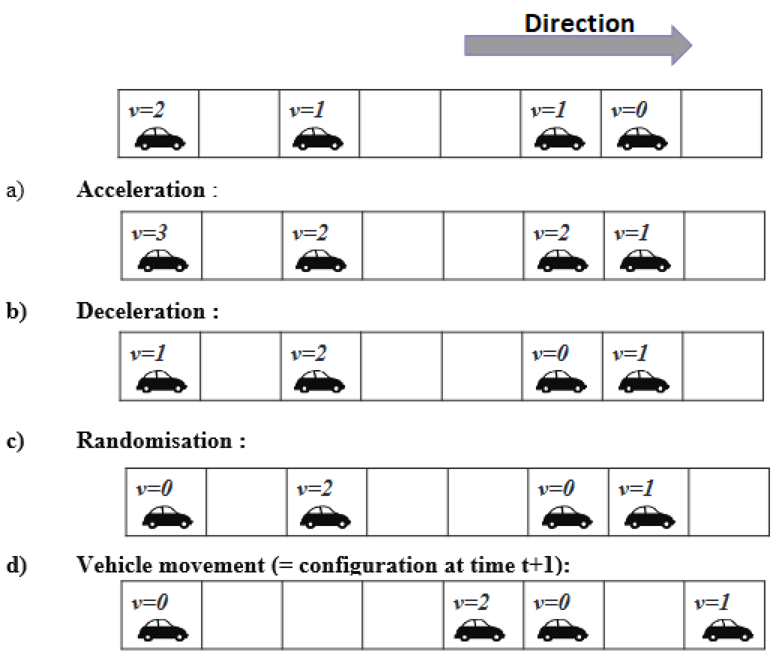

FIGURE II.4: The NaSch model rules for $v_{max} = 2$.

The diagram fundamental of this model, obtained for periodic boundary and steady-state conditions, is shown in the figure (Figure II.6).
Figure II.6 present the current J as a function of density for different maximum velocities $(v_{max} = 1, 3, 5)$, and different braking probabilities $(p = 0.1, 0.4, 0.7)$. We see two branches in the diagram fundamental:

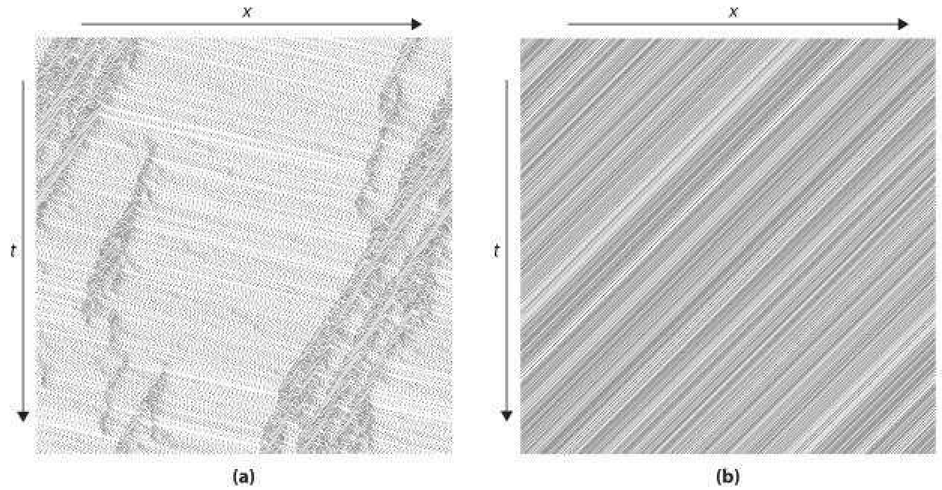

FIGURE II.5: Space-time diagrams of the NaSch model with $v_{max} = 5$ and (a) $p = 0.25$, $\rho = 0.20$, (b) $p = 0, \rho = 0.5$. Each horizontal row of dots represents the instantaneous positions of vehicles moving to the right while successive rows of dots represent the positions of the same vehicles in successive time steps.

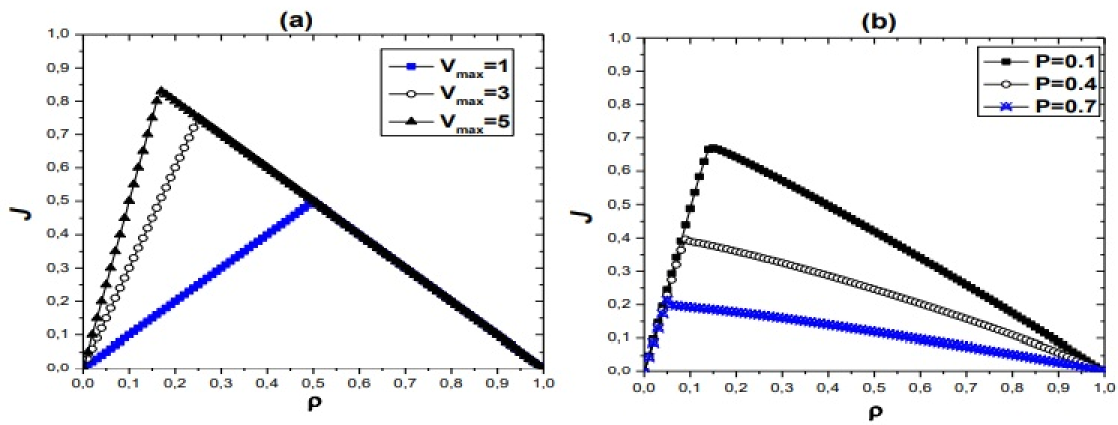

FIGURE II.6: Fundamentals diagrams of the Nagel-Schreckenberg model, (a) For various maximum speeds $(v_{max} = 1,3,5)$ with $p = 0$, (b) For different values of the braking probability p with $v_{max} = 5$.

- Branch corresponds to free-flow traffic where the density is lower than the critical density (it is the density corresponding to the maximum value of the current for each v_{max}. The flow increases with the density until it reaches a maximum value and then enters a second Branch (congested traffic).

- Branch corresponds to congested-flow traffic where the density is higher than the critical density.

Increasing $v_{max}(v_{max} > 1)$ breaks the symmetry free-space – particle. Hence, the symmetry of the fundamental diagram is broken (i.e., no symmetry for $\rho = \frac{1}{2}$). However, the increase in braking probability p leads to a large fluctuation in velocities resulting in the collapse of the current at lower densities.

II.3.3 Extensions of the NaSch model in a single-lane

The NaSch model is a minimal model in the sense that any simplification of the rules can no longer produce realistic traffic behaviour [40]. It is able to reproduce the basic properties of road traffic.
The movement of a vehicle in this model could have unrealistic characteristics, such as linear acceleration (Step 1 of NaSch), stopping in a one-time step instead of linear deceleration of speed (Step 2 of NaSch).
On the other hand, vehicles take into account the distance instead of the speed of vehicles in front of them [41]. The NaSch model is unable to capture many aspects of the fine structure of traffic dynamics, in particular, the existence of metastable states [40] or synchronized traffic [41]. Consequently, modifications have been proposed to obtain a more realistic description [41–44, 49–55].
Hence, It is impossible to discuss all of them, so we have limited ourselves to the most popular and successful ones that have introduced other interesting aspects to the dynamics. The NaSch model is flexible enough to be modified to refine other properties by adding new rules to modify motion behaviours. Takayasu and Takayasu (T^2) [42], Benjamin, Johnson and Hui (BJH) [43] and Barlovic et al (VDR) [40], modified the randomization rule to model the delayed acceleration of a vehicle after stopping (driver reaction time). The randomization rule can be modified also to create synchronized traffic [56]. The NaSch model has also been modified to take into account the synchronization of distances between vehicles in order to obtain the synchronized phase [41]. Fukui and Ishibashi [57] introduced another variation on the basic model in which the speed increase may not be progressive and the stochastic delay is applied only to high-speed vehicles. Another model was developed to add vehicle anticipation to determine the speed of the vehicle being followed [44].

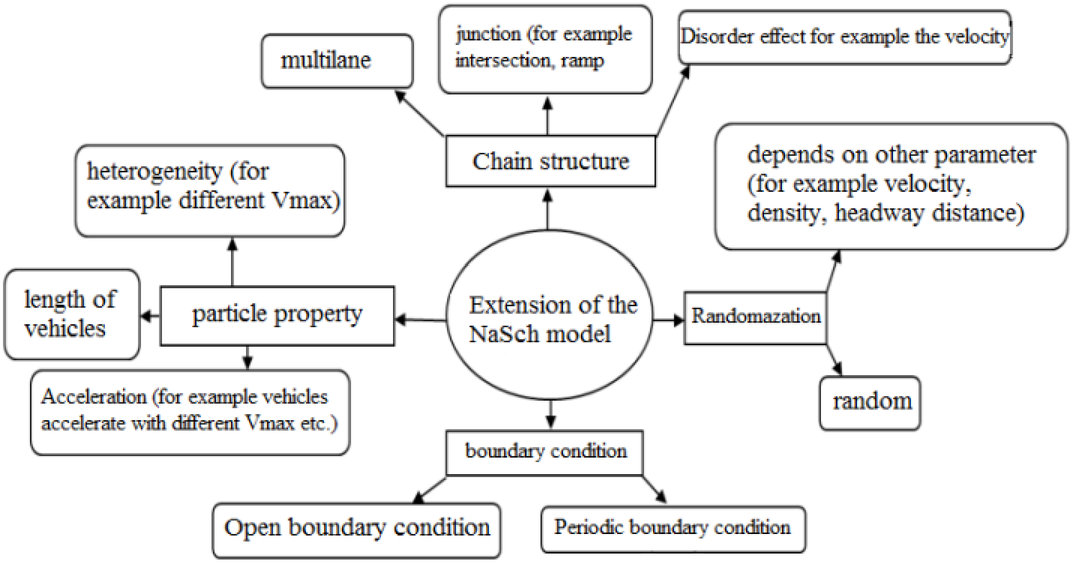

FIGURE II.7: The Extension of the NaSch model

II.3.4 Synchronized traffic flow

The three-phase traffic theory is a traffic flow theory that was developed by Boris Kerner in the 1990s. It is based on the observation that traffic flow can be divided into three distinct phases: free flow, synchronized flow, and wide moving jams.

The three-phase traffic theory has been supported by empirical data from a variety of traffic systems. It has also been used to develop traffic models that can be used to predict traffic congestion and to improve traffic management.

- Free flow is the state of traffic when vehicles are moving freely and there is no congestion.
- Synchronized flow is the state of traffic when vehicles are moving at a reduced speed and are interacting with each other.
- Wide moving jam is the state of traffic when vehicles are moving slowly or stopped in a long queue.

Here is a more detailed explanation of each of the three phases:

-Free flow

In free flow, vehicles are moving freely and there is no congestion. Vehicles are spaced out at a comfortable distance from each other and are able to maintain a constant speed. Free flow is the most efficient state of traffic, as it allows the maximum number of vehicles to pass through a given point in a given time.

-Synchronized flow

Synchronized flow is a state of traffic that occurs when the traffic density is high enough that vehicles begin to interact with each other. This interaction can cause vehicles to slow down and to bunch together. Synchronized flow is still a relatively efficient state of traffic, but it is less efficient than free flow.

-Wide moving jam

A wide moving jam is a state of traffic that occurs when the traffic density is too high for vehicles to interact with each other in a coordinated way. In a wide moving jam, vehicles are moving slowly or stopped in a long queue. Wide moving jams are the least efficient state of traffic.

The three-phase traffic theory has been used to develop traffic models that can be used to predict traffic congestion and to improve traffic management. For example, traffic engineers can use the theory to identify areas where congestion is likely to occur and to implement measures to reduce congestion. The Kerner-Klenov-Wolf (KKW) model is a cellular automata model of traffic flow that was developed by Boris Kerner, Sergey Klenov, and Dieter Wolf in 2002 [45]. The model is based on the three-phase traffic theory and is able to reproduce a wide range of traffic phenomena, including free flow, synchronized flow, and wide moving jams.

II.3.4.1 The Kerner-Klenov-Wolf (KKW) model

The KKW model is a discrete-time, continuous-space model. The space is divided into a grid of cells, and each cell can be occupied by a vehicle or be empty. The time is divided into discrete time steps, and at each time step, each vehicle moves forward one cell or remains stationary.

The movement of vehicles in the KKW model is governed by a set of rules. The main rule is that a vehicle can move forward if the cell in front of it is empty. However, there are also a number of other rules that govern the movement of vehicles, such as the following:

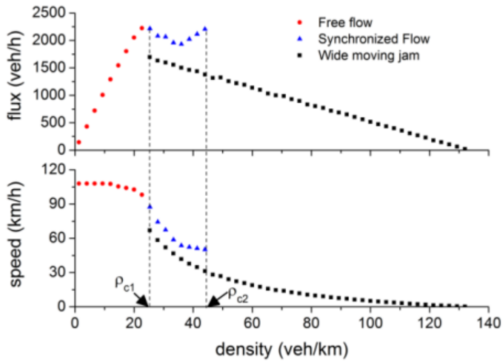

FIGURE II.8: The fundamental diagram of the KKW model on a circular road

- Vehicles cannot overtake each other.
- Vehicles slow down when they are close to the vehicle in front of them.
- Vehicles speed up when they have a long distance to the vehicle in front of them.

The KKW model has been used to study a wide range of traffic phenomena, including the following:

- The formation of free flow, synchronized flow, and wide moving jams.
- The propagation of traffic waves.
- The effects of traffic signals and other traffic control measures.

The KKW model is a valuable tool for understanding and modeling traffic flow. It is able to reproduce a wide range of traffic phenomena, and it can be used to study the effects of different traffic control measures.

II.3.4.2 Two-state model and its improved version

A) Two-state (TS) model

The two-state model is a more complex model than the KKW model, but it is able to reproduce a wider range of traffic phenomena. For example, the two-state model is able to reproduce the formation of wide moving jams, which the KKW model is not able to do.

The two-state model is based on the following assumptions:

- Vehicles travel at a constant speed in free flow.

- Vehicles slow down when they encounter a vehicle in front of them.
- Vehicles stop when they cannot move forward.
- Vehicles can change lanes.

The two-state model is able to reproduce a number of traffic phenomena, including the following:

- The formation of traffic jams.
- The propagation of traffic waves.
- The effects of traffic control measures.

The two-state model is a valuable tool for understanding and modeling traffic flow [46]. It is more complex than the KKW model, but it is able to reproduce a wider range of traffic phenomena.

1. Deterministic speed update (for a time step Δt = 1 s):

$$v'_{det} = min(v + a, v_{max}, d_{anti}) \tag{II.3}$$

2. Stochastic deceleration:

$$v' = \begin{cases} max(v'_{det} - b_{rand}, 0) & \text{with probability p} \\ v'_{det} & \text{otherwise} \end{cases} \tag{II.4}$$

3. Determination of stop time t_{st}:

$$t_{st} = \begin{cases} t_{st} + 1 & \text{if } v = 0 \\ 0 & \text{otherwise} \end{cases} \tag{II.5}$$

4. Position update:

$$x' = x + v' \tag{II.6}$$

In the given context, the variables and parameters have the following meanings:

- v and x represent the speeds and positions at the current time step, respectively.
- v' and x' represent the speeds and positions at the next time step, respectively.
- $d_{anti} = d + \max(v_{anti} - g_{safety}, 0)$ is the anticipated space gap, where d is the real space gap ($d = x_l - x - L_{veh}$), L_{veh} is the length of the vehicle, and x_l is the position of the leading vehicle.

- $v_{anti} = \min(d_l, v_l + a, v_{max})$ is the expected speed of the preceding vehicle in the next time step, where d_l is the distance to the leading vehicle, v_l is the speed of the leading vehicle, a is the maximum acceleration, and v_{max} is the maximum speed.

- g_{safety} is a safety parameter used to prevent accidents, and it should satisfy the constraint $g_{safety} \geq b_{rand}$.

The randomization probability is denoted as p, and the randomization deceleration is denoted as b_{rand}:

$$p = \begin{cases} p_b & \text{if } v = 0 \textit{ and } t_{st} > t_c \\ p_c & \text{else if } v \leqslant d_{anti}/T \\ p_a & \text{otherwise} \end{cases} \tag{II.7}$$

$$b_{rand} = \begin{cases} a & \text{if } v \leqslant d_{anti}/T \\ b_{defense} & \text{otherwise} \end{cases} \tag{II.8}$$

In the given model, the effective safe time gap is denoted as T. The stopped time of vehicles is represented by tst. The Two-state model incorporates two driver states: a defensive state and a normal state. The defensive state is activated when the condition $v > d_{anti}/T$ is met, indicating that the vehicle is maintaining a speed greater than the ratio of the anticipated space gap (danti) to the effective safe time gap (T). Otherwise, the drivers are assumed to be in the normal driving state.

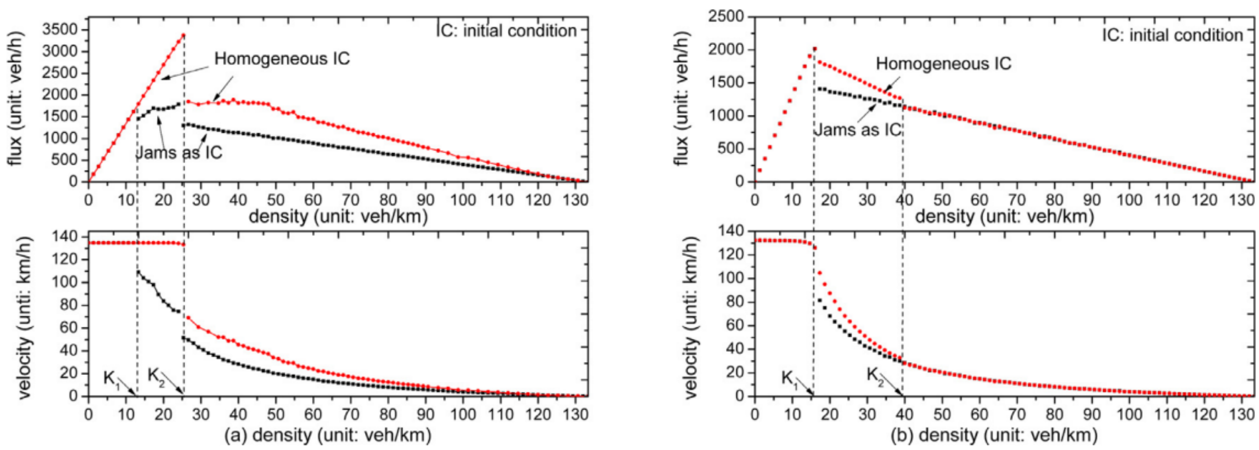

FIGURE II.9: The flow-density and speed-density diagrams show the results of simulations using two versions of the Two-state model: (a) with a cell length of 0.5 meters and (b) with the default cell length of 7.5 meters. In the diagrams, "Homogeneous IC" refers to the initial condition where the traffic distribution is initially homogeneous, while "Jams as IC" refers to the initial condition where the traffic distribution is initially in a mega-jam state.

B) Two-state safe-speed (TSM) model

To enhance the realism of the Two-state model and address intrinsic large fluctuations, certain modifications are introduced. In accordance with a previous study [47], two new variables are incorporated: the safe speed v_{safe} and the logistic function for the randomization probability $p_{defense}$. These additions aim to mitigate large decelerations and fluctuations within the model. The variables are defined as follows:

$$v_{safe} = [-b_{max} + \sqrt{b_{max}^2 + v_l^2 + 2b_{max}d}] \tag{II.9}$$

$$p_{defense} = p_c + \frac{p_a}{1 + e^{\alpha(v_c - v)}} \tag{II.10}$$

The logistic function introduced in the model includes parameters a (steepness) and v_c (midpoint). The round function, denoted as $[x]$, returns the integer closest to the value of x. The safe speed v_{safe} accounts for kinematic limitations by considering the maximum permissible speed of a vehicle based on its space gap d and the speed v_l of the preceding car.

1. Deterministic speed update (for a time step Δt = 1 s):

$$v'_{det} = min(v + a, v_{max}, d_{anti}, v_{safe}) \tag{II.11}$$

2. Stochastic deceleration:

$$v' = \begin{cases} max(v'_{det} - b_{rand}, 0) & \text{with probability p} \\ v'_{det} & \text{otherwise} \end{cases} \tag{II.12}$$

3. Position update:

$$x' = x + v' \tag{II.13}$$

where the randomization deceleration b_{rand} is defined by :

$$b_{rand} = \begin{cases} a & \text{if } v < b_{defense} + \lfloor d_{anti}/T \rfloor \\ b_{defense} & \text{otherwise} \end{cases} \tag{II.14}$$

while the randomization probability p is redefined as:

$$p = \begin{cases} p_b & \text{if } v = 0 \\ p_c & \text{else if } v \leqslant d_{anti}/T \\ p_{defense} & \text{otherwise} \end{cases} \tag{II.15}$$

In the Two-state model (TSM), the floor function denoted as $\lfloor x \rfloor$ returns the largest integer less than or equal to x. Unlike the KKW (Krauss-Kühne-Weidlich) model, the TSM incorporates a behavioral change when the anticipated time gap, represented as d_{anti}/v, falls at or below the threshold value T, rather than a specific range of indifference for the gaps. Additionally, the TSM introduces a safe speed that limits the braking deceleration in all normal scenarios.

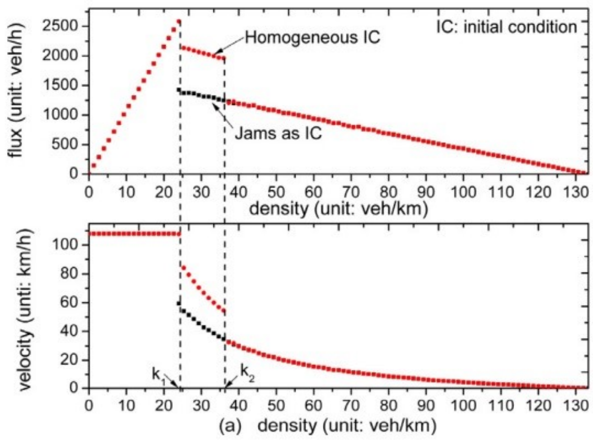

FIGURE II.10: The flow-density and speed-density diagrams obtained from simulations of the Two-state model (TSM) on a ring road illustrate the average flow (or speed) of traffic as a function of the overall density. The upper branch, observed between densities K_1 and K_2, represents a coexistence of free-flowing traffic and synchronized flow. On the other hand, the lower branch, observed at densities above K_1, represents a coexistence of free-flowing traffic and congested areas (jams).

II.3.4.3 Modified NaSch (mNaSch) model

Modified NaSch (mNaSch) model [48], is a model which considers a real acceleration and deceleration of vehicles. Where The vehicles are described by two parameters namely the position x_i and speed v_i at the time t. The updated of position and speed of each vehicle can be as follow:

$$v_i(t+1) = \begin{cases} v_i(t)+1 & \text{if } v_i(t)+1 \leqslant \varphi(v_{i+1}(t), g_i(t)) \; and \; rand() \leqslant P \\ v_i(t) & \text{if } v_i(t)+1 \leqslant \varphi(v_{i+1}(t), g_i(t)) \; and \; rand() \geqslant P \\ \varphi(v_{i+1}(t), g_i(t)) & \text{otherwise} \end{cases} \tag{II.16}$$

v_{i+1} represents the speed of the vehicle located in front of vehicle i at time t. The empty space between vehicle i and $i+1$ is denoted as $g_i(t)$, which is calculated as the difference in positions: $g_i(t) = x_{i+1} - x_i - 1$. The variable P represents the randomization probability, which can be interpreted as the likelihood of random acceleration.

$\varphi(v_{i+1}(t), g_i(t))$ is a function that takes into account both the speed of the vehicle $i+1$ and the empty space $g_i(t)$ between vehicle i and $i+1$ at time t. This function captures the anticipation behavior of the vehicles, considering both the speed and the distance from the leading vehicles where:

$$\varphi(v_{i+1}(t), g_i(t)) = min\{\lfloor \frac{1}{2}\sqrt{8g_i(t) - 7 + 4v_{i+1}(t)(v_{i+1}(t) - 1)} - \frac{1}{2}\rfloor, v_{max}\} \tag{II.17}$$

here, the floor function $\lfloor , \rfloor$ is used to round down a value to the nearest integer. The variable $g_i(t)$ represents the distance between vehicle i and vehicle $i+1$ at time t. The maximum allowed speed is denoted by v_{max}, and it is constrained to integer values.

II.3.5 Limitations

Like any other model, the cellular automata model for single lane traffic has its limitations, which are outlined below.

- A single-lane model in cellular automaton is not suitable for realistic traffic scenarios as it assumes homogeneous traffic, where all vehicles are assumed to have identical characteristics including size, speed, and acceleration. However, in real-world traffic, there is a diverse mix of vehicles such as cars, trucks, and buses, each with their own unique characteristics and behavior.

- Moreover, this model also does not take into account external factors such as weather conditions, traffic signals, and road infrastructure, which can significantly affect traffic flow. In real-world scenarios, these factors play a crucial role in determining the traffic condition.

- A single-lane traffic model may not accurately represent the complex dynamics of real-world traffic. In reality, there may be multiple lanes.

So, two-lane models have been introduced to meet some requirements, which could be related to traffic flow, safety, or efficiency. Additionally, three rules have been added to allow for the exchange of vehicles between the lanes.

II.3.6 Extensions of the NaSch model in a two-lane

II.3.6.1 Left- and right-hand traffic

Left-hand traffic **(LHT)** and right-hand traffic **(RHT)** are the two primary practices for traffic flow in bidirectional traffic (See Figure II.11). In left-hand traffic, vehicles keep to the left side of the road, while in right-hand traffic, vehicles keep to the right side of the road.

FIGURE II.11: Left and right-hand traffic

These practices help ensure consistency and orderliness in traffic movement, particularly in countries where there are no specific rules or regulations dictating which side to drive on [58].

The choice between left-hand traffic and right-hand traffic is largely influenced by historical, cultural, and practical factors. Different countries and regions around the world have adopted one of the two practices, and it generally remains consistent within a particular country or region.

In left-hand traffic countries, drivers typically sit on the right side of the vehicle and drive on the left side of the road. This practice is prevalent in countries like the United Kingdom, Australia, India, Japan, and several others. On the other hand, in right-hand traffic countries, drivers sit on the left side of the vehicle and drive on the right side of the road. This is the dominant practice in countries like the United States, Canada, most of Europe, and many others.

Right-hand traffic **(RHT)** is indeed prevalent in the majority of countries and territories worldwide. Approximately 165 countries and territories drive on the right side of the road, including the United States, Canada, most of Europe, China, and many others. **RHT** is the dominant practice in terms of the number of countries and territories that follow it. While left-hand traffic **(LHT)** is indeed used in approximately 72 countries and territories. Some notable examples include the United Kingdom, Australia, India, Japan, South Africa, and several countries in the Caribbean. **LHT** is followed in these countries, where vehicles drive on the left side of the road, and the driver's seat is typically on the right side of the vehicle [59].

II.3.6.2 Lane changing

The introduction of lane changing in traffic models was indeed a response to the limitations of the single lane model in representing realistic traffic conditions. In reality, traffic consists of vehicles with different desired velocities, sizes, and characteristics, which can lead to variations in speeds and behaviors among drivers.

The single-lane model assumes a homogeneous traffic flow, where all vehicles travel at the same speed and maintain a constant distance between each other. While this model can provide a simplified understanding of traffic behavior, it fails to capture the complexities and dynamics of real-world traffic scenarios.

In reality, drivers have different desired velocities based on factors such as vehicle type, road conditions, and personal preferences. This variation in desired velocities can lead to differences in driving speeds, resulting in the need for lane changing. Lane changing allows vehicles to adjust their position on the road to match their desired velocity or to overtake slower vehicles.

In the generic two-lane model, two parallel single-lane models are combined to represent a road with two lanes of traffic. The periodic boundary conditions imply that the ends of the road are connected in a way that allows vehicles to continue their motion from one end to the other seamlessly.

Each single-lane in the two-lane model operates based on the principles of the single-lane model, where vehicles travel at a homogeneous speed and maintain a constant distance between each other. However, the introduction of two lanes allows for lane changing maneuvers, which simulate vehicles moving between lanes to adjust their position or overtake slower vehicles.
Lane changing in the two-lane model can be governed by various rules or algorithms, these rules determine when and how vehicles change lanes based on factors like desired velocity, distance to other vehicles, and available gaps in the adjacent lane.

II.3.6.3 STCA models of two lane traffic

The model formulated by Nagatani (reference [62]) for two-lane traffic is indeed an oversimplified model that makes certain assumptions to simplify the analysis. One of the assumptions in this model is that the maximum allowable speed of each vehicle is identical.

By assuming that all vehicles have the same maximum allowable speed, the model neglects the natural variations in desired velocities among different types of vehicles or individual drivers. In reality, vehicles on the road can have different speed limits, performance capabilities, or driver preferences, which can result in variations in their maximum speeds. However, it's important to note that this assumption may not accurately represent real-world traffic conditions, where vehicles with different maximum speeds coexist. In practice, speed limits, vehicle types, and driver behaviors can significantly influence the flow and interactions in a multi-lane traffic scenario.

While oversimplified models like Nagatani's provide valuable insights and serve as a starting point for understanding basic traffic behavior, more sophisticated models that account for variations in maximum speeds and desired velocities are often used for comprehensive traffic studies and simulations. These models consider the heterogeneity of vehicles and drivers, allowing for a more accurate representation of real-world traffic dynamics. Some of the notations that will be used in this thesis to mark the lane gaps are as follows:

- g_i = gaps in front of i_{th} vehicle in its present lane.
- g_{other} = gaps in front of i_{th} vehicle in other lane.
- g_{back} = gap in the other lane behind the site.

At each time step, the states of the vehicles are changed in two steps in all of the two-lane models discussed in this section, as well as all of those suggested in the following sections: First, all of the vehicles are assumed in parallel for lane changing based on various specified rules, and then, after parallel application of the exploration's findings, all of the vehicles are moved in parallel at their respective lanes.
For forward movement through a lane, all of these models use the NS algorithm except for the rule controlling the changes of lanes. Every set of rules for changing lanes is made up of two parts. A motive or a trigger condition ("Do I wish to change lane?") and a safety condition ("Is changing-lane safe?"). The lane is changed only if both questions are answered.
While the safety condition for all the rules considered in the literature are quite similar, and only relate to the conditions of the targeted lane, The proposed triggers differ significantly, and in most cases, they are dependent on both lanes.

The two-lane is controlled by lane-changing rules, where these rules can be **symmetric** or **asymmetric** with respect to lanes or the types of vehicles.

A) The symmetric lane changing rules

In the **symmetric** rules for lane changing in the two-lane model suggested by Rickert et al. [63]:

1. Lane Selection:

   - Each vehicle determines whether to change lanes based on its desired velocity and the velocities of the vehicles in both lanes. The decision is made to maximize progress towards the desired velocity while maintaining safety.

2. Gap Evaluation:

   - If there is not enough gap in the current lane in front of the vehicle, it considers changing lanes. The vehicle evaluates the gap in the target lane in front of it to determine if it is adequate for lane changing. The adequacy of the gap is determined based on predefined criteria, such as minimum distance or time headway.

3. Collision Avoidance:

   - Before initiating a lane change, the vehicle checks if the lane change can be performed without collision. It ensures that there are no vehicles occupying the space it intends to move into in the target lane. Blocking Avoidance:

     The vehicle also verifies that its lane change will not block the path of other vehicles. It ensures that the lane changing activity will not hinder the movement of other vehicles in either lane.

4. Lane Change Probability:

   - If all the above conditions are met, the vehicle decides to change lanes with a certain probability, denoted as "ch". The probability allows for stochastic behavior in lane changing decisions.

5. Lane Change Process:

   - If the vehicle decides to change lanes, it initiates the lane change process gradually, adjusting its position towards the target lane. The lateral movement is controlled to avoid collisions with neighboring vehicles. The lane change is completed when the vehicle reaches the desired lane.

These rules incorporate the considerations of gap adequacy, collision avoidance, blocking avoidance, and a probabilistic decision-making process for lane changing, ensuring that the lane changing activity is performed safely and does not impede the movement of other vehicles.

The above statements are rules derived from the following equations. II.21 to II.20

- Incentive criterion:

$$g_i < min(v_i + 1, v_{max}) \tag{II.18}$$

- Safety criterion:

$$g_{other} > g_i \tag{II.19}$$

$$g_{back} \geq v_{max} \tag{II.20}$$

The rules II.21 and II.32 and II.20 are referred to as the trigger criteria and the safety criterion, respectively. These guidelines apply to lane changes from the left to the right as well as from the right to the left, and they change the lane with probability *ch*.

Numerical Example

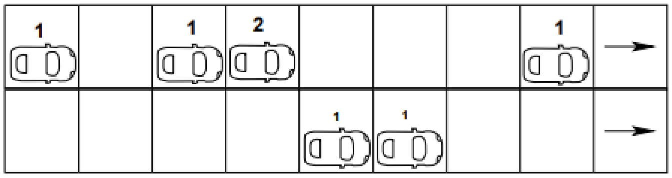

FIGURE II.12: Sketch of a road segment before applying changing lane rules

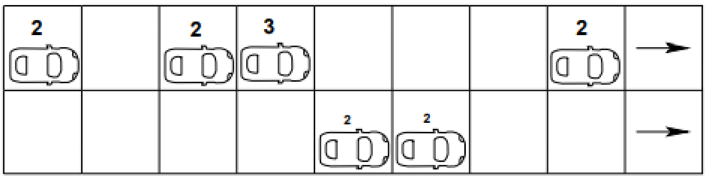

FIGURE II.13: Sketch of a road segment after applying changing lane rules

Consider a two-lane road that has nine cells in each lane. Vehicles are positioned in the first (1), third (1), fourth (2), and eight (1) cells in the first lane, and the fifth (1) and sixth (1) cells in the second lane. The velocities of the different vehicles are indicated by the numbers in the brackets.(See Figures(II.12,II.13).)

The solution begins with the acceleration stage of the vehicles, when the acceleration rule $(v_i = min(v_i + 1), v_{max})$ is applied to the vehicles, every vehicle with a velocity below the maximum velocity has increases by one unit. As a result, the stage of the vehicles following acceleration is depicted in Fig. II.13. Lane changing is necessary for $lane1(1), lane1(2)$ and $lane2(1))$. Here "$lane1(1)$" denotes a number in the subscript as its lane number and the superscript as its vehicle number in the corresponding lanes.

✓ Rule 1 : ($g_i < v_i + 1$)

- The first vehicle's velocity is two, and the gap ahead of it in its current lane is also two. According to the rule ($v_i + 1 > g_i$), the vehicle satisfies the rule and can change lanes. $lane1(1) = (2 < 2+1)$ is satisfied. Similarly, checking for all the other vehicles: $lane1(2) = (1 < 2+1)$ ... satisfied, $lane2(1) = (1 < 2+1)$ ... satisfied.
  g_i) is commonly defined in two different ways. One interpretation is the distance between the bumper-to-bumper of the vehicles. The other interpretation is the number of empty cells in front of a vehicle. In this discussion, we are using the first interpretation, but it ultimately depends on the reader's preference. A slight modification can be made by adding 1 to the other side of the equations.

✓ Rule 2 : ($g_{other} > v_i + 1$)

- The first vehicle has a velocity of two, and the gap in the target lane ahead of it is four. Therefore, the rule (gap in target lane > velocity + one) is satisfied for the first vehicle. $lane1(1) = (4 > 2+1)$ is satisfied. Similarly, when checking the other vehicles, we obtain the following results: $lane1(2) = (2 \ngtr 2+1)$ is rejected, and $lane2(1) = (34 \ngtr 2+1)$ is rejected.

✓ Rule 3 :

- According to the provided pattern, there are no observed collisions between vehicles.

✓ Rule 4 : ($g_{back} > v_{max}$)

- The maximum velocity allowed for any vehicle is four, and the gap behind the first vehicle in the target lane is five, which is greater than the maximum velocity. Therefore, the vehicle satisfies the rule and is eligible for a lane change. $L_1(1) = (5 > 4)$. Consequently, the first vehicle in the first lane satisfies all four rules.

Rickert and coworkers suggested the following criteria:

- Incentive criterion:

$$g_i < min(v_i + 1, v_{max}) \tag{II.21}$$

- Safety criterion:

$$g_{other} > g_i \tag{II.22}$$

$$g_{back} \geq v_{max} \tag{II.23}$$

Additionally, as stated by Wagner [64], the safety criterion is symmetric, similar to the one proposed by Rickert et al. However, there is a difference in the trigger conditions for changing lanes from right ($lane1$) to left ($lane2$) and vice versa.

$(a : R \longrightarrow L)\, g_i < v_{max} + 1$, and

$(b : R \longrightarrow L)\, g_{other} > g_i$, whereas

$(a : L \longrightarrow R)\, g_i > v_i + 1 + v_{off}$,and

$(b : L \longrightarrow R)\, g_{other} > v_i + 1 + v_{off}$.

v_{off}. is a parameter which delays the return to the right lane.

In the context of multilane traffic, there is a specific focus on studying systems that involve various types of vehicles and incorporate asymmetric lane-changing rules. This concept was initially introduced by Rickert et al. In their proposed cellular automaton (CA) models, the update process occurs in two steps.

1. During the first step, vehicles undergo lane changes based on a probability value, denoted as ch. The lane-changing probability is determined by both the vehicle type (slow or fast) and the lane itself. Specifically, ch^f_{lane1} and ch^f_{lane2} represent the probability of lane change for fast vehicles from lane 1 to lane 2 and from lane 2 to lane 1, respectively. Similarly, ch^s_{lane1} and ch^s_{lane2} represent the probability of lane change for slow vehicles in the corresponding directions.

2. In the second step, the vehicles proceed straight ahead based on the NaSch rules [39]. Additionally, each vehicle has the opportunity to perform a lane-change manoeuver if certain conditions are satisfied:

   - Incentive condition: The condition states that a vehicle cannot reach its desired speed due to insufficient space in its current lane, expressed as $g_i < v_{hope}$.
   - Improvement condition: This condition indicates that the available free space ahead of a vehicle in the other lane of the road is greater than the free space in its current lane, denoted as $g_{other} > g_i$.

- Safety condition: Before changing lanes, a vehicle must ensure that the available free space behind it, denoted as g_{back}, is greater than or equal to the maximum velocity of either a fast vehicle, v^f_{max}, or a slow vehicle, v^s_{max}. This condition ensures that the vehicle does not disrupt the flow of incoming vehicles in the other lane during the lane-change maneuver.

In this scenario, the desired speed of vehicle i is determined as $v_{hope} = min(v_i + 1, v^{(fors)}_{max})$, where $v^{(fors)}_{max}$ represents the maximum allowable speed.

The terms g_{other} and g_{back} refer to the number of empty cells in front of vehicle i and its two neighboring vehicles in the other lane at time t, respectively. (Refer to Figure II.14 for visualization.)

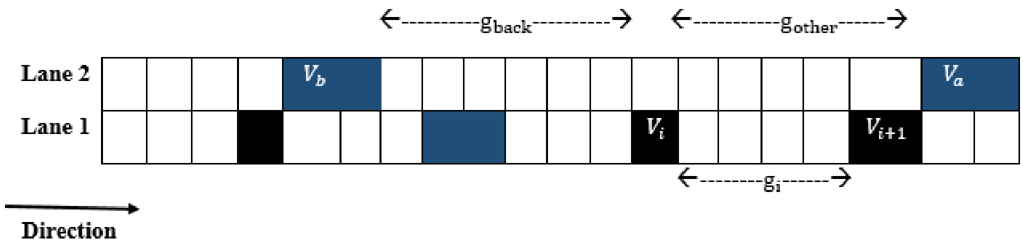

FIGURE II.14: The road model sketch showcases various variables associated with vehicle i traveling at speed v_i in lane1. Fast vehicles are depicted in black, while slow vehicles are represented by the color blue.

In the given context, the variables are defined as follows:

- v_i represents the speed of vehicle i.
- x_i indicates the position of vehicle i.
- g_i represents the available free space in front of vehicle i. This is calculated as the difference between the position of the next vehicle, x_{i+1}, and the current vehicle's position, x_i, minus the length of the next vehicle, denoted as l^{i+1}_{fors}. For fast vehicles, l_f is equal to 1, while for slow vehicles, l_s is equal to 2.
- p denotes the probability of randomization.
- $v^{(fors)}_{max}$ represents the maximum allowable speed for either fast or slow vehicles.

B) The asymmetric lane changing rules

The rules governing the update of vehicle states in the asymmetric model differ based on the characteristics of the vehicles (specifically, vehicles with different maximum velocities, denoted as v^f_{max} for fast vehicles and v^s_{max} for slow vehicles) as well as the lanes. The rules for changing lanes from the left lane to the right lane differ from those for changing lanes from the right lane to the left lane. In this context, the left and right lanes are referred to as the fast and slow lanes respectively. It should be noted that, in the case of asymmetric lane-changing rules, overtaking is prohibited in one lane, such as the right lane in many European countries. The asymmetric rules can be divided into two parts:

1. The rules for a slow vehicle changing lanes from the right lane to the left lane remain the same as in the symmetric model mentioned earlier. However, for a fast vehicle to change lanes from the right lane to the left lane, the probability of lane change is determined by the variable *ch*.

   (i) Incentive criterion:

   (a) In situations where the vehicle immediately ahead in the current lane is a fast vehicle

   $$g_i < min(v_i + 1, v_{max}) \tag{II.24}$$

   (b) In cases where the vehicle directly in front in the current lane is a slow vehicle

   $$g_i < v^f_{max} \tag{II.25}$$

   (ii) Safety criterion:

   $$g_{other} > g_i \tag{II.26}$$

   $$g_{back} > v_{max} \tag{II.27}$$

2. The rules for changing lanes from the left lane to the right lane for slow vehicles are as follows:

   (i) Incentive criterion:

   $$g_{other} > v_i \tag{II.28}$$

   (ii) Safety criterion:

   $$g_{back} > v_{max} \tag{II.29}$$

   For the fast vehicles:

   (i) Incentive criterion:

   (a) In situations where the preceding vehicle in the target lane is a fast vehicle.

   $$g_{other} > v_i \tag{II.30}$$

(b) When the vehicle immediately ahead in the target lane is a slow vehicle.

$$g_{other} > v^{f}_{max} \tag{II.31}$$

(ii) Incentive criterion:

$$g_{back} > v_{max} \tag{II.32}$$

II.4 Simulation method

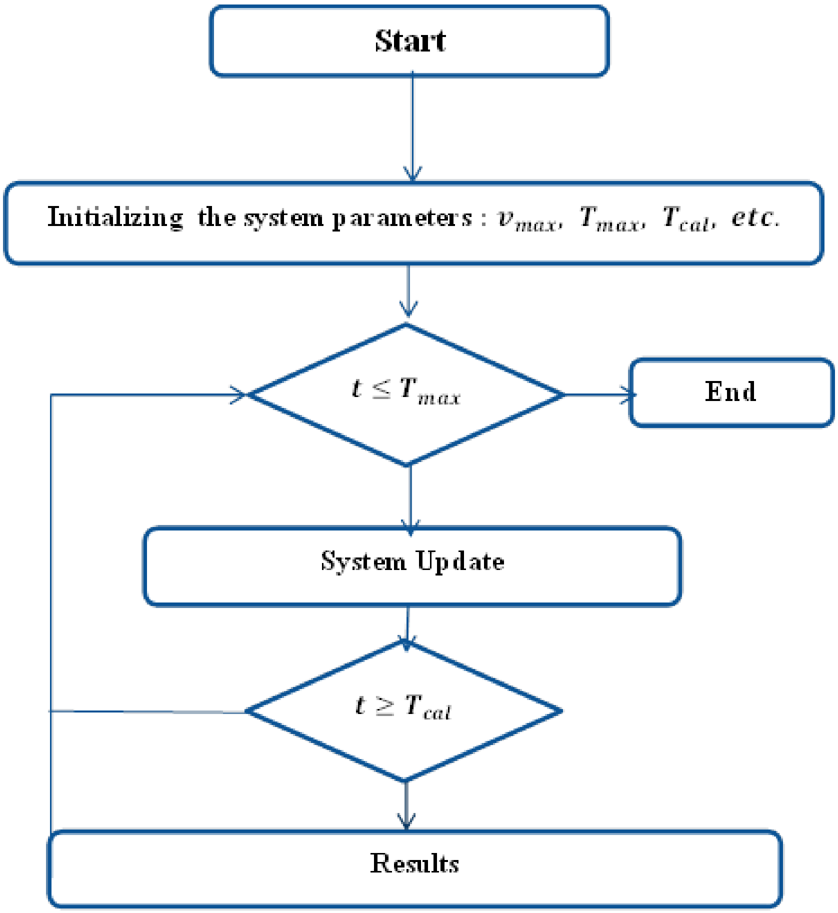

FIGURE II.15: Monte Carlo steps.

In this thesis, the Monte Carlo method was employed as an effective and versatile approach to numerically solve complex problems. The term "Monte Carlo" was coined by scientists Stanislaw Ulam, John von Neumann, and Nicholas Metropolis in the late 1940s, when they utilized this method to address particle transport problems in nuclear weapons research [65].

The calculation process relies on generating a sequence of random numbers that adhere to statistical laws, enabling the simulation of the desired process. This approach is referred to as stochastic, as the precise outcome of the simulation slightly varies when the procedure is repeated with a different sequence of random numbers. The results exhibit a random distribution and are characterized by a statistical mean value and an associated standard deviation. This is distinct from deterministic calculations, where the outcome remains consistent for the same set of input parameters.

In the following section, we provide a brief overview of the method employed to calculate road traffic variables.

1) In each simulation, we first choose the Monte Carlo time T_{max} (number of iterations) and the time after which the calculation will perform T_{cal}. The latter presents the stationary state.

2) Initially, the vehicles are randomly positioned on the road in accordance with the desired density, which represents the number of vehicles present.

3) We apply the rules of the chosen model on each vehicle in each iteration (t). In this thesis, the basic model is the NaSch model in two lanes plus other rules that depend on the shape of the road (intersection, limited speed zone, bottleneck). These rules lead to a new configuration.

4) If the current iteration is in the stationary state $(t > T_{cal})$ the calculation of the variables is performed.

5) We apply the rules of the model again until iteration $t = T_{max}$.

A very important aspect of road traffic in many modelling approaches are **fundamental diagram, satisfaction rate, energy dissipation, emissions** and **the occurrence of accidents**.

II.5 Energy of Dissipation

The issue of traffic congestion, and the energy dissipation caused by traffic have become increasingly significant in modern society. According to Ref. [66], over 20% of fuel consumption and air pollution can be attributed to the interruptions and "stop-and-go" traffic. Recent studies have focused on investigating energy dissipation in traffic systems using car-following and city traffic models, resulting in valuable findings [67, 70].

However, it is worth noting that the relationships between energy dissipation and factors such as speed limits, stochastic noise, and stop-and-go vehicles have not been explored yet. These factors can be incorporated rapidly into cellular automata (CA) models and should be further examined using statistical physics approaches.

To assess the impact of vehicles, we adopt energy dissipation as a measure of the dissipated kinetic energy. The kinetic energy of a vehicle is given by $\frac{mv^2}{2}$, where m and v represent the mass and speed of the vehicle, respectively. For the purpose of this study, we disregard other forms of dissipation, such as rolling and air drag, and focus solely on the dissipation occurring during deceleration. Energy dissipation is defined as the difference between the initial and final kinetic energy of a vehicle, as follows:

$$E_d(t) = \begin{cases} 0, & \text{if } (v_i(t+1) \geq v_i(t)) \\ \frac{m}{2}[v_i^2(t) - v_i^2(t+1)], & \text{if } (v_i(t+1) < v_i(t)) \end{cases} \tag{II.33}$$

Here, $v_i(t+1)$ and $v_i(t)$ refer to the speeds of the ith vehicle at time $t+1$ and time t, respectively.

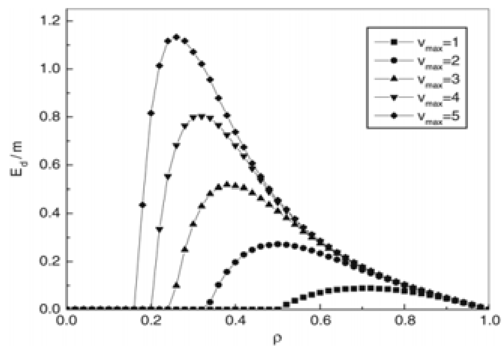

FIGURE II.16: The energy dissipation rate E_d (normalized by the mass m) is examined in relation to the car density ρ within the deterministic NS model, considering different speed limit values v_{max}.

Wei Zhang et al. conducted a study to examine the impact of the speed limit v_{max} on energy dissipation within the deterministic NS model. Their investigation focused on the deterministic case, disregarding stochastic braking (i.e., $p = 0$). Figure II.16 illustrates the relationship between the energy dissipation rate E_d and the car density ρ for different values of the speed limit v_{max}.

As depicted in Figure II.16, a critical density $\rho_c = v_{max}/(v_{max}+1)$ is observed, indicating the threshold at which energy dissipation occurs. Below this critical density, no energy

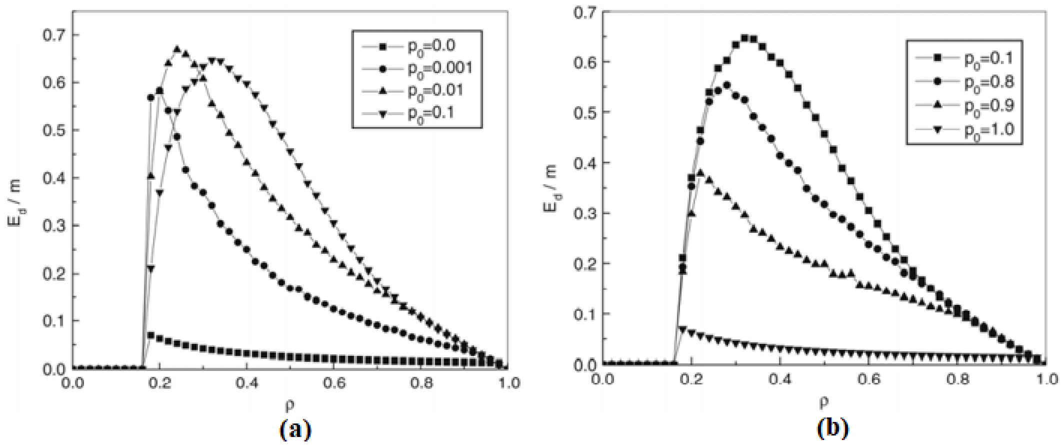

FIGURE II.17: The energy dissipation rate E_d (normalized by the mass m) is investigated in the deterministic NS model, considering its dependence on the vehicle density ρ. Specifically, the analysis is conducted for two scenarios: (a) The case of a fixed speed limit, $v_{max} = 5$, (b) Various values of the probability p_0, while keeping other parameters constant.

dissipation is present, as all vehicles move at the maximum velocity v_{max} without any instances of braking. This region represents the free-flowing dynamical phase. Moreover, the critical density shifts towards lower density regions as the speed limit increases. When $\rho > \rho_c$, the energy dissipation rate E_d initially increases with density ρ until it reaches a maximum value, after which it starts to decrease. This region corresponds to the jammed phase. The maximum value and the corresponding density at which it occurs are influenced by the speed limit. In the density range between the free-flowing and jammed phases, the energy dissipation rate increases with the speed limit. However, in the high density region, where most vehicles are stationary and the maximum speed is limited to 1, the speed limit has no influence on energy dissipation.

Additionally, Figure II.17(a) and (b) display the relationship between the energy dissipation rate E_d and the car density, considering various values of the stochastic braking probability p_0, while maintaining $v_{max} = 5$. The results were obtained by averaging over 100 different random seeds and simulating $10,000$ time steps after discarding the initial $20,000$ time steps. These figures demonstrate that the stochastic braking probability p_0 significantly affects the energy dissipation rate E_d above the critical density ρ_c, but does not influence ρ_c itself. When p_0 is small, E_d increases within the density range $0.32 < \rho < 1.0$. However, when p_0 is large, E_d decreases within the density range $\rho_c < \rho < 1.0$, as depicted in Figure II.17(a) and (b) respectively. Near the critical density, E_d exhibits a sharp increase when p_0 transitions from zero to a nonzero value, but further increases in p_0 do not result in a higher energy dissipation rate.

II.6 Satisfaction rate

Traffic is influenced by many natural, environmental and human factors. In many cases, a non-uniform distribution of speed has been considered [71, 73] , in this sense, studies on the formation of variability and the resulting distribution have been made [74, 75]. According to these studies, which for us constitute scientific references, our attention will not be focused on the distribution of real speed, but on the heterogeneity of drivers, which in turn leads to a kind of speed distribution. As road or weather conditions change regularly, the distribution of the desired speed also changes. This change affects not only the actual speeds but also the traffic. The effect of lane changes on traffic has been modelled and analyzed, demonstrating that voids caused by such a change can reduce traffic flow. Furthermore, under realistic conditions where all vehicles are travelling at the same speed, lane changing is essential to maintain the flow. If there is no opportunity for lane changing, the slower vehicle dominates the speed while pushing all other vehicles in the lane to reduce theirs. In addition, empirical studies on the distribution of desired speeds have been carried out [76], for which Lipshtat has proposed a model that consists of a single and/or multi-lane motorway.

In this thesis, the satisfaction rate is employed as a measure to evaluate the condition of vehicles, whether they are able to move at their desired speed or if they experience hindrance due to other vehicles. The satisfaction rate is defined as follows:

$$\mu = \frac{v_{max}^{(sorf)}}{v_{max}^{(sorf)}} \tag{II.34}$$

Additionally, we will utilize the percentage of satisfied vehicles ($\%\eta$) to assess the proportion of vehicles with $\mu = 1$. Here, $v_{max}^{(sorf)}$ represents the actual speed of vehicle i and the desired speed (i.e., the maximum speed), respectively. It is important to note that $v_{max}^{(sorf)}$ corresponds to the vehicle's speed under ideal conditions, where vehicles can move freely without any hindrance. When the average satisfaction rate $<\mu>$ equals 1, it implies an ideal flow where all vehicles are able to drive at their desired speeds. Lower values of $<\mu>$ indicate reduced traffic flow in the system, resulting in slower vehicle movements. Hence, $<\mu>$ serves as an alternative measure to quantify the traffic state. Furthermore, we define the standard deviation as follows:

$$C_v = \mu \times v_i^{(sorf)}. \tag{II.35}$$

II.6.1 Effect of traffic heterogeneity on the satisfaction rate

The wide distribution of desired speeds is accompanied by great variability in the actual speed and as long as the actual speed is greater, this results in many slow vehicles forcing those behind to drive slower. On the other hand, the satisfaction rate on the roads is drastically reduced. Furthermore, and in only one lane, there is no possibility of avoiding slow vehicles, so μ decreases rapidly according to C_v. This decrease does not depend on the average speed $v_i^{(sorf)}$ (Figure II.18).

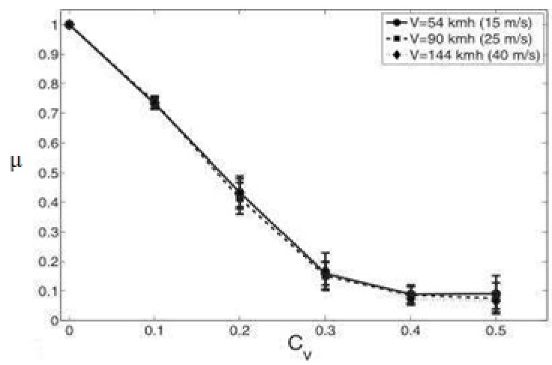

FIGURE II.18: Satisfaction as a function of the coefficient of variance: effect of the coefficient of variance in the case of a single lane with a mixture of vehicles.

II.6.2 Effect of multi-lane highway on the satisfaction rate

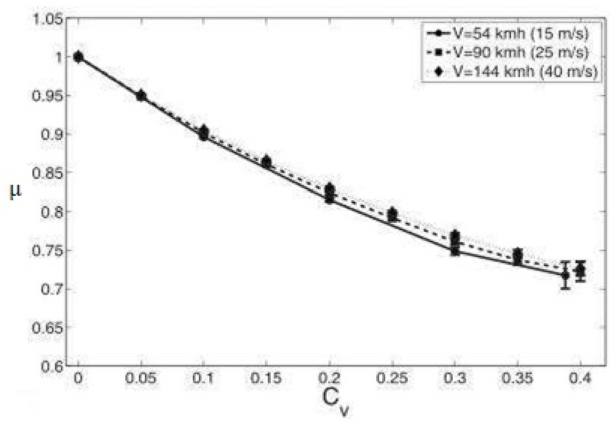

FIGURE II.19: The satisfaction rate as a function of the coefficient of variance. On a five-lane motorway, overtaking and changing lanes allows the traffic flow to be smooth [76].

The presence of multiple lanes, which enables overtaking, has a significant positive impact on traffic flow. However, a critical question arises: does this improvement depend on the speed distribution or the average speed? Numerical simulations indicate that the width of the speed distribution plays a more crucial role than the absolute speeds themselves (see Figure II.19). Specifically, an increase in the coefficient of variation results in a decrease in traffic efficiency.

This phenomenon can be explained by two opposing effects. Firstly, a high variability in speeds leads to congestion due to slower vehicles, causing undesirable delays for faster vehicles. This congestion negatively affects traffic efficiency. On the other hand, the same speed variability creates larger gaps between successive vehicles, which makes lane changes more favorable. These larger gaps facilitate smoother and more efficient traffic flow.

(Note: The original text refers to "Figure II.19". However, as a text-based AI, I cannot see or refer to specific figures. Please make sure to refer to the appropriate figure in the document or provide a description of the figure for further paraphrasing.)

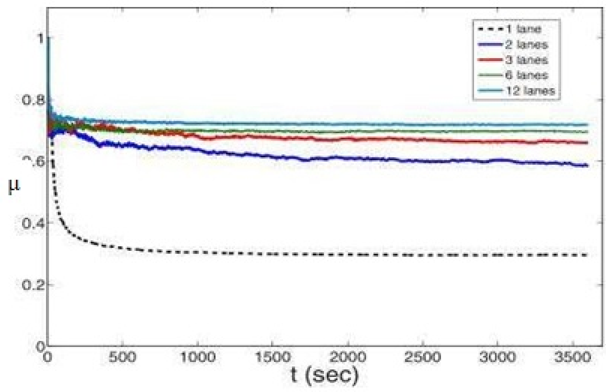

FIGURE II.20: The dotted line indicates a single lane, and the solids (from bottom to top) are lanes for 2, 3, 6 and 12. (Single simulation for each number of highway, $C_v = 0.25$) [76].

The satisfaction rate can be affected by the number of lanes. It can be assumed that several of these will result in efficient traffic flow, which is the case to some extent. In this respect, a significant improvement is observed by changing a single lane into two lanes. However, the contribution of any additional lanes is minor (Figure II.20). As long as the number of lanes increases, the satisfaction rate also increases.

II.7 Pollution from road traffic

II.7.1 Pollutants emitted by vehicles

Car traffic contributes to air pollution both through the direct emission of pollutants from vehicle use (primary pollutants) and through the derived or secondary pollutants formed after chemical reactions in the atmosphere from chemical species (known as precursors) emitted by vehicles (e.g. ozone and the secondary fraction of fine particles). Pollutants fall into two broad categories: particulate matter (emitted from the exhaust or from vehicle wear and tear, road surfaces, and resuspension), and gaseous pollutants (exhaust and fuel evaporation). Some exhaust pollutants may be semi-volatile and therefore present as both particles and gases.
More specifically, the pollutants emitted by vehicles on the road are mainly :

-**Carbon dioxide** (CO_2 , also known as carbon dioxide) which is emitted by the combustion of fossil fuels (tailpipe emissions). Carbon dioxide has no impact on public health (except at very high concentrations), but it does contribute to the greenhouse effect that leads to climate change.

- **Carbon monoxide** (CO) which results from incomplete combustion (exhaust emission). It slowly oxidises to carbon dioxide in the atmosphere with a lifetime of about one month. It is a well-known pollutant in terms of its harmful effect on health.

- **Nitrogen oxides** (NO_x), which are formed at high combustion temperatures by the recombination of nitrogen and oxygen in the air. They include nitric oxide (NO), which is in the majority, and nitrogen dioxide (NO_2). NO_x = NO + NO_2 ; the relative fractions of these two chemical species depend on the type of vehicle, the driving style and the pollution control system. The origin of these pollutants was 75% due to road traffic in 2005. Nitrogen oxides are involved in the formation of ozone, particulate matter, acid rain and nitrogen deposition. NO2 also has adverse health effects.
- **Ozone** (O_3) which is a secondary pollutant resulting from the reaction of nitrogen oxides and volatile organic compounds (VOC_s) under the effect of the sun (photochemistry). Ozone formation is a complex mechanism involving many chemical and climatic aspects (temperature, sunshine, etc.). Ozone is not a local pollutant because it is formed over the course of several hours. It reacts almost instantaneously with nitric oxide (NO) emitted by motor vehicles to form nitrogen dioxide (NO_2). Ozone is a pollutant of a rather regional. It is an oxidant that has adverse effects on health and vegetation; it is also a greenhouse gas.
- **Sulphur dioxide** (SO_2) is related to the sulphur content in diesel fuel and to a lesser extent

in petrol. It is emitted from the exhaust. For many years, diesel vehicles have contributed to SO_2 pollution, but decrees reducing the sulphur content of fuels have significantly reduced emissions from cars. SO_2 has adverse health effects and is also a sulphate precursor, which contributes to fine particle levels and acid rain.

- **Ammonia** (NH_3) which is emitted from the exhaust. It does not affect health, but it plays an active role in the neutralization of acids, in the formation of atmospheric particles, and in nitrogenous deposition on surface waters and soils. It should be noted that it is only marginally present in the transport sector; although pollution control technologies tend to increase its emission, its emissions are currently dominated by agriculture.

- **Nitrous oxide** (N_2O): A small proportion of nitrous oxide emissions is attributed to road traffic, particularly catalytic converters. It is one of the most important greenhouse gases contributing to global warming after water vapor (H_2O), carbon dioxide (CO_2) and methane (CH_4).

- **Particulate matter** (PM) comes from exhaust (mainly from diesel vehicles without particulate filters), non-exhaust emissions and resuspension. Exhaust fine particles are formed from solid carbonaceous cores to which other compounds are attached, such as unburnt semi-volatile hydrocarbons from oils and fuel, and oxidised and/or aromatic combustion products. Ultra-fine particles from the exhaust are formed from nucleation of sulphuric acid followed by condensation of semi-volatile products (sulphuric acid, organic compounds); they then coagulate with fine particles. It should be noted that a distinction should be made between particles with an aerodynamic diameter of less than 10 µm (PM_{10}) and those with a diameter of less than 2.5 µm ($PM_{2,5}$). In addition, particles contain toxic substances such as heavy metals, soot carbon and organic compounds.

- **Volatile Organic Compounds** (VOC_s), which result on the one hand (and mainly) from incomplete combustion and are found in the exhaust (especially when cold), and on the other hand from fuel evaporation. VOC emissions from evaporation represent about 9% compared to 91% from exhaust (André et al., 2012).

II.7.2 Emission model

There are various models that have been developed to estimate traffic emissions, including the PANIS (Prediction of Air Pollution from NOx and VOCs in an Urban Area) model. PANIS is a comprehensive model that simulates the emissions of nitrogen oxides (NOx) and volatile organic compounds (VOCs) from traffic in urban areas. The model takes into account factors such as vehicle fleet composition, driving patterns, and traffic congestion. It uses data on vehicle speeds, vehicle counts, and meteorological conditions to estimate emissions from different sources, such as on-road vehicles, non-road engines, and industrial sources. The PANIS model can be used to identify the most significant sources of air pollution, and to evaluate the effectiveness of different emission control strategies.

The global form of a function of emission rates is expressed by a different parameter (average speed, type, instantaneous acceleration, age and other properties of the vehicles). In this thesis we will consider the model proposed by panis et al that depends on the instantaneous acceleration and speed of vehicles and six coefficients.

$$e_i(t) = Max(e_0, f_1 + f_2 v_i(t) + f_3 v_i^2(t) + f_4 a_i(t) + f_5 a_i^2(t) + f_6 v_i(t) a_i(t)) \tag{II.36}$$

Where $v_i(t)$ and $a_i(t)$ are the speed and the acceleration of a ith vehicle at time t. e_0 present the specified minimum emission (g/s) for each type of vehicles and pollutant $(e_0 = 0)$, f_1 to f_6 are the specific constants of emission for each kind of vehicles and contaminated and each amount of emission varies according to whether the ith vehicle is in acceleration $(a \geq -0.5m/s^2)$ or deceleration $(a < -0.5m/s^2)$, and it given in detail in the table II.1:
Thus, the average emission rate is:

$$E_m = \frac{1}{T}\frac{1}{N}\sum_{t=t_0+1}^{t_0+T}\sum_{i=1}^{N} e_i(t) \tag{II.37}$$

Where N is the number of vehicles in the lane and t_0 is the relaxation time (i.e., taken as a long enough time for the system to reach a steady state).

II.8 Accidents

Road Accidents are a major economic, social and public health problem according to the World Health Organization (WHO 2015). According to the same reference, statistics show that every year, nearly 1.25 million people die in traffic accidents, and another 20 to 50 million are injured worldwide which results from the global growth in population (4% between 2010 and 2013) and the number of motor vehicles (16%). WHO and World Bank data show that, if left unchecked, the number of such injuries will increase dramatically by 2020, especially in countries experiencing rapid motorization.
Road Accidents cause 518 billion dollars in losses and cost countries between 1% and 3% of their GDP, more than they (some developing countries) receive in development aid [**?**].

TABLEAU II.1: Emission functions for the 2010 fleet of urban traffic

Pollutant	Vehicle type	e_0	f_1	f_2	f_3	f_4	f_5	f_6
CO_2	Petrol car	0	5.53 e -01	1.61 e-01	-2.89 e-03	2.66 e-01	5.11 e-01	1.83 e-01
	Diesel car	0	3.24e-01	8.59e-02	4.96e-03	-5.86e-02	4.48e-01	2.30e-01
	LPG car	0	6.00e-01	2.19e-01	-7.74e-03	3.57e-01	5.14e-01	1.70e-01
	HDV	0	1.52e+ 00	1.88e+ 00	-6.95e-02	4.71e+ 00	5.88e + 00	2.09e + 00
	Bus	0	9.04e-01	1.13e+ 00	-4.27e-02	2.81e+ 00	3.45e + 00	1.22e + 00
NO_x	Petrol car (a≥-0.5 m/^{2})	0	6.19e-04	8.00e-05	-4.03e-06	-4.13e-04	3.80e-04	1.77e-04
	Petrol car (a<-0.5 m/^{2})	0	2.17e-04	0.00e+ 00	0.00e+ 00	0.00e+ 00	0.00e+00	0.00e + 00
	Diesel car (a≥-0.5 m/s^2)	0	2.41e-03	-4.11e-04	6.73e-05	-3.07e-03	2.14e-03	1.50e-03
	Diesel car (a<-0.5 m/s^2)	0	1.68e-03	-6.62e-05	9.00e-06	2.50e-04	2.91e-04	1.20e-04
	LPG car (a≥-0.5 m/s^2)	0	8.92e-04	1.61e-05	-8.06e-07	-8.23e-05	7.60e-05	3.54e-05
	LPG car (a<-0.5 m/s^2)	0	3.43e-04	0.00e+ 00	0.00e + 00	0.00e+ 00	0.00e + 00	0.00e + 00
	HDV	0	3.56e-02	9.71e-03	-2.40e-04	3.26e-02	1.33e-02	1.15e-02
	Bus	0	2.36e-02	6.51e-03	-1.70e-04	2.17e-02	8.94e-03	7.57e-03
VOC	Petrol car (a≥-0.5 m/s^2)	0	4.47e-03	7.32e-07	-2.87e-08	-3.41e-06	4.94e-06	1.66e-06
	Petrol car (a<-0.5 m/s^2)	0	2.63e-03	0.00e+ 00	0.00e + 00	0.00e+ 00	0.00e + 00	0.00e + 00
	Diesel car (a≥-0.5 m/s^2)	0	9.22e-05	9.09e-06	-2.29e-07	-2.20e-05	1.69e-05	3.75e-06
	Diesel car (a<-0.5 m/s^2)	0	5.25e-05	7.22e-06	-1.87e-07	0.00e+ 00	-1.02e-05	-4.22e-06
	LPG car (a≥-0.5 m/s^2)	0	1.44e-02	1.74e-07	-6.82e-09	-8.11e-07	1.18e-06	3.96e-07
	LPG car (a<-0.5 m/s^2)	0	8.42e-03	0.00e+ 00	0.00e + 00	0.00e+ 00	0.00e + 00	0.00e + 00
	HDV	0	1.04e-03	4.87e-04	-1.49e-05	1.27e-03	2.10e-04	1.00e-04
	Bus	0	1.55e-03	8.20e-04	-2.42e-05	1.86e-03	3.21e-04	1.36e-04
PM	Petrol car	0	0.00e+ 00	1.57e-05	-9.21e-07	0.00e+ 00	3.75e-05	1.89e-05
	Diesel car	0	0.00e+ 00	3.13e-04	-1.84e-05	0.00e+ 00	7.50e-04	3.78e-04
	LPG car	0	0.00e+ 00	1.57e-05	-9.21e-07	0.00e+ 00	3.75e-05	1.89e-05
	HDV	0	2.14e-04	3.35e-04	-2.22e-05	2.07e-03	1.80e-03	2.27e-04
	Bus	0	2.23e-04	3.47e-04	-2.38e-05	2.08e-03	1.76e-03	2.23e-04

Almost half of all road deaths worldwide are among the least protected road users: motorcyclists (23%), pedestrians (22%) and cyclists (4%). In contrast, the likelihood of a motorcyclist, cyclist or pedestrian losing their life on the road varies from region to region: the African Region has the highest percentage of pedestrian and cyclist deaths (43% of road casualties), while these rates are relatively low in the South-East Asian Region.
Because of all these consequences, traffic accidents have become a real problem that threatens human life, but also one that can be prevented and tackled by theoretical studies. There are three major types of collisions: **Rear-end collisions**, **lane-changing collisions** and **head-on collisions.**

II.8.1 Rear-end collisions

A **Rear-end collision** is an accident in which a stopped or slow-moving vehicle collides with a moving vehicle in the same direction.
In NaSch's model, accidents cannot occur, because of the second rule ($v_i = min(v_i, g_i)$), which helps to avoid collision between vehicles. Indeed, accidents can occur if drivers do not respect the safety distance, and especially when a moving vehicle suddenly stops.
The first study of accidents that take into account the probability of the rear-end collision in

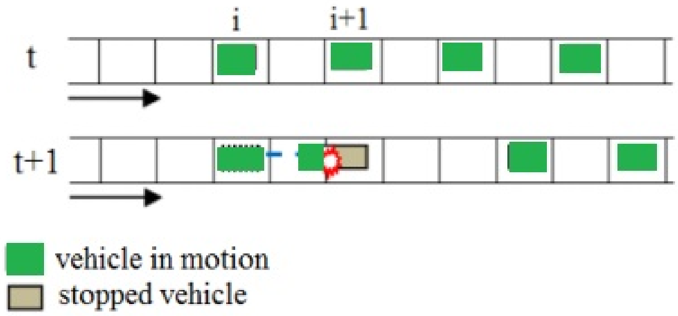

FIGURE II.21: Mimic representation of rear-end collisions.

a single lane CA model model was proposed by Boccara and his co-workers [77], where the conditions for an accident to occur are:

(1) : $g_i(t) \leq v_{max}$: The number of empty sites in front of the i−th vehicle is less than or equal to the maximum speed of the vehicle.

(2) : $v_{i+1}(t) > 0$: the vehicle ahead is moving.

(3) :$v_i(t+1) = 0$: The vehicle ahead comes to a stop in the next iteration.

If these conditions are met, there is a probability p that the vehicle will cause an accident. The probability of an accident, P_{acc}, is defined as:

$$P_{acc}/p = \frac{1}{T}\frac{1}{N}\sum_{t=t_0}^{t_0+T} n_i(t) \tag{II.38}$$

Where:

N : is the total number of vehicles.

t_0: is the time at which the calculation starts..

T : is the duration of the calculation.

When the density ρ is below the critical density $\rho_c = 1/(1+v_{max})$, the average number of free spaces between two consecutive vehicles exceeds v_{max}. In this scenario, the fraction of stopped vehicles n_o is zero, and no accidents occur (See Figure II.22). However, when $\rho > \rho_c$, the average speed of vehicles is lower than v_{max}. The fraction n_o increases with ρ, indicating reckless driving behavior. As the density approaches 1, where all vehicles come to a stop, the number of accidents tends towards zero. Therefore, the probability of a vehicle accident reaches its maximum within a vehicle density range between ρ_c and 1.

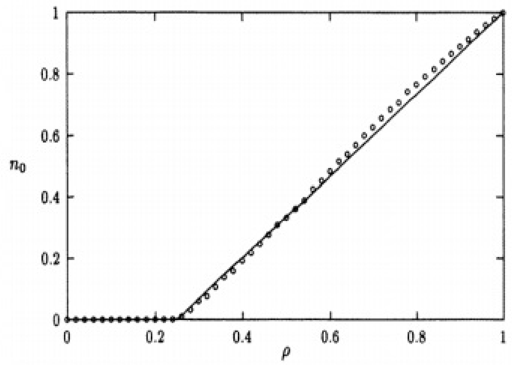

FIGURE II.22: The relationship between the fraction of stopped vehicles, n_o, and the density ρ, with $v_{max} = 3$, is depicted in the graph. The continuous line in the graph represents the linear approximation given by the equation $n_o = \dfrac{(\rho - \rho_c)}{(1 - \rho_c)}$ [77].

As it shown in Figure II.23 . The analytical part was also highlighted by Boccara [78]. He gave the following analytical form of P_{acc}:

$$P_{acc} = p\rho(1 - (1-\rho)^{v_{max}+1})\frac{(\rho - \rho_c)(1-\rho)}{(1-\rho)^2}(see(Rf.[74]) \tag{II.39}$$

The analytical results found are not confused with those of the simulation.

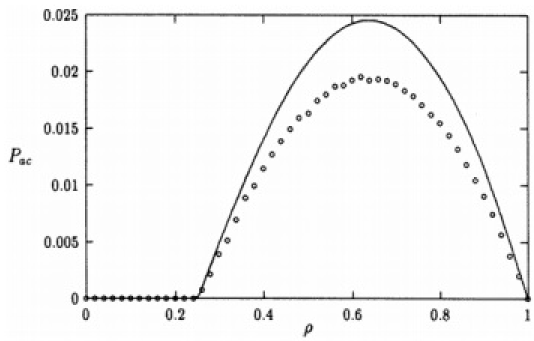

FIGURE II.23: The probability of accidents P_{acc}, as a function of vehicle density ρ, with $v_{max} = 3$. The continuous line represents the analytical results [77].

This analytical problem has been solved by other researchers [79, 80]. They found the exact analytical results of P_{acc} as shown in Figure II.24 .
Subsequently, a number of studies have examined rear-end collisions in the deterministic and non-deterministic case [81] and with open boundary conditions [82].

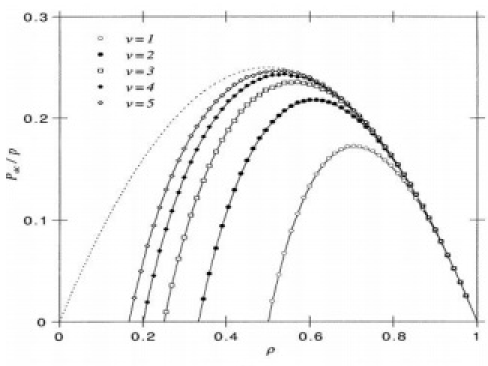

FIGURE II.24: The probability accidents P_{acc}, as a function of density. The solid lines represent the exact analytical results [80].

II.8.2 Lane-changing collisions

A lane-changing collision refers to a situation where a vehicle attempts to switch back to its original lane and collides with the vehicle following it on the same lane. Specifically, in a two-lane traffic system, such collisions can occur due to unsafe lane-changing maneuvers by vehicles, where the vehicles fail to adhere to safety criteria for lane-changing. It's important to note that our system does not actually experience accidents; instead, we calculate the probability of an accident occurring. The probability of a lane-changing collision is computed when the following rules are satisfied:

- Incentive criterion
  - $g_o(t) > g_i(t)$.
  - $g_b(t) < v_d(t+1)$.

Here, v_d represents the expected speed of the approaching vehicle in the destination lane. This refers to the lane that the vehicle attempting a lane change hopes to switch to in order to improve its speed. It is crucial to consider this expected speed as it indicates the potential collision risk between the vehicle attempting the lane change and the approaching vehicle in the desired lane.

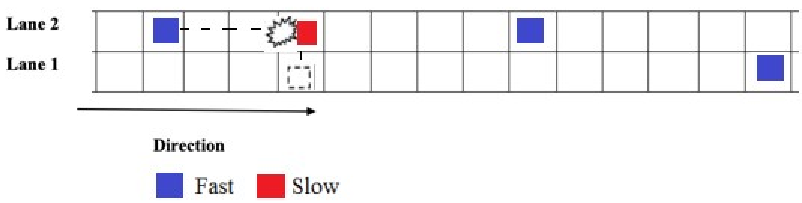

FIGURE II.25: Mimic representation of Lane-changing collisions.

II.8.3 Head-on collisions

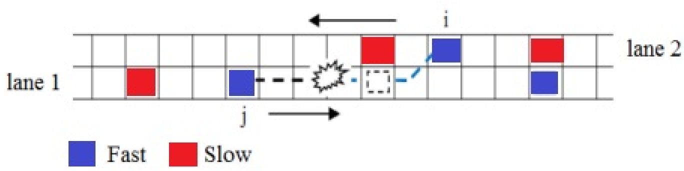

FIGURE II.26: Mimic representation of Head-on collisions.

A frontal collision, or head-on collision, is a collision in which the front ends of two vehicles collide first. This type of collision is extremely dramatic because of the energy generated by the impact. For this reason, vehicles that need to travel fast benefit from divided roads, such as highways or expressways, which are designed to avoid head-on collisions.

N. Moussa [83] studied head-on collisions on a two-way road. He found that the risk of collision increases when there is a low density of vehicles in one lane but a high density in the other lane. Moreover, the presence of slow-moving vehicles on the road has an impact on the occurrence of this particular type of accident. The conditions of having this type of collisions are given in the follow:

- $\Delta(t) * v_i(t) > g_i(t) - v_{j+1}(t+1)$.
- Vehicles are on the same lane with an opposite's direction in the bidirectional roads.

II.8.4 Time to collision (TTC)

Time to collision (TTC) is a measure of the time it will take for two vehicles to collide if they continue traveling at their current speeds and on their current paths. TTC is calculated using the following formula:

$$TTC_i(t) = \frac{x_{i-1}(t) - x_i(t) - L}{v_i(t) - v_{i-1}(t)} \quad and \quad v_i(t) > v_{i-1}(t) \tag{II.40}$$

where:

L represents the length of the vehicle, while $x_i(t)$ and $x_{i-1}(t)$ represent the positions of the front and rear vehicles, respectively. $v_i(t)$ and $v_{i-1}(t)$ represent the front and rear vehicles speeds, respectively.

TTC can be used to assess the risk of a collision and to determine whether a driver needs to take evasive action. For example, a TTC of 2 seconds or less is considered to be a high risk of collision, and a driver should take action to avoid a collision.

Here are some examples of TTC values and their corresponding risk levels:

- TTC of 2 seconds or less: High risk of collision.
- TTC of 3 to 4 seconds: Medium risk of collision.
- TTC of 5 seconds or more: Low risk of collision.

TTC cellular automata models have been shown to be effective at predicting collisions in a variety of traffic scenarios. They have been used to study the effects of different traffic control measures, such as speed limits and traffic signals, on the likelihood of collisions. They have also been used to study the effects of driver behavior, such as tailgating and aggressive driving, on the likelihood of collisions.

TTC cellular automata models are a valuable tool for traffic engineers and safety researchers. They can be used to identify potential problem areas on the road and to develop strategies to reduce the risk of collisions.

II.8.4.1 Advantages and disadvantages of using TTC cellular automata models

Here are some of the advantages of using TTC cellular automata models:

- They are relatively easy to implement and use.
- They can be used to simulate a wide variety of traffic scenarios.
- They can be used to predict the likelihood of collisions with a high degree of accuracy.

And the disadvantages of using TTC cellular automata models are:

- They can be computationally expensive to run.
- They can be sensitive to the initial conditions of the simulation.
- They can be difficult to use to predict the behavior of individual vehicles.

Conclusion

The first and second chapters are a general representation where we have presented the general context of our research work. We have highlighted the importance of road traffic simulation. Then we gave a brief history of road traffic and the pioneering work in this field. afterward we discussed the concept of global and local phenomena and the link between them. Various empirical results were also presented such as the empirical fundamental diagram, inter-vehicle time.

In the literature, there are three models for modeling road traffic: macroscopic, mesoscopic, and microscopic models. This thesis is based on the cellular automata (CA) model which is presented as an intermediate approach between macroscopic and microscopic models because it allows on the one hand to study traffic as a fluid (calculation of flow, average speed, density...), and on the other hand, it allows to study the individual behavior of vehicles and the interactions between them.
Since the road in the real case does not depend on a single lane most of the time, we have extended the single-lane road to a two-lane road and we discussed the concept of particle hopping models and the asymmetric simple exclusion process. The two types of lane-changing rules (i.e., symmetric and asymmetric) are introduced. Finally, we discussed different types of emissions resulting from traffic, and the most important previous results related to energy dissipation, rate of satisfaction, and accidents.

Chapter III

Dissipation energy and satisfaction rate for A two-Lane traffic model with two types of vehicles

III.1 Introduction

Traffic flow problems have attracted much attention from different perspectives [84–90]. One of the biggest challenges of traffic is its heterogeneity. As we know in road traffic, we can find different categories of vehicles such as cars and trucks, bicycles, etc. The number of lanes changing increases significantly when the slow vehicles are present on the road. The phenomena of the lane changing from a lane to another have attracted tremendously the researchers especially from the perspective of modeling [91–93]. Nagatani [94, 95] proposed a simple cellular automaton (CA) model composed of two lanes where vehicles either move forward or change lanes. Rickert et al. [96] developed a two-lane CA model based the Nagel and Schreckenberg model (NaSch) [97]. Ou and Tang [98] developed a two-lane car-following model to study the influences of inter-vehicle communication on each vehicle's movement when an incident occurs. Zhu et al. [99] studied the effect of the blockage induced by an accident on a two-lane CA model. They showed that the jam caused by a car accident in one lane merge to the other lane of the road. Furthermore, the mixture of traffic in multi-lane was also investigated. Chowdhury et al. [100] proposed a two-lane CA model where the system have two type of vehicles namely slow and fast with different values of maximum speed (v_{max}). They found that even for small densities, the slow vehicles affected the stability of traffic flow in the system. Knospe el al. [101] studied the effects of disorder in two-lane traffic CA model. They noticed that even a small number of slow vehicles can initiate the formation of platoons at low densities. Jia et al. [102] studied the effect of the honk on the lane change in a two-lane CA model. They found that when the traffic is homogenous the effect of honk is slightly. However, in heterogeneous traffic, the honk enhances the traffic situation especially in the intermediate density regime. Qian et al. [103]

proposed a three-lane CA model under two different lane control conditions. They analyzed the relationship between mixing ratio of different vehicles, density, and overtaking ratio. Li et al. [104] proposed a symmetric two-lane CA model where the aggressive lane-changing is considered. They found that when fast vehicles perform an aggressive lane-changing the plugs formed by slow vehicles reduced especially at the intermediate density range.
As we saw in the former slow vehicles affect the traffic flow by creating plugs moving with a slow speed which creates unsatisfied vehicles in the system (i.e. vehicles that moves with a speed much lower than its desired speed). Hence, slow vehicles increase the energy dissipation. In this work, we are going to study the effect of slow vehicles and their distribution on the traffic flow in a two-lane CA model. Also, the satisfaction rate and the energy dissipation were used as parameters to understand the effect of slow vehicles in the system.

This chapter is organized as follows: in next Section we will explain the model, in Sec. III.3 we will discuss the results, the conclusion is given in Sec. III.4.

III.2 Models

In this chapter, we use a CA model to simulate a unidirectional two-lane traffic flow. The system consists of two parallel single-lanes, each lane is composed of L cells, every cell corresponds to $7.5m$. We consider two types of vehicles that differ with their length and the maximum speed. The fast vehicles occupy only one cell and their maximum allowed speed is v^f_{max}. The slow vehicles occupy two cell and their maximum allowed speed is v^s_{max}, where $v^f_{max} > v^s_{max}$. For the longitudinal movement of vehicles, we use NaSch model, where the vehicles are handled in parallel during one-time step according to the four rules of the NaSch model (see II.3.2.3):

The two-lane are controlled by lane-changing rules, where these rules can be symmetric or asymmetric with respect to lanes or to the types of the vehicles. In asymmetric rule the slow vehicles of one lane have a lower changing probability than the slow of the other lane. Here only fast vehicles can move between the two-lane while the slow vehicles have a favorite lane. For the symmetric rules, both fast and slow vehicles have the right of passing between the lanes with the same probability. For the lane changing rules we are going to use the model proposed by Rickertet al (see II.3.6.3).

We consider the periodic boundary condition. Besides the fractions of the fast and the slow vehicles are f_{fast} and f_{slow}, respectively where:

$$f_{fast} = 1 - f_{slow} \tag{III.1}$$

III.3 Results And Discussions

In our computational studies, we consider two lanes each of them is composed of 5000 sites. The vehicles are distributed randomly around the two lanes according to their fractions (i.e. $f_{fast} = 0.8$ and $f_{slow} = 0.2$). As mentioned above the simulation was done in the case of mixture of two types of vehicles which differ according to their lengths (i.e. slow vehicles $l_s = 2$ and fast one $l_f = 1$) and characterized by two different values of the maximum allowed speed (i.e. $v^f_{max} = 5$ and $v^s_{max} = 3$). All vehicles have the same randomization probability $p = 0.2$. We carry out the simulations of the system model under the periodic boundary condition. The system run for 60000 time-steps to ensure that the steady state is reached. The sampling for the calculation of the results is done for the last 10000 time-steps. We are interested in the case where the probabilities of lane changing are asymmetric, where the following parameters are considered ($ch^f_{lane1} = 1$, $ch^s_{lane2} = 1$, $ch^f_{lane2} = 1$) . This mimics the real case that it is illegal for slow vehicles obstructing traffic while driving continuously in the lane for passing.

III.3.1 Homogeneous systems

As previously stated, based on the experimental situation, an appropriate lane-changing rule set must be selected. First, we'll look at symmetric lane-changing rules, which are useful for relevant in cities and on highways where overtaking is permitted on both lanes. In this subsection, we are interested in studying the case where the system is homogeneous, where only one type of the vehicles on the two-lane is introduced (i.e., slow or fast ones) with the same length.

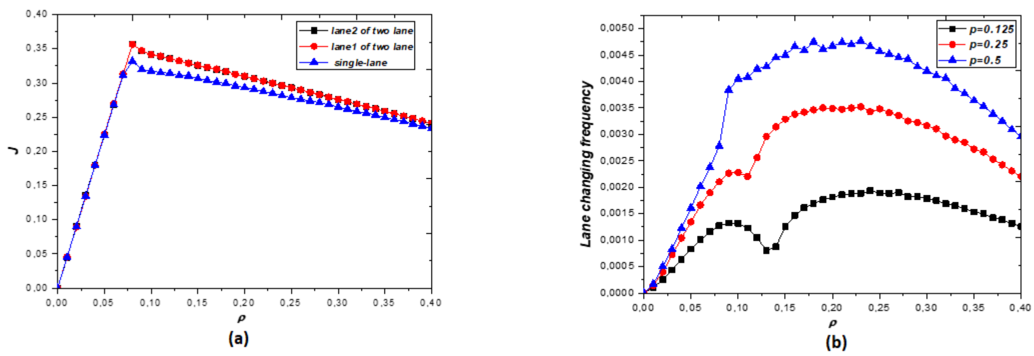

FIGURE III.1: The fundamental diagram of the single-lane model compared with the two-lane model for systems with $v_{max} = 5$ and $p = 0,5$. (b) Lane-change frequency in the two-lane model for different braking parameters p.

Figure III.1 investigated the fundamental diagram of a periodic two-lane traffic flow model, as well as the density dependence of the lane-changing frequency. The simulations

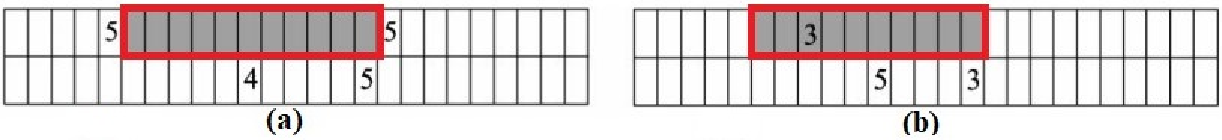

FIGURE III.2: (a) Necessary safety gap for a lane change in the free-flow regime. (b) Possible positions of slow vehicles which lead to a plug. The vehicles are driving from left to right.

show an improvement in the maximum flow per lane compared to a single-lane traffic flow. In addition, there are some unexpected new findings, such as the presence of a local minimum of lane-changing frequency near the density of maximum flow J in the case of a small value of braking noise p. Obviously traffic jams can be partly prevented by changing lanes, therefore the system's capacity is marginally improved. In order to trigger a lane changing, two prerequisites must be required. First, the situation on the other lane must be more favorable and second, in the free flow regime, a lane-changing operation usually needs $2v_{max}+1$ empty spaces on the target lane (Figure III.2). Hence, for a small value of p where the vehicles are ordered homogeneously, a local maximum of the lane-changing frequency can be observed near to $\rho_s = 1/2(v_{max}+1)$. In other hand for a greater value of the braking probability (i.e., $p = 0,5$) There is no local maximum founded, but when we increase the density p for a sufficiently small values of p, a minimum of the lane-changing frequency is observed. This is can be illustrated in the limit $p \longrightarrow 0$ for $\rho = 1/(v_{max}+1)$, where the vehicle is perfectly ordered with a v_{max} sites between successive vehicles, in this situation both the incentive and safety conditions are never fulfilled and the lanes are entirely decoupled. For small braking noise, the ordering mechanism remains active, reducing the number of lane changes to value approach to $\rho = 1/(v_{max}+1)$. For a large value of p this kind of ordering is prevented since the fluctuations of the space between successive vehicles become larger. Therefore, large gaps become better than in the case of deterministic limit and lane-changing become possible once again. Furthermore, the increase in density reduces the probability to find adequate free space on the other lane. Obviously, the maximum is achieved at higher values of p, because the incentive criterion is fulfilled and at intermediate densities large gaps are still observed because of the inhomogeneity of the microscopic states.

III.3.2 Inhomogeneous systems

After this brief overview of the results for homogenous systems. We now discuss different types of vehicles with the same length, which is more significant for practical purposes, we chose two types of vehicles as the first step toward realistic distributions of free flow velocities, e.g. slow vehicles with $v^s_{max} = 3$ and fast vehicles with $v^f_{max} = 5$, similar to Ref. [105]. The simulations were carried out with 5% of slow vehicles, which are placed randomly in

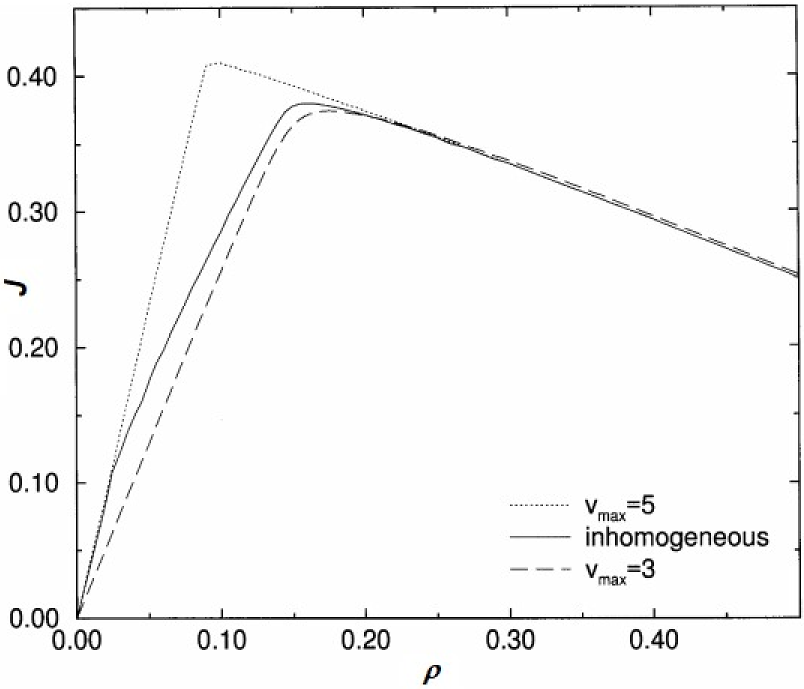

FIGURE III.3: Comparison of the flow per lane of the inhomogeneous model with the corresponding homogeneous models for $p = 0.4$.

the beginning. Both fast and slow vehicles are allowed to use both lanes, i.e. both vehicles are treated similarly in terms of lane-changing behavior.

Figure III.3 compares the impacts of slow vehicles on the average flow of a two−lane system to the fundamental diagram of a single-lane road with one slow vehicle. Because passing is not permitted in a single-lane system, the slow vehicle dominates the average flow at low densities, resulting in platoon formation [106–110]. Surprisingly, the two-lane system exhibits identical behavior, although passing is permitted and the proportion of slow vehicles is minimal, which is consistent with the findings of Ref. [100]. It was demonstrated in Ref. [105] that two slow vehicles driving side by side can form a "plug" and obstruct the lane. References [100, 111] have made similar observations. Both cars don't have to drive side by side to form such a plug. A fast vehicle with a velocity of $v = v^{s}_{max}$ moving behind a slow vehicle will require $v^{f}_{max} + 1$ vacant cells in the driving direction and vacant cells in the following direction. As a result, two slow vehicles can create a plug, even though there is a gap of $9 - cell$ between them (see Figure III.2).

In the rest of this chapter, we will consider two categories of vehicles fast and slow with different length.

III.3.3 Homogeneous Initial Configuration (HIC)

III.3.3.1 Fundamental Diagram

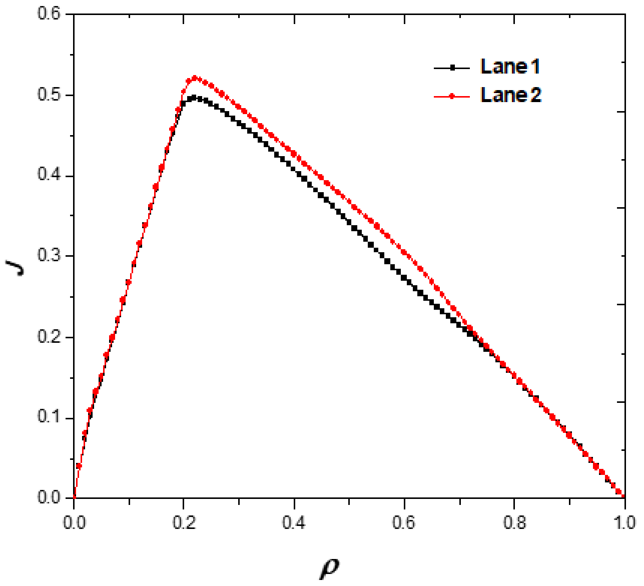

FIGURE III.4: Fundamental diagram for each lane in two-lane road for homogeneous traffic. $ch^{s}_{lane1} = 0.1$.

At the first step, we are going to study the case where the initial configuration is homogeneous which means that the slow and fast vehicles are distributed all over the two lanes. To compare the two lanes throughput, we show the fundamental diagram for the traffic flow in both lanes. Fig. III.4 shows the current as a function of density for lane 1 and lane 2. The full squares represent the plot of current against density in the lane 1. Full red circles represent the plot of the current against density in lane 2 where $ch^{s}_{lane1} = 0.1$. We can see that both fundamental diagrams have similar features; the current J increases with density ρ, until it reaches the maximal current, and then decreases with increasing the density ρ. Hence, the fundamental diagrams coincide with each other for low and high densities. However, at intermediate densities, the flow in lane 2 is a little higher than that in lane 1.

As shown in the corresponding lane-changing frequency of the vehicles (see Fig. III.5). At the low-density fast vehicles in both lanes have the same lane-changing frequency. In that case slow vehicles do not obstruct continuously fast vehicles in both lanes because at low density there are large spaces between vehicles which lead to an easy lane change for vehicles to improve their individual situation. In another hand, at high density we can see that the values of the lane-changing frequency become zero, in that case, traffic in both lanes become denser which make the finding of adequate space for a safe lane changing an impossible task. Thus, the vehicles in both lanes keep moving straight forward in their lanes. For

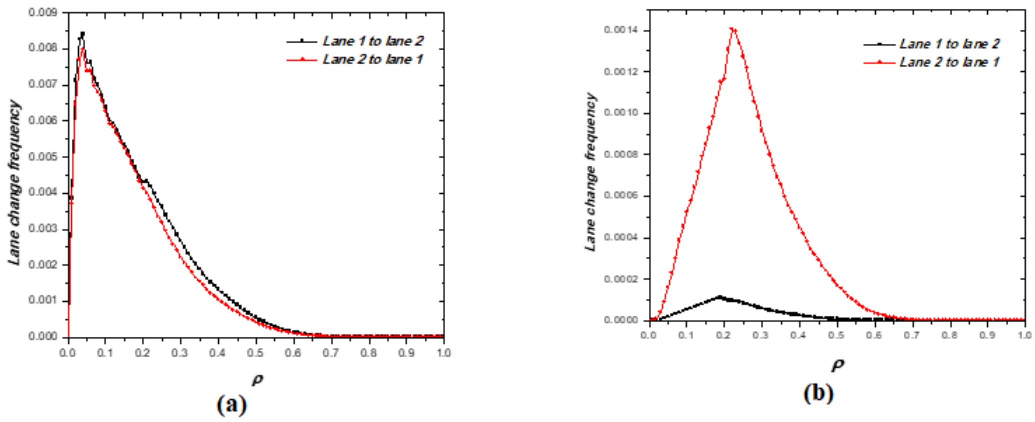

FIGURE III.5: lane change frequency against the total density for homogeneous traffic (a) fast vehicles, (b) slow vehicles for $ch^{s}_{lane1} = 0.1$.

the intermediate density we can see that the lane-changing frequency of fast vehicles from lane 1 to lane 2 is greater that this from lane 2 to lane 1. In that case, the effect of slow vehicles in the lane 1 start affecting the fast vehicles by imposing their speed in the lane 1 which make the fast vehicles goes to the lane 2. Hence, for the slow vehicles (see Fig. III.5(b)) the lane-changing frequency from the lane 2 to the lane 1 is higher as compared with the lane-changing frequency for the lane 1 to lane 2. This is due to the asymmetric lane changing probability that give the right of going to the lane 2 only to 10% of slow vehicles of the lane 1, within these slow vehicles control the lane 1 especially at intermediate densities, this explains why the traffic in the lane 2 shows better performance than this in the lane 1.

Another important remark, from the fundamental diagram for the $0.01 < \rho < 0.05$the current increase rapidly and as the density increase ($\rho \geq 0.05$) the slop of the line decreases which means that the relation between the current and the density is not straight line in the free flow region (see Fig. III.6). Here, the lane change frequency of the fast vehicles increases rapidly which means that the fast vehicles change the lane to improve their speed consequently the plugs created by slow vehicles is reduce thereby increasing the flow in both lanes (i.e. higher speed means higher flow rate) (Fig. III.6). As the density increases ($\rho \geq 0.05$) the lane changing frequency decreases which means the plugs formed by slow vehicles become consistent and starts controlling the lanes. This, explains why the relationship between the flow and density is not a straight line in the free flow region. In addition, we should not that the flow is slightly higher in the lane 2 than in the lane1 for $\rho > 0.01$. In this case, the asymmetric lane changing probability for slow vehicles makes more fast vehicles confined in lane 2 which increases the flow as compared to lane 1.

To better see these effects, we plot the space time diagrams (see Fig. III.7). For low

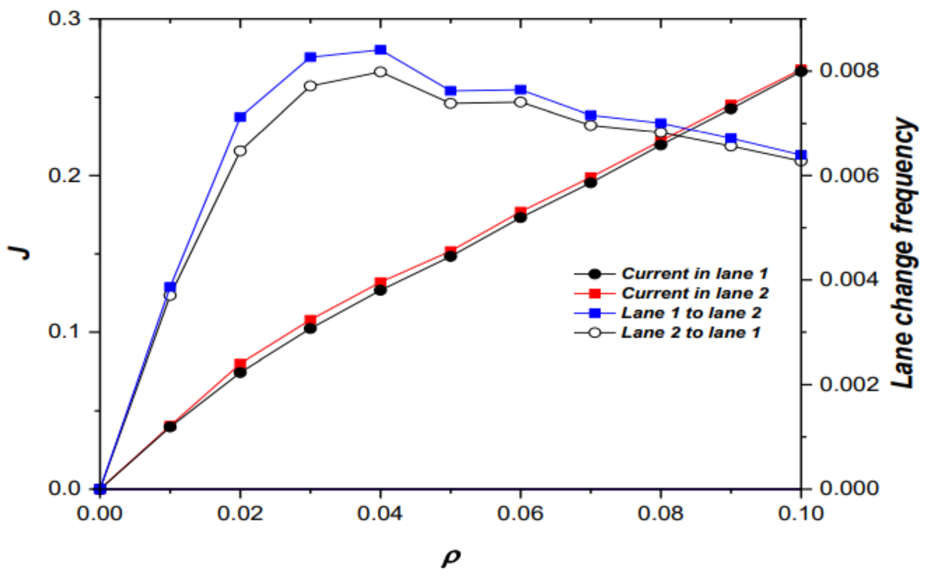

FIGURE III.6: The current and the lane change frequency of fast vehicles as a function of the density for homogeneous traffic for $ch^{s}_{lane1} = 0.1$.

density ($\rho = 0.1$), in both lanes traffic situation is quite similar; clusters of slow-moving vehicles are observed.

Nevertheless, free space is also observed which helps fast vehicles in both lanes to improve their traffic situation. For intermediate density ($\rho = 0.4$), traffic in lane 1 becomes denser because a large number of slow vehicles are confined in this lane. Thus, the traffic flow is slightly improved in the lane 2. In the case of high-density ($\rho = 0.8$), traffic situation worsens in both lanes the jam spread all over the two lanes. Despite that the number of the slow vehicles in the lane 1 is greater than this in the lane 2, but the traffic situation in both lanes is quite similar. In that case, only one slow vehicle in the lane could control the traffic situation because of the impossibility of lane changing for fast vehicles.

As we saw above, the slow vehicles affect the traffic flow in the system especially if those vehicles are confined in one lane which gives rise in some case to the moving blocks in both lanes when a slow vehicle tries to overtake another slow one.

III.3.3.2 Energy Dissipation And Satisfaction Rate

As we know the stop and go events induced by slow moving vehicles is often observed in those system. However, in order to quantify this behavior one of the methods that could be useful is to study the dissipation energy. The former is the difference between the initial and final kinetic energy of each vehicle.

Fig. III.8 shows the relation between energy dissipation per vehicle and the density of both types of vehicles in the two lanes (lane 1, lane 2). For fast vehicles the energy dissipation

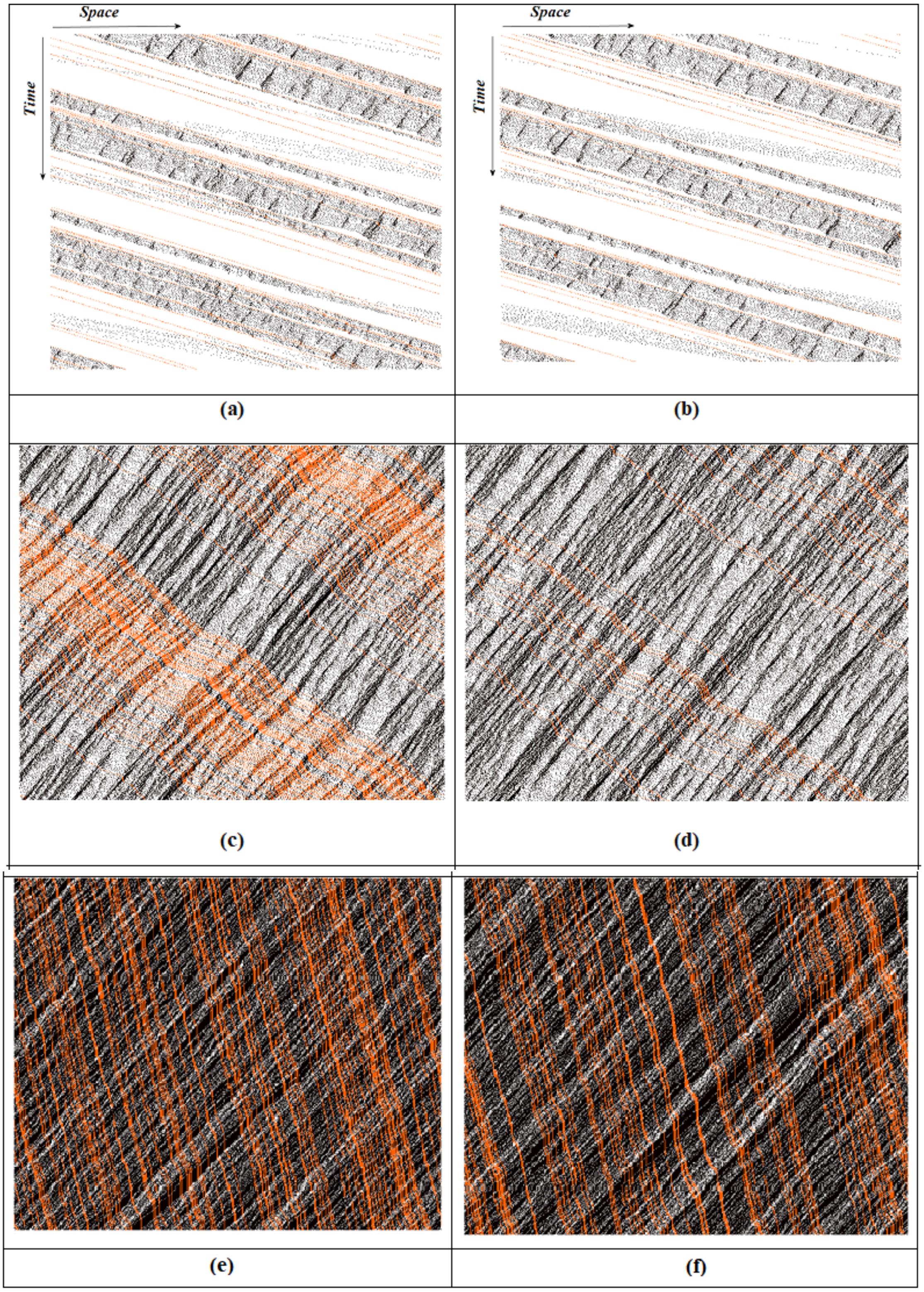

FIGURE III.7: Space time plots of the proposed homogeneous traffic in both lanes, white color is the empty space and the black color corresponds to fast vehicles, red color corresponds to slow vehicles. Lane 1: (a) $\rho = 0.1$ (c) $\rho = 0.4$ (e) $\rho = 0.8$. Lane 2: (b) $\rho = 0.1$ (d) $\rho = 0.4$ (f) $\rho = 0.8$.

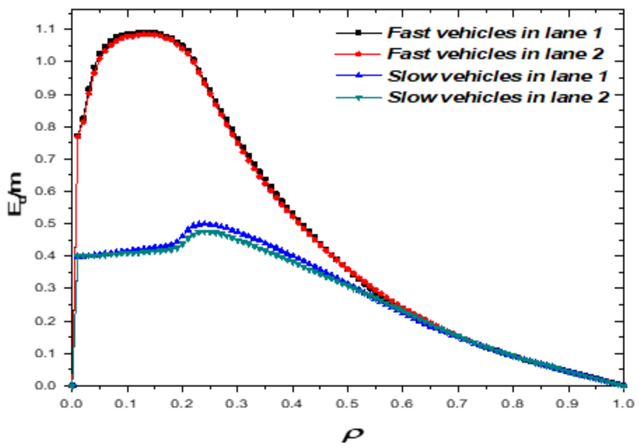

FIGURE III.8: Energy dissipation against the density in both lanes for homogeneous traffic and for both type of vehicles with $ch^s_{lane1} = 0.1$.

in both lanes shows a similar feature. The energy dissipation increases with an increase of density before reaching a changeless plateau, after that it decreases with an increase of density. Besides, for the case of the slow vehicles the energy dissipation increases with an increase of density before reaching a maximum value then it decreases with an increase of density. We should note that the energy dissipation of both types of vehicles in the two lanes coincide at high density. In this case, the two lanes become denser, the speed of vehicles in both lanes is determined only by the headway between the vehicles in the same lane (i.e. the lane change is impossible see Fig. III.5). In addition, we can see that the energy dissipation in the lane 1 for both type of vehicles is slightly greater than this in the lane 2 especially at intermediate density. Thus, the lane 1 becomes denser and the stop and go events become higher which increase the energy dissipation for both type of vehicles.

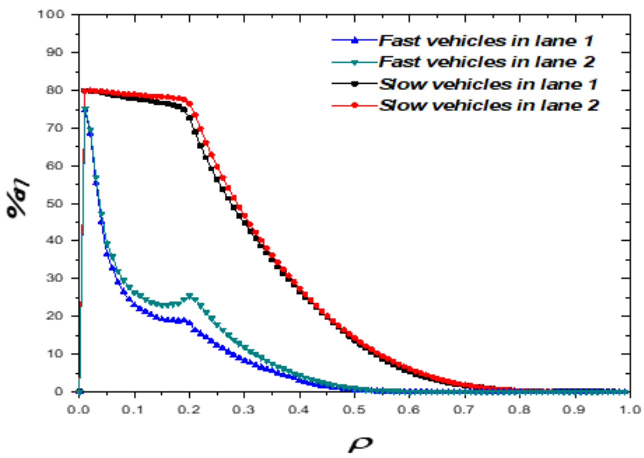

FIGURE III.9: The percentage of satisfied vehicles against the density for homogeneous traffic with $ch^s_{lane1} = 0.1$.

From this section we found that the slow vehicles control the lane 1 by imposing their speed all along this lane which give rise to large cluster of vehicles behind the slow vehicles. As we can see from Fig. III.9, the percentages of vehicles that can move with their desired speed never reach the 100%. The maximum observed value equal 80% this is due to the braking probability $p = 0.2$. Besides, the percentage of satisfied fast vehicles in both lanes shows a similar behavior; it decreases rapidly as the density increases before reaching a local maximum then it decreases again with the density. Additionally, the percentage of satisfied fast vehicles in lane 2 is slightly higher than this in lane 1. Hence, for the slow vehicles in the lane 2 the number of satisfied vehicles is bigger than this in the lane 1. We should note that the critical density shown for the case of slow vehicles (see Fig. III.9) correspond to the maximum of the lane changing frequency.

III.3.4 Inhomogeneous Initial Configuration (IC)

III.3.4.1 Fundamental Diagram

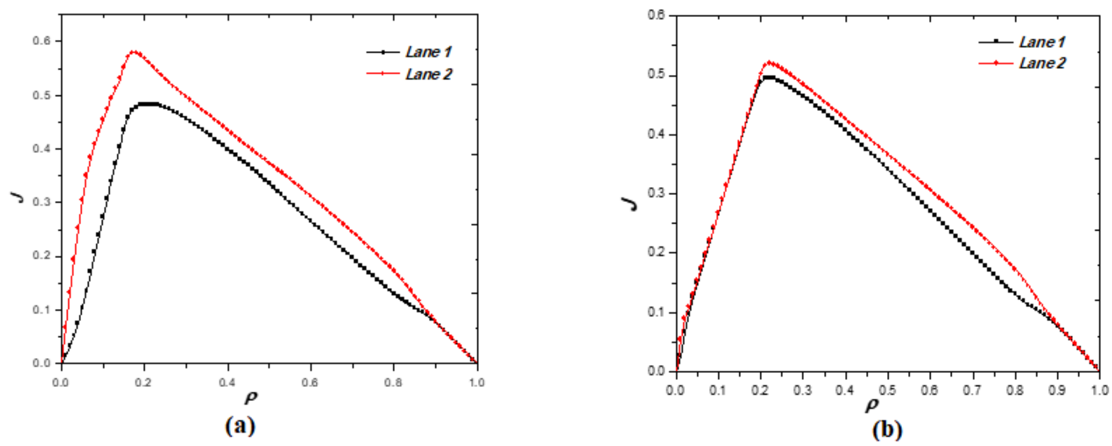

FIGURE III.10: Fundamental diagram for each lane in two-lane road for inhomogeneous traffic. (a) $ch^s_{lane1} = 0$ (b) $ch^s_{lane1} = 0.1$.

In this section, we study the case where the initial configuration is inhomogeneous which means the slow vehicles start with a random distribution only in the lane 1. However, the fast vehicles are disturbed all over the two lanes.

As we can see from (Fig. III.10(a)), for the case of $ch^s_{lane1} = 0$, the traffic flow in the lane 2 shows better performance as compared to the lane 1. The slow vehicles prevent fast vehicles to move with their desired speed. In that case, the fast vehicles emigrate from the lane 1 to the lane 2 which explain the large lane change frequency especially in the low densities (see Fig. III.11(a)).

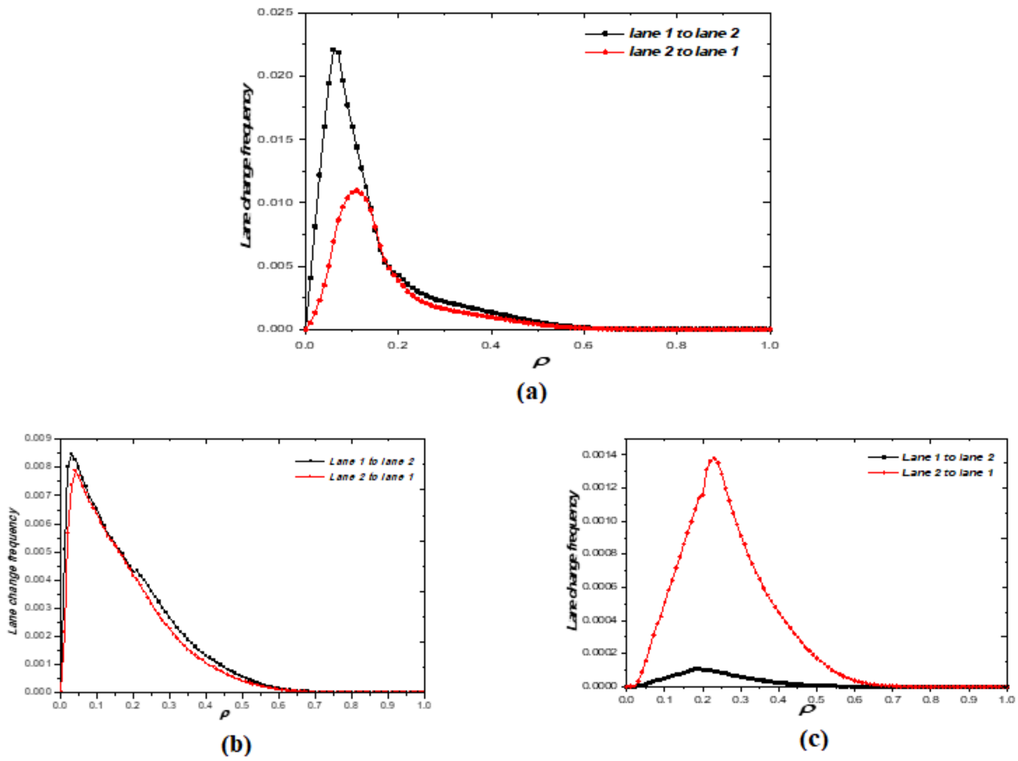

FIGURE III.11: Lane change frequency against the total density for inhomogeneous traffic (a) fast vehicles for $ch^{s}_{lane1} = 0$ (b) fast vehicles for $ch^{s}_{lane1} = 0.1$ (c) slow vehicles for $ch^{s}_{lane1} = 0.1$.

Thus, the number of fast vehicles in the lane 2 increases (by comparing the lane change frequency for fast vehicles in both lanes) in this way their contribution in the total flow increases which enhances the flow in the lane 2 at the expense of the lane 1 (see Fig.III.12). This explains the no straight-line increase for both lanes in the free flow region (i.e. the curve of the flow shows a concave up increasing in the lane 2, in the other way for the lane 1, the flow exhibits a concave down increasing).

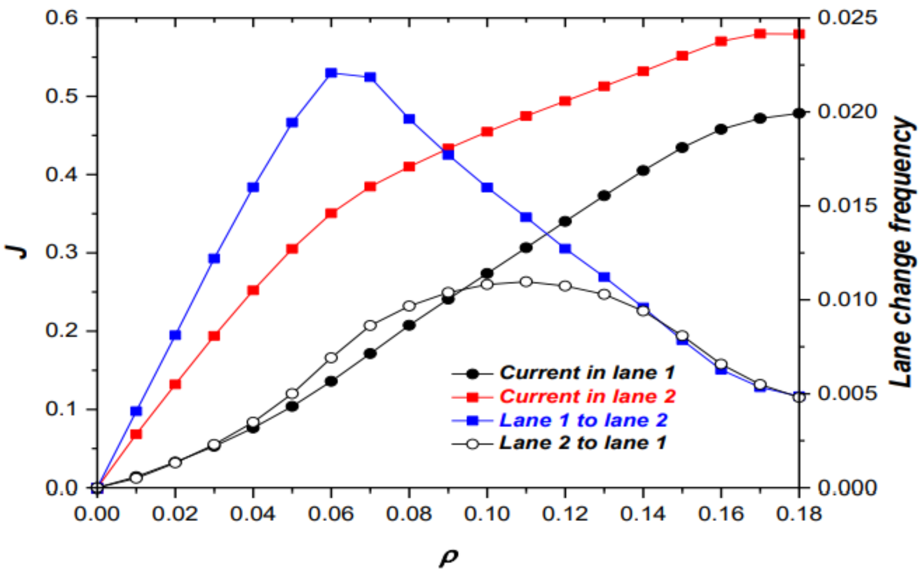

FIGURE III.12: The current and the lane change frequency of fast vehicles as a function of the density for inhomogeneous traffic for $ch^s_{lane1} = 0$

It is worth mentioning that beyond the $\rho = 0.6$ the lane changing rate becomes null, unlike the flow in lane 2 remain better than the flow in lane 1. We can explain this by the fact that the slow vehicles are confined to the lane 1 which make them impose their speed in the lane 1. Here the flow is determined only by the longitudinal interaction between vehicles and as we know that the braking probability ($p = 0.2$) creates the fluctuation of the free space between vehicles which increase the flow in the lane 2 because it holds only fast vehicles. However, beyond the $\rho = 0.9$ the situation worsens in both lanes here the current in both lanes is the same.

For the case of $ch^s_{lane1} = 0.1$ (see Fig. III.10(b)) we get the same current as in the Fig. III.4 except when ρ goes beyond $\rho = 0.6$, the current is only defined by the longitudinal interactions between vehicles. In that case, the traffic flow in the lane 1 is lower than the one of the homogenous initial configurations of the Fig. III.4. Hence, we get the same lane changing frequency (see Fig. III.11(b)-(c)) as the Fig. III.5. However, the current of the lane 2 is slightly better than this in the Fig. III.4 especially in the high-density region. We can explain this by the distribution of slow vehicles in the initial configuration that allows them to

be confined in the lane 1. In addition, as the density is larger, the vehicles in both lanes cannot find adequate space for the lane changing which increases the longitudinal interactions at the expense of the lateral interactions that increases the flow in the lane 2 as compared to lane 2 of the Fig. III.4 (i.e., because the lane 2 in Fig. III.4 is composed of a mixture of slow and fast vehicles).
As we saw the initial configuration affect strongly the traffic flow in both lanes especially when the slow vehicles have not the right of changing the lane (i.e., $ch^{s}_{lane1} = 0$). However, even the lane changing probability is lower, thus the distribution of slow vehicles becomes homogenous over the time which explain the similarity of the results of Fig. III.10(b) and Fig. III.10. In another hand, what is the effect of the distribution of the slow on the energy dissipation and the percentage of satisfied vehicles in both lanes?

III.3.4.2 Energy Dissipation And Satisfaction Rate

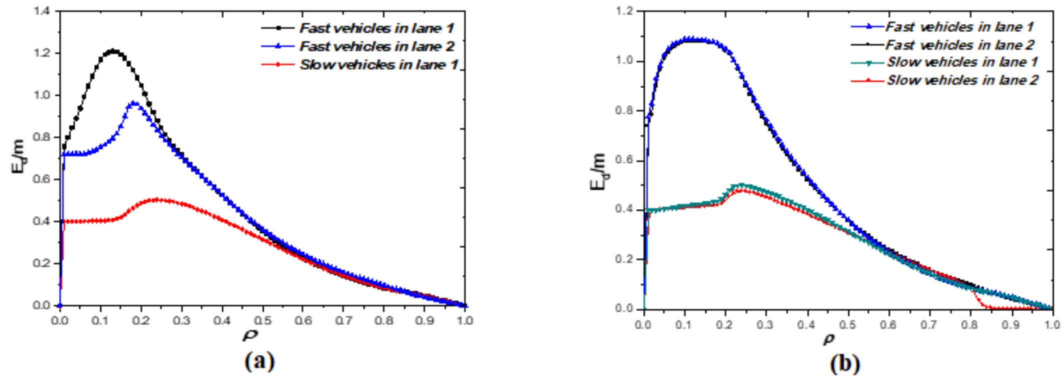

FIGURE III.13: Energy dissipation against the density in both lanes and for both types of vehicles for inhomogeneous traffic (a) $ch^{s}_{lane1} = 0$ (b) $ch^{s}_{lane1} = 0.1$.

As we can see from Fig. III.13(a) the energy dissipation of fast vehicles in the lane 1 is higher than this in the lane 2. Here, the slow vehicles impose their speed in the lane 1, which give rise of a large energy dissipation. However, for the large density the three curves of the energy dissipation coincide with each other. Here the lane change frequency becomes null (see Fig. III.4(a)), and therefore the dissipation energy in both lanes depends only on the longitudinal interactions of vehicles. As compared to the case where the initial configuration is homogeneous (see Fig. III.8), the fast vehicles in the lane 1 for the inhomogeneous initial configuration (Fig. III.13(a)) show a higher energy dissipation when the $\rho < 0.3$. As we said before the slow vehicles are confined in the lane 1 which implies their speed on the fast vehicles that gives rise of a higher dissipation energy for the fast vehicles that could not pass to the other lane. However, as the density increase, the effect of the slow vehicles decreases at the expense of the lack of free space between vehicles in both lanes as well as in both initial configurations (i.e., homogeneous, inhomogeneous) which implies the same features in the dissipation energy. Nevertheless, for Fig. III.13(b) the energy dissipation of both type of vehicles and in the two lanes show a similar feature as that in the Fig. III.8 except for the case of slow vehicles in the lane 2 especially in the high density where the energy dissipation becomes null. We can explain this by the fact that at high density the slow vehicles cannot change the lane, where the slow vehicles become confined in the lane 1.

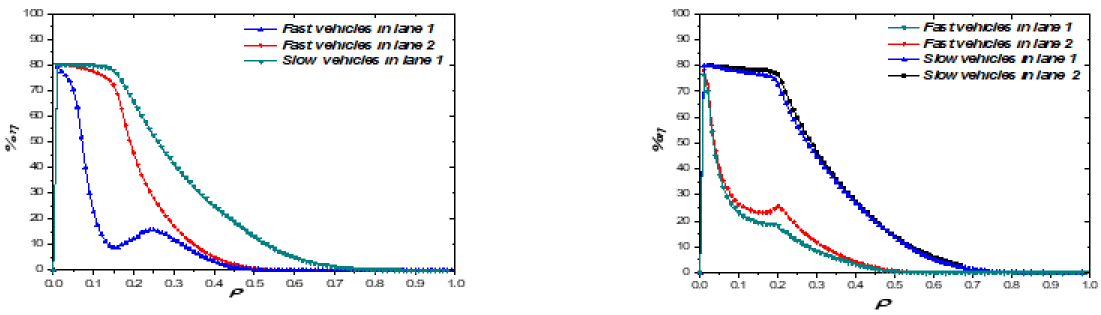

(a) (b)

FIGURE III.14: The percentage of satisfied vehicles against the density for inhomogeneous traffic (a) $ch^{s}_{lane1} = 0$. (b) $ch^{s}_{lane1} = 0.1$.

Furthermore, form Fig. III.14 in both cases (i.e.(a) $ch^{s}_{lane1} = 0$ (b) $ch^{s}_{lane1} = 0.1$) the percentage of satisfied vehicles for the fast vehicles in the lane 1 is the lowest. Thus, the slow vehicles control the lane 1 which reduces the speed of fast vehicles. Hence, fast vehicles try to improve their speed by the lane changing which gives rise to a local maximum in the percentage of satisfied vehicles especially in the intermediate density. However, the percentage of satisfied vehicles for the case of the fast ones become null before the slow ones, which means that the slow vehicles control the traffic situation especially at intermediate density. For the high density, the traffic situation is worsening the free space between vehicles is reduced, a large number of vehicles came to a halt, which reduces the speed of vehicles and as a result, the satisfaction rates become null even for the slow vehicles.

III.4 Conclusion

In this chapter, we studied the effect of slow vehicles on the traffic flow stability in two lanes cellular automata model. The energy dissipation was evaluated for both types of vehicles. We found that slow vehicles obstruct fast ones while driving continuously in the same lane. This affects the speed of fast vehicles which give rise to a large number of unsatisfied vehicles that drive with speed lower than their maximal speed. The influence of slow vehicles is observed especially at the intermediate density. Hence, the effect of the initial configuration of slow vehicles is evaluated. The inhomogeneous initial configuration where the slow start in one lane is studied. We found that the slow vehicles control this lane by imposing their speed on the fast one, which gives rise to a large number of unsatisfied fast vehicles and a high frequency of lane changing. However, when the lane changing probability for slow vehicles increases, the distribution of the slow vehicles over the two lanes becomes homogenous which reduces the flow in both lanes.

Chapter IV

Effects of slow vehicles on Carbon dioxide emission in a two-lane cellular automata model

IV.1 Introduction

Over the past decade, the world has witnessed significant economic and urban activity, also many factories and huge projects have been established. The quality of leaving has been enhanced where the number of residential buildings, water sanitation networks, the use vehicles has increased. As the result of this huge increase, the industrial and transportation emissions and among other effects became the main causes of the environmental pollution. Moreover, the air quality has been affected which affect the health of the population [112–114]. This situation is expected to be exacerbated in recent years, as the continuous rise in the standard of living leads to a significant increase in air pollutants due to fuel combustion. One of the principal causes of gas pollutants in the air is automobile engines.
The list of atmospheric pollutants of automobile origin is long, among of them, one finds the oxides of carbons (CO and CO_2, the oxides of nitrogen (NO and NO2 regrouped under the name NOx), volatile organic compounds (VOCs) and particulate matter (PM). These substances cause many diseases for humans, including cancer, respiratory infections, eye pain, and nervous system dysfunction [115, 116]. Besides the pace of experiments and research aimed at reducing harmful emissions from the vehicle has not subsided, and the field of research has exceeded the modifications made to the vehicle, to reduce fuel consumption and thus extend to the road and driving behaviors [117, 118] .
It is well established that vehicle emissions are intrinsically linked to traffic flow status, transient driving patterns, which are created by repeated decelerations and accelerations of the vehicle and frequently occur at junctions or during self-organized jamming phases on roadways (e.g., stop-and-go), produce a significant extra quantity of released exhaust pollution [119]. As a result, microscopic models must be used to examine the precise evolution

of vehicular flow, which gives a strong approach to anticipating vehicle emissions. Micro-traffic flow simulations may provide a comprehensive description of a moving vehicle queue [120, 123]. Traditionally, car-following models have been employed to replicate the behavior of single vehicles [124]. Recently, cellular automata (CA) models, which are discrete in both space and time, have emerged as a viable technique for micro-simulation based on the Nagel-Schreckenberg model (NS) is a stochastic CA model for single-lane roadway [125]. Despite the simplicity of this model, it can simulate the basic phases of real-world traffic, namely free flow and traffic jams. Since then, this model has been extended to a two-lane traffic model induced by lane-changing maneuvers in numerous ways and used to analyze a variety of real-world traffic problems [126–129]. Hence, many researchers relied on the microscopic models to investigate the vehicles emissions. Some scholars have studied the PM emissions due to their health and environmental implications [130, 133]. Qiao et al [134] studied the PM emission in a single lane using two types of slow-to-start models namely VDR [135] and TT [136] under periodic boundary and open boundary conditions. However, the PM effects can be mild if it was considered far from the cities like highways or expressway. In another hand, the effect of CO_2 emission on global warming cannot be neglected even though far from cities. As we know the global warming is a serious problem that can induce climatic change [137] etc. Scholar studied the effect of many metrics in vehicular traffic on the CO_2 emission. Binoua et al [138] studied the effect of two types of traffic lights controlling methods in a single lane CA model on the CO_2 emission and energy dissipation. Pérez-Sansalvador et al [139] investigated the influence of speed humps on traffic flow and on the exhaust emissions of CO_2, NOx, VOC, and PM. Recently, Wang et al [140], studied the pollutant emissions of mixed traffic flow which is composed of vehicles with different length and the maximum speed. Li-Dong and Wen-Xing [141] analyzed the signal control strategy for reducing CO_2 emission based on proposing a new relative speed discrete traffic flow model, which is derived from traditional coupled map car-following model. As we know the heterogeneity of traffic increase the energy consumption which negatively affect the vehicles emissions. The heterogeneity of speed can be induced by slow vehicles or with fixed bottlenecks. In two lanes traffic the vehicles that driver over the time in one lane can induce a change in the emission of vehicles. This chapter aims to investigate the CO_2 emission of a mixture traffic flow model which is composed of vehicles distinguished by their lengths and their maximum speed in two lanes CA model. The dependence of emission to the density as well as the impact of a homogeneous and inhomogeneous initial configuration on the CO_2 emissions were studied. Speed frequency is also investigated.

The remainder of this chapter is structured as follows. In the next section, the motion model that describe the straightforward movement, lane changing rules and the traffic emission model are presented, the simulation results are discussed in section IV.3. Conclusions are given in section IV.4.

IV.2 Methodology

In this section, the model used for the simulation of the car-following and lane-changing rules will be described, and the method used in the calculation of the CO_2 emission is also showed.

We considered the model proposed by Nagel-Schreckenberg II.4 where the space and time are discrete. The road is considered as a lattice of L sites, here we consider two parallel lattices to mimic the two-lane road scenario. Each site can either be empty or occupied by one vehicle, the accumulation is forbidden. In this chapter we consider of the heterogeneity of vehicles which can be long-slow vehicles or short-fast vehicles. The slow vehicle occupies two cells while the fast one occupies one cell where f_s is the fraction of slow vehicles in the system. Hence, the periodic boundary condition is adopted where the conservation of the number of vehicles is assured. The length δx of each site in real world equal $7.5m$. The straightforward motion is described as mentioned before with the NS model (See chapter1).

When a vehicle is obstructed or cannot move with its desired speed (i.e., $v_{max}^{f\,or\,s}$) in its actual lanes, in real traffic driver try to find solution to enhance his individual situation by lane changing. In our computation model we are going to adopt the rules proposed by Rickert et al II.3.6.2:

IV.2.1 Carbon dioxide emission model

In this chapter we will consider the model proposed by Panis et al [142] that depends on the instantaneous acceleration, velocity of vehicles and six coefficients. We should note that fast vehicles use petrol as a source of energy, while the slow ones use diesel as a source of energy (See table II.1).

IV.3 Results and discussion

Simulations are conducted to examine the exhaust emissions in two-lane model. In our computational study, we consider two lattices consists of $L = 5000$ sites. The simulation was performed with two categories of vehicles which distinguished by their length and maximum speed (i.e., slow vehicles ($l_s = 2; v_{max}^s = 3$) and fast one with the couple ($l_f = 1; v_{max}^f = 5$). Vehicles at the beginning of the simulation are distributed randomly all along the two lanes according to their fractions (i.e., $f_f = 0.8$ for fast and $f_s = 0.2$ for slow one). The closed boundary condition is adopted which means the number of vehicles in the lattices is conserved. We carry out the simulation with the same value of randomization $p = 0.2$. We are focused on the situation where the lane-changing are asymmetric, where the following measures are assumed $(ch^{f}_{lane1} = 1, ch^{s}_{lane2} = 1, ch^{f}_{lane2} = 1)$, the slow vehicles in the lane 1 have a different probability of lane-changing (i.e., this mimics the real case where the slow vehicles slow moving vehicles must remain in the slow lane). The system runs for $80,000$ steps of time. The calculation is done after the last 10 000 iterations, where the results were averaged over 100 times (i.e., 100 is the number of the different initial configuration of the vehicles).

IV.3.1 Homogeneous configuration

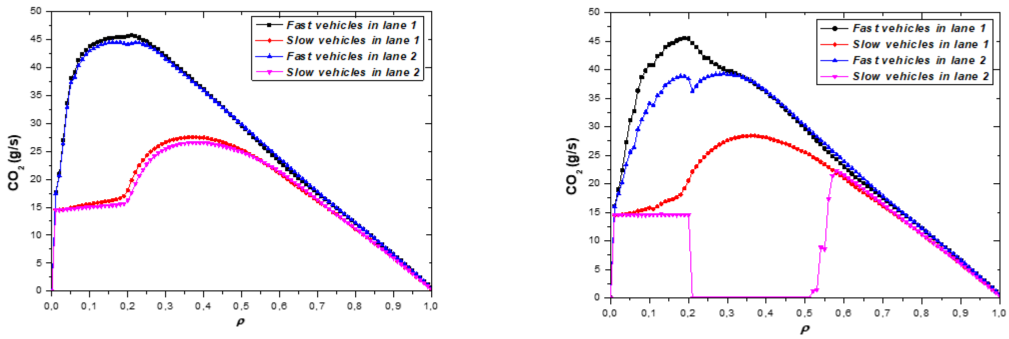

(a) **(b)**

FIGURE IV.1: The average CO_2 emissions against density ρ in homogeneous traffic in two-lanes. For a) $ch^{s}_{lane1} = 0.1$, b) $ch^{s}_{lane1} = 0$.

In this subsection we will investigate the homogeneous configuration which means that the slow vehicles are distributed overall both lanes.

The slow vehicle in real traffic has a great effect on traffic flow they condense the vehicles after them into a cluster of slow vehicles. The only way to escape from this situation is to find adequate space to do a safety lane-changing, however, in some cases, the slow vehicles also change lanes to increase their speed. In that case, fast vehicles sometimes can be trapped behind two slow-moving vehicles in both lanes. This situation can affect the traffic flow as well as the CO_2 emission. Hence, the distribution of the slow vehicles along the two-lane can drastically affect the fast vehicles flow. One of the ways that change the distribution of the slow vehicles in the two lanes model is the lane changing probability that mimics the aim of the vehicles to change the lane when the conditions are met (i.e., the safety and incentive criterion). Some countries have restriction that is prohibited for slow vehicles to occupy a lane continuously (or prohibited that the slow vehicles occupy the right lane) on the road with multilane. As a preliminary step we are going to investigate the effect of the ch^{s}_{lane1} on the CO_2 emission on both lanes. Figure IV.1 shows the CO_2 emission for several values of ch^{s}_{lane1} $(ch^{s}_{lane1} = 0.1, ch^{s}_{lane1} = 0)$. Fig. IV.1(a) displays the average CO_2 emissions against density ρ for fast and slow vehicles in two-lane for $ch^{s}_{lane1} = 0.1$. For slow vehicles, we can see that the CO_2 emissions increases with a small slope as the density increases, until a critical density $\rho = 0.2$, we observe a dramatic rise in CO_2 emission to a maximum value, followed by a sharp drop to a value approach to zero. We should note that for large densities the curves of CO_2 emissions coincide with each other which means that the CO_2 emissions depend only on the longitudinal interactions of vehicles. For fast vehicles, the CO_2 emissions show qualitatively and quantitatively the same behavior for all densities ranges except where $\rho \in [0.15; 0.22]$. For the case of $ch^{s}_{lane1} = 0$, Fig. IV.1(b) depicts the CO_2 emission as a function of the density ρ. In the lane 1, the CO_2 emissions of the slow vehicles increase with ρ, till reaching a maximum value then decays and converge to value approached to zero. In the lane 2, the CO_2 emissions were almost unchanged in the density range $[0, 0.2]$ for slow vehicles. As the density increases the CO_2 emissions drop rapidly and reach zero values in the density range $[0.21, 0.51]$. Subsequently, the CO_2 emissions rise rapidly pass through a maximum then started decrease gradually till reaching the $0.553 g/s$ which correspond to f_1. For the CO_2 emission of the fast vehicles in both lanes show similar feature expect in intermediate density where the CO_2 emission in the lane 1 is higher than that in lane 2.

To better understand the features of Fig. IV.1 it is better to understand the microscopic interaction between vehicles which is the main cause of the change in the CO_2 emission. Hereafter, in order to understand the difference between the CO_2 emission of the two lanes we investigate the spacetime configurations where the evolution of the vehicles in space and time is exploited. For lane 1, when $ch^{s}_{lane1} = 0.1$ and $\rho = 0.2$, the number of the slow vehicles is slightly bigger than that in lane 2 (see the red color in Fig. IV.2(a), (b)). That can explain why the CO_2 emissions in lane 1 are slightly higher than that in lane 2 (see Fig IV.1(a)). Here the low changing lane probability of the slow vehicles in the lane 1, increases the number of slow vehicles which imped the fast vehicles to move at their desired speed, thus increase moderately the CO_2 emission of the fast vehicles in the lane 1. For the case when $ch^{s}_{lane1} = 0$ and $\rho = 0.21$, the lane change probability prohibits the slow vehicles to change their lane even though the situation in lane 1 is not suitable for them to move with the desired speed. In this case, all slow vehicles in lane 2 merge into lane 1, which means that lane 2 is controlled by fast vehicles this explains why the CO_2 emission in lane 2 for the slow vehicles equals zero in the density range $[0.21, 0.51]$. In the same way, the presence of slow vehicles in one lane can increase the CO_2 emission of the fast vehicles in this lane, which explains why lane 1 shows a higher CO_2 emission compared to the lane 2.

As the lane changing affect drastically the distribution of vehicles in both lanes. The lane changing frequency can show us when the longitudinal interaction is the responsible for the CO_2 emission. Fig. IV.3 depicts the lane-changing frequency of the vehicles in two-lane for

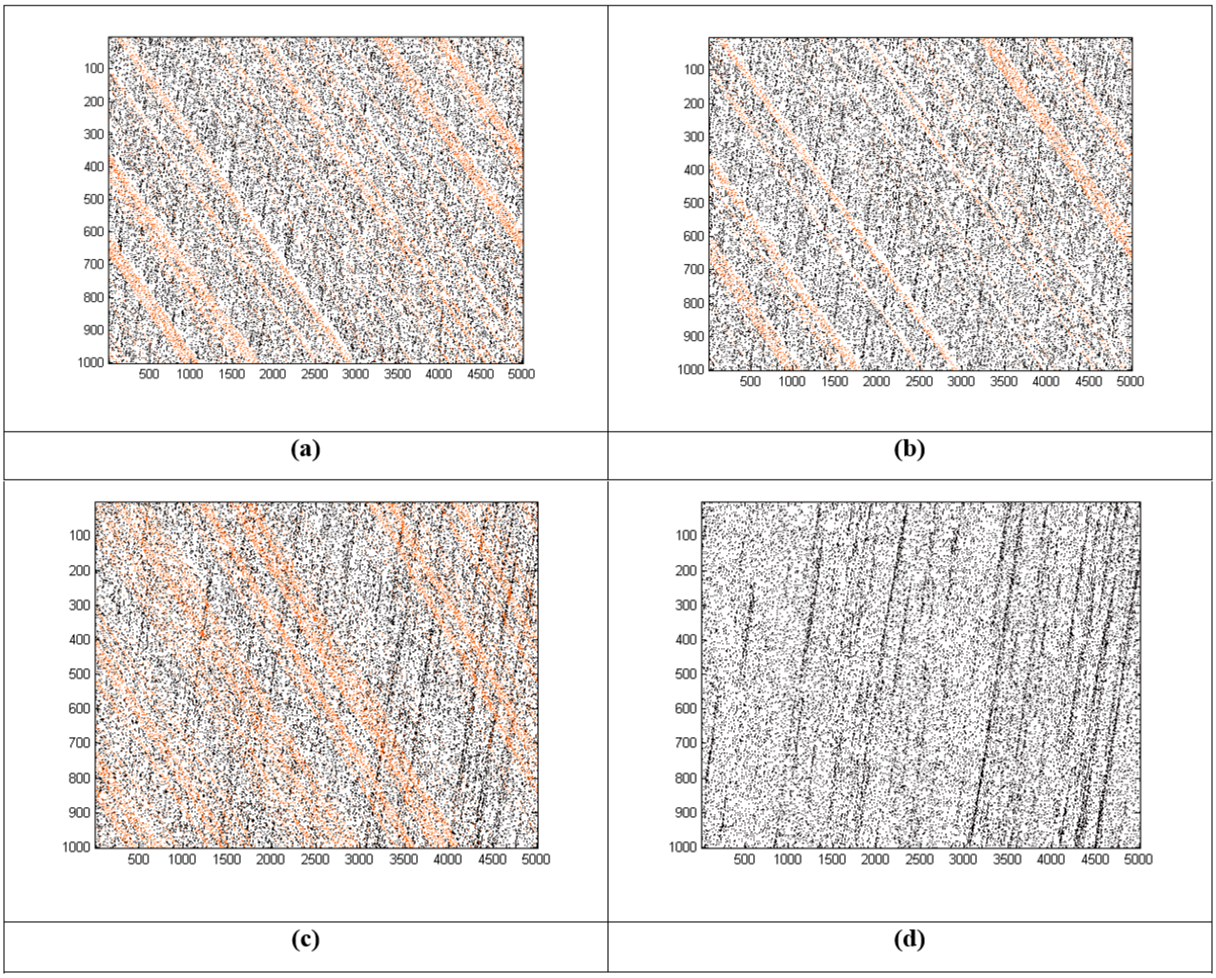

(a) (b) (c) (d)

FIGURE IV.2: Space time diagram for the two-lane. For $ch^s_{lane1} = 0.1$ and $\rho = 0.2$ (a) lane 1 (b) lane2. For $ch^s_{lane1} = 0.$ and $\rho = 0.21$ (c) lane 1. (d) lane2. Where the white color is the free-space and the black color corresponds to fast vehicles, orange color corresponds to slow vehicles.

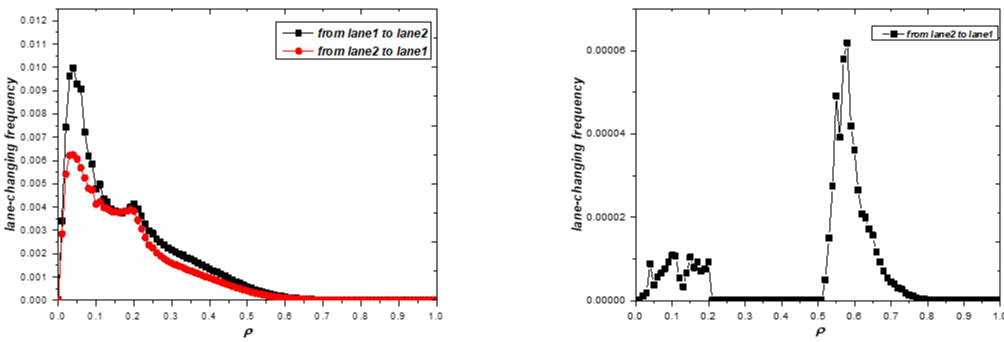

(a) (b)

FIGURE IV.3: Lane change frequency against the density for inhomogeneous traffic in two-lanes (a) fast vehicles, (b) slow vehicles for $ch^s_{lane1} = 0$.

a mixture traffic for $ch^{s}_{lane1} = 0$. As we can see at low-density, the lane-changing frequency of fast vehicles from lane1 to lane2 is larger than that for lane 2 to lane 1. In this situation the presence of the slow vehicles in lane 1 increase the lane changing frequency. At high density the CO_2 emission becomes the same for all vehicles we can explain that by the impossibility of lane changing for both types of vehicles in the two lanes, because of that the longitudinal interactions are the main cause of the CO_2 emissions. Another important note to discuss in Fig IV.3(b) where in the density range $[0.21, 0.51]$ the lane changing frequency equals zero, here the slow vehicles back to the lane 1 over the time before steady state and then for that they become trapped in the lane 1(we recall the initial configuration of both vehicles is homogenous which means that the slow vehicles re distributed equiprobably in both lanes). However, for $\rho > 0.5$ the slow vehicles that initialized at the beginning of the simulation in the lane 2 cannot find adequate space to do a safe lane changing which explains the presence of the slow vehicles in the lane 2 permanently even though if we increase the calculation time, and this mimics the real case near fixed bottleneck or in jams cases.
As one of the main causes of the lane changing of the fast vehicles is the variability of speed or the uneven speed distribution overall the two-lane which may provoke an increase in the CO_2 emission. The slow vehicles play the role of a moving obstacle for the fast vehicles and the speeds of the slow vehicles have a great effect on the CO_2 emission. Therefore, subsequently, we are going to study the effect of changing the speed of slow vehicles on the CO_2 emission in both lanes for the asymmetric case, where the slow vehicles in lane 1 have a low changing lane probability. This restriction causes the slow vehicles to have a preferred lane which is in this case lane 1.

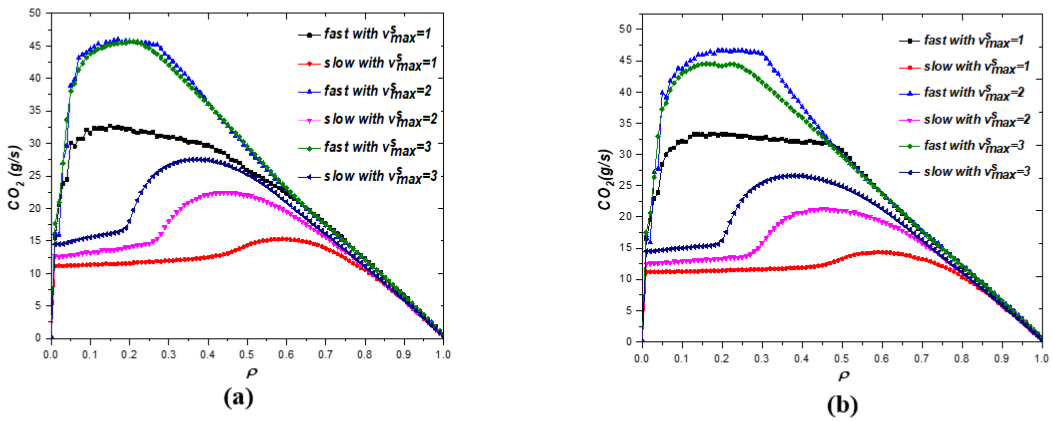

FIGURE IV.4: CO_2 emissions as a function of the density ρ in a heterogeneous traffic with $v^f_{max} = 5$, $v^s_{max} = 0.1$ and for several values of for $v^s_{max} \in 1, 2, 3$ (a) Lane1, (b) Lane2.

As we can see from Fig. IV.4 the CO_2 emission for the slow vehicles that have the maximum allowed speed equal to 1 vehicle is the lowest, the slow vehicles keep a stable emission rate even the density increase, however near to the value $\rho = 0.45$ the CO_2 emission shows a slight increase till a maximum value then start to decrease with the increasing of the density. In this case, the slow vehicles have a speed of 1 that only affected when the stopped vehicles appear in the system (by the large density or with the braking probability effect). The increase of the v^s_{max} increase the CO_2 emission for slow vehicles and the critical density that correspond to the maximum values of the CO_2 emission shift toward the lowest values of the density. As shown in the spacetime diagrams (see Fig. IV.5) the slow vehicles in the case of v^s_{max} can drive with their desired speed, the perturbation observed (see the slight deviation of the orange line in the space time for Fig. IV.5,IV.6, IV.7 (a) and (b)) is due to the braking probability that can affect the motion of the slow vehicles. However, in intermediate the distance shrunk, and the stopped vehicles appears which increase the stop and go process that explain the rise of the CO_2 emission. Hence, as the density increase the number of stop vehicles become predominant which meanly decrease the CO_2 emission. We should note that the main cause of the CO_2 emission in low densities for low values of v^s_{max} is the speed of vehicles. However, the contribution of the acceleration process become important when the stopped vehicles appear, and the heterogeneity of speed become highest. As comparted to CO_2 emission of slow vehicles in both lanes, the lane 1 shows the highest emission this is simply explained by the fact that the slow vehicles in the lane 1 have a lower changing probability $ch^s_{lane1} = 0.1$, which create a denser space even for low densities that increase the CO_2 emission. However, the slow vehicles have the same CO_2 emission as the fast ones in the high density (see the graph that become identic in the high density $\rho > 0.8$).

As for fast vehicles, in the high density even though we change the speed of slow vehicles the CO_2 emission in this case the spacetimes configurations show the almost the same features for the different values of the slow vehicles speed (see Fig. IV.5, IV.6, IV.7(e) and (f)). Hence, for intermediate densities we can observe a non-linear feature in the CO_2 emission of the fast vehicles where the CO_2 emission for $v^s_{max} = 1$ is the lowest and the highest for $v^s_{max} = 2$. Here, the slow vehicles in the case of $v^s_{max} = 1$ have a local effect on the fast vehicles. As seen in the spacetime the slow cluster provoked by slow vehicles is only observed behind the slow ones and moderate free space is observed between the clusters (see Fig. IV.5(c) and (d)). However, for the case of $v^s_{max} = 2$ the presence of slow vehicles provokes the perturbation overall the lane (Fig. IV.5(c) and (d)). Hence for the case of $v^s_{max} = 3$ a small number of slow vehicles is observed in the lane 2 this provokes a low CO_2 emission for the fast vehicles. Hence, in order to understand why the $v^s_{max} = 2$ show higher CO_2 emission than the case of $v^s_{max} = 3$, Fig. IV.8 depict the speed frequency of vehicles in both lanes. For the case of $v^s_{max} = 2$, the number of slow vehicles or speed vehicles is higher than that for the

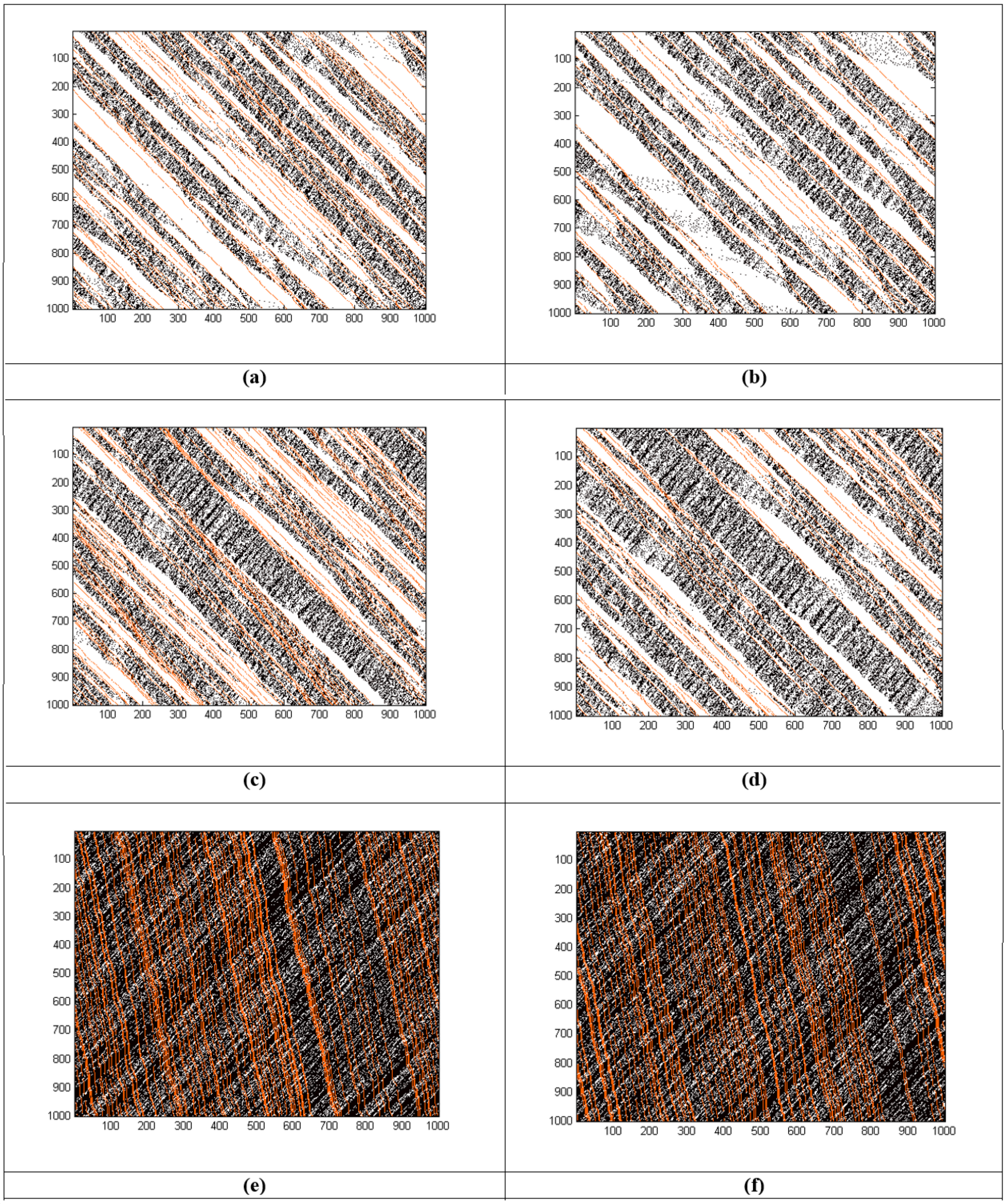

FIGURE IV.5: Space time plots of the proposed homogeneous traffic in both lanes, white color is the empty space, and the black color corresponds to fast vehicles, red color corresponds to slow vehicles for $v^s_{max} = 1$. Lane 1: (a) $\rho = 0.27$ (c) $\rho = 0.35$ (e) $\rho = 0.83$. Lane 2: (b) $\rho = 0.27$ (d) $\rho = 0.35$ (f) $\rho = 0.83$. with $ch^s_{lane1} = 0.1$.

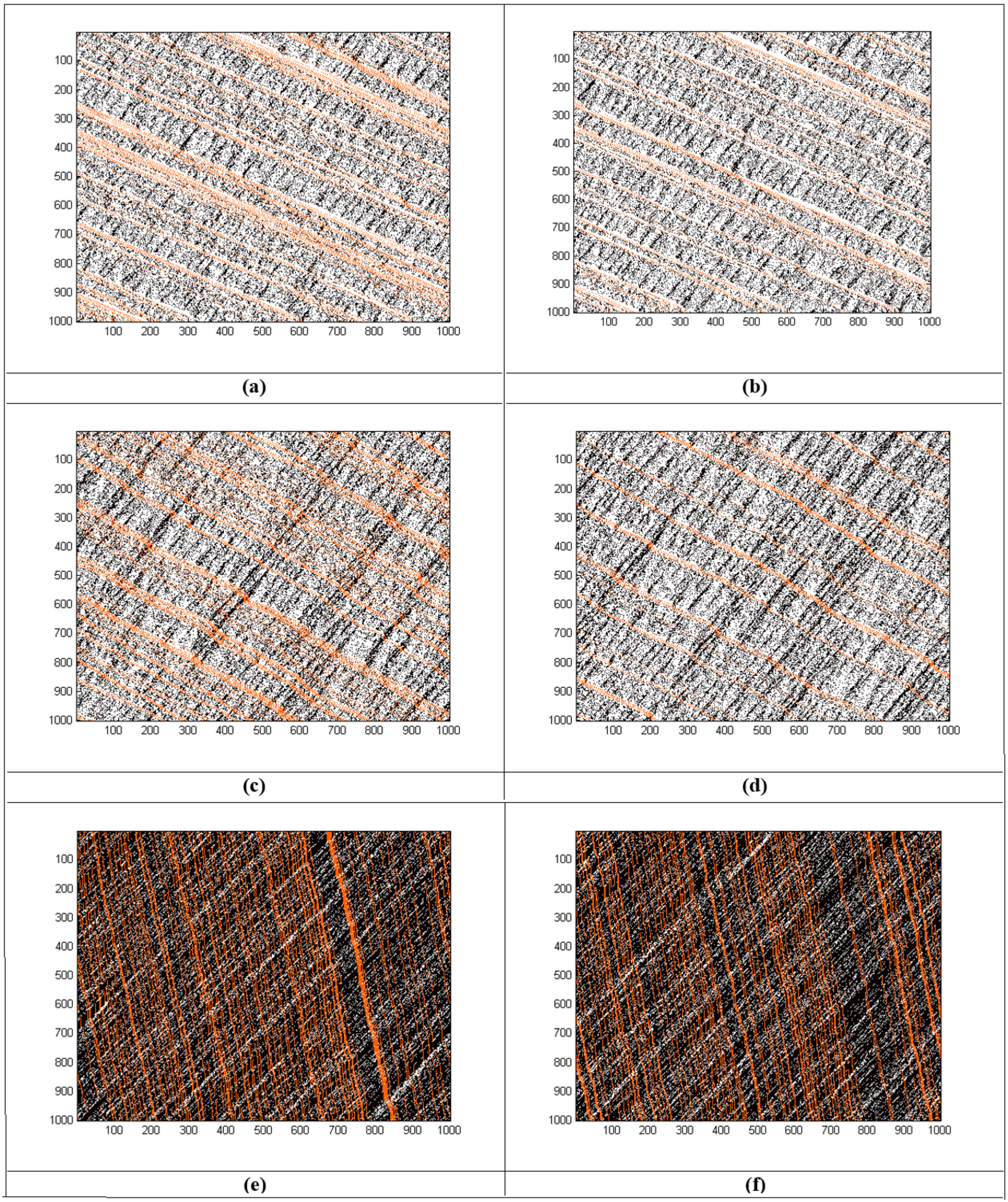

FIGURE IV.6: Space time plots of the proposed homogeneous traffic in both lanes, white color is the empty space, and the black color corresponds to fast vehicles, red color corresponds to slow vehicles for $v^s_{max} = 2$. Lane 1: (a) $\rho = 0.27$ (c) $\rho = 0.35$ (e) $\rho = 0.83$. Lane 2: (b) $\rho = 0.27$ (d) $\rho = 0.35$ (f) $\rho = 0.83$. with $ch^s_{lane1} = 0.1$.

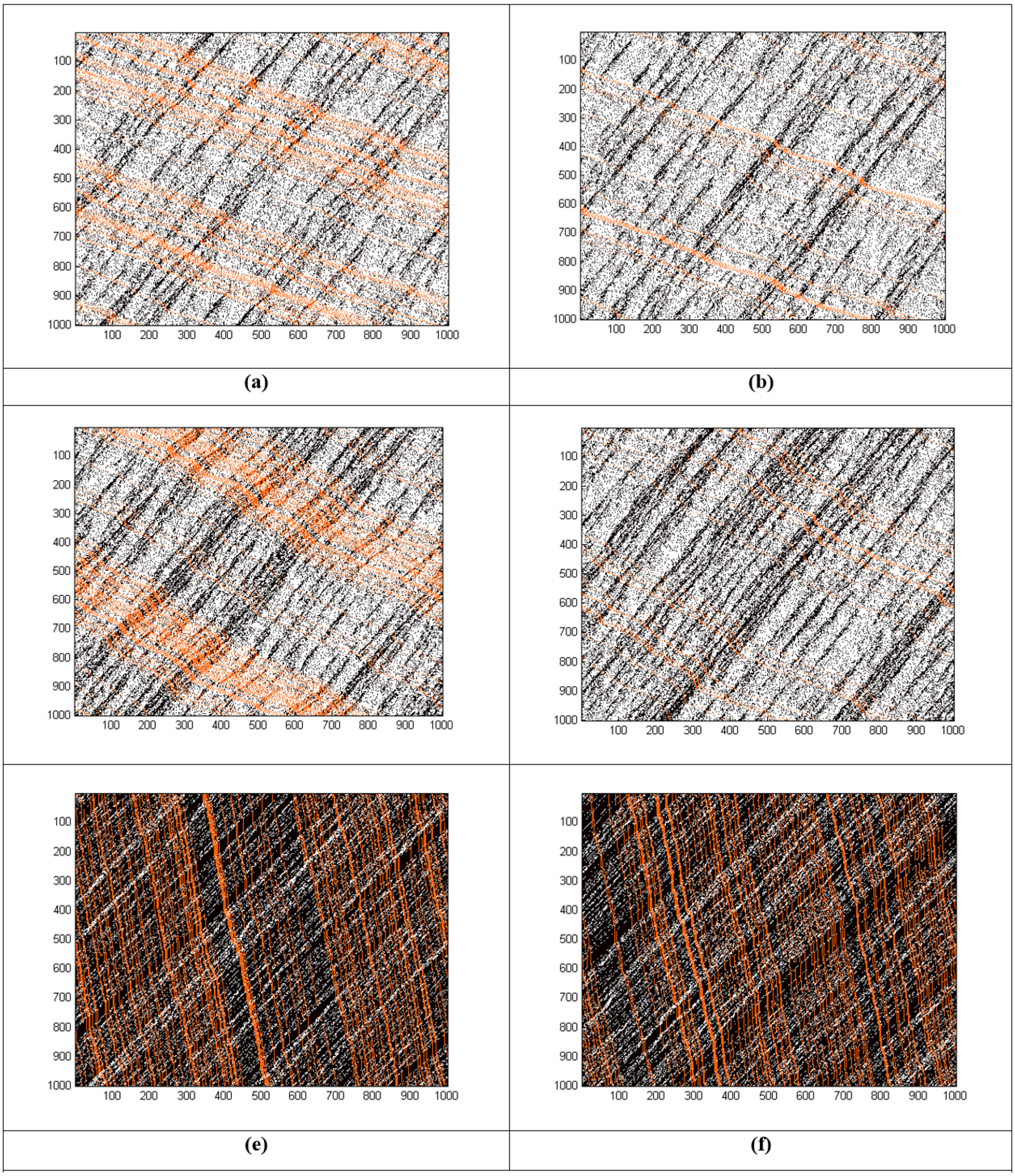

FIGURE IV.7: Space time plots of the proposed homogeneous traffic in both lanes, white color is the empty space, and the black color corresponds to fast vehicles, red color corresponds to slow vehicles for $v^s_{max} = 3$. Lane 1: (a) $\rho = 0.27$ (c) $\rho = 0.35$ (e) $\rho = 0.83$. Lane 2: (b) $\rho = 0.27$ (d) $\rho = 0.35$ (f) $\rho = 0.83$. with $ch^s_{lane1} = 0.1$.

case of $v^s_{max} = 3$, thus provokes the stop and go more often for the case of $v^s_{max} = 2$ which explain why the CO_2 emission is higher as compared to the case of $v^s_{max} = 3$.

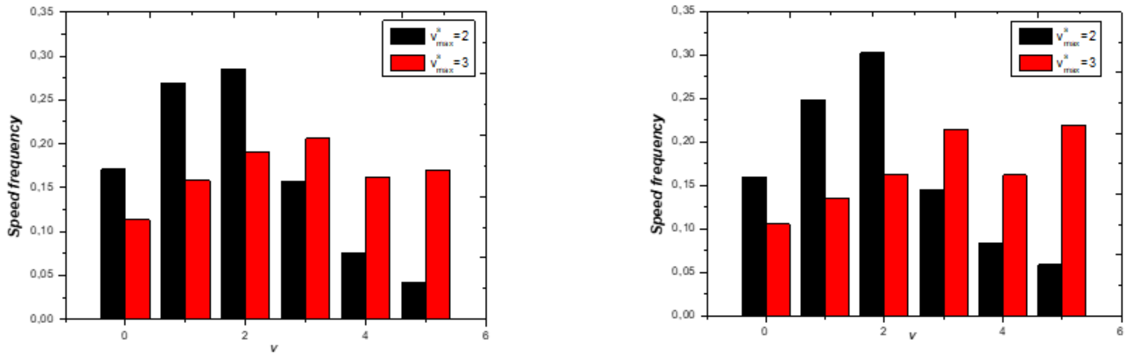

(a) **(b)**

FIGURE IV.8: The histogram of speed frequency for fast vehicles in (a) lane 1, (b) lane2 at the case of $v^s_{max} = 2,3$ with $\rho = 0.2$ and $ch^s_{lane1} = 0.1$.

IV.3.2 Inhomogeneous configuration

In this subsection, we will investigate inhomogeneous initial configurations, which means that slow vehicles are distributed randomly only on lane 1 while fast ones are distributed on both lanes. Fig. IV.9(a) depicts the CO_2 emission of vehicles in both lanes in the case where the slow vehicles in lane 1 have a lane-changing probability of 0.1. As we can see the CO_2 emissions of both kinds of vehicles in two lanes display a similar feature as seen in Fig. IV.1(a) except in the region where $\rho \in [0.62; 0.83]$, here, the CO_2 emission in the lane 2 is slightly bigger than that in the lane 1. The situation of finding an adequate space to do a safe lane changing become smaller in the density range $[0.62; 0.83]$ and because $ch^s_{lane1} = 0.1$ which can reduce the lane-changing frequency. We explain this by the fact that the initial configuration of the slow vehicles in lane 1 reduce drastically the speed of vehicles which reduces the heterogeneity of speed that affect the acceleration process thereby reducing the CO_2 emission in this lane. We should note that the CO_2 emission is higher when the traffic status is heterogeneous. Hence, for the large density (i.e., $\rho > 0.85$), the slow vehicles cannot change their lanes which make the slow vehicles confined in the lane 1. That explain why we get a zero in CO_2 emission value for the slow vehicles of the lane 2. As the ch^s_{lane1} decrease (see Fig. IV.9(b)) which affect the distribution of the slow vehicles in the system. The slow vehicles become confined in lane 1, which affects the speed of the fast vehicles, that is why we can explain the higher values of CO_2 emission, especially in the low densities. Hence, as the density increase, the effect of the slow vehicles becomes seldom. Hereafter, the only cause that determinate the CO_2 emission of the vehicles is the longitudinal interaction between vehicles no matter how type the vehicles is, because the traffic is denser. We should note that the CO_2 emission of the slow vehicles in lane 2 equals a zero because there are no slow vehicles in this lane because all slow vehicles keep moving in the lane 1.

For low density (see Fig. IV.10,IV.11 (a), (b)) the cluster is only observed for the case $ch^s_{lane1} = 0.1$, fast vehicles get trapped behind slow ones in both lanes. In other hand for $ch^s_{lane1} = 0$ fast vehicles can easily escape from slow ones by changing their lane and because the lane 2 has no slow vehicles this reduce the CO_2 emissions. For intermediate density (see Fig. IV.10,IV.11 (c), (d)), traffic situation in both lanes is similar, as the stop and go are observed all over the two lanes. For extremely high density (see Fig. IV.10,IV.11 (e), (f)) slow vehicles become confined in lane 1 even though that we change the probability of lane changing, where CO_2 emissions are the same for both lanes (types of vehicles).

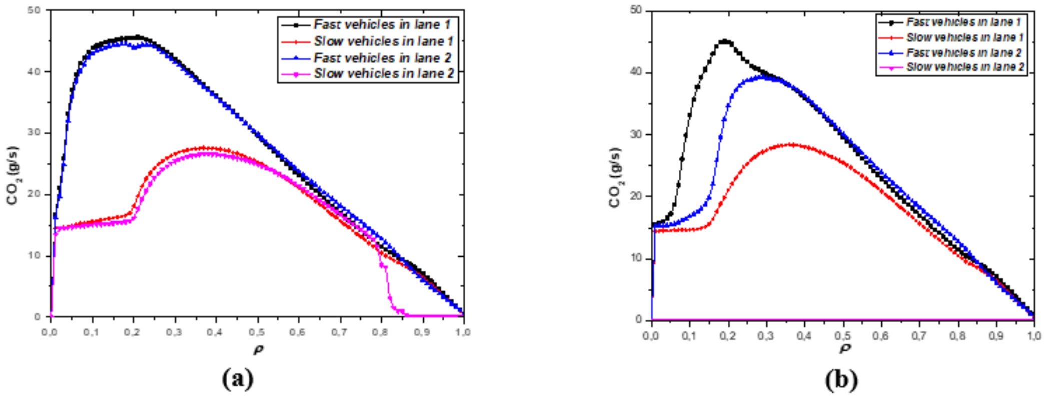

FIGURE IV.9: The average CO_2 emissions against density ρ in inhomogeneous traffic in two-lanes. For a) $ch^s_{lane1} = 0.1$, b) $ch^s_{lane1} = 0$.

IV.4 Conclusion

Traffic heterogeneity impedes fast vehicles from reaching their target speed and increases carbon dioxide emissions. In this chapter we propose a cellular automata model to investigate the effect of slow vehicles on the CO_2 emissions and on the microscopic structure of traffic. The asymmetric scenario is evaluated, where the slow vehicles have a different lane changing probability. This situation mimics the real case where slow vehicles are prohibited to move continuously in the fast lane. The initial configuration is evaluated, where we call homogenous case when the slow vehicles likewise the fast vehicles can be distributed over the two lanes. Hence, in the inhomogeneous configuration the slow vehicles can start in slow lane only, however for both cases the fast vehicles are disturbed randomly in both lanes. We found that in both initial configurations, fast vehicles emit more pollutants than slow in terms

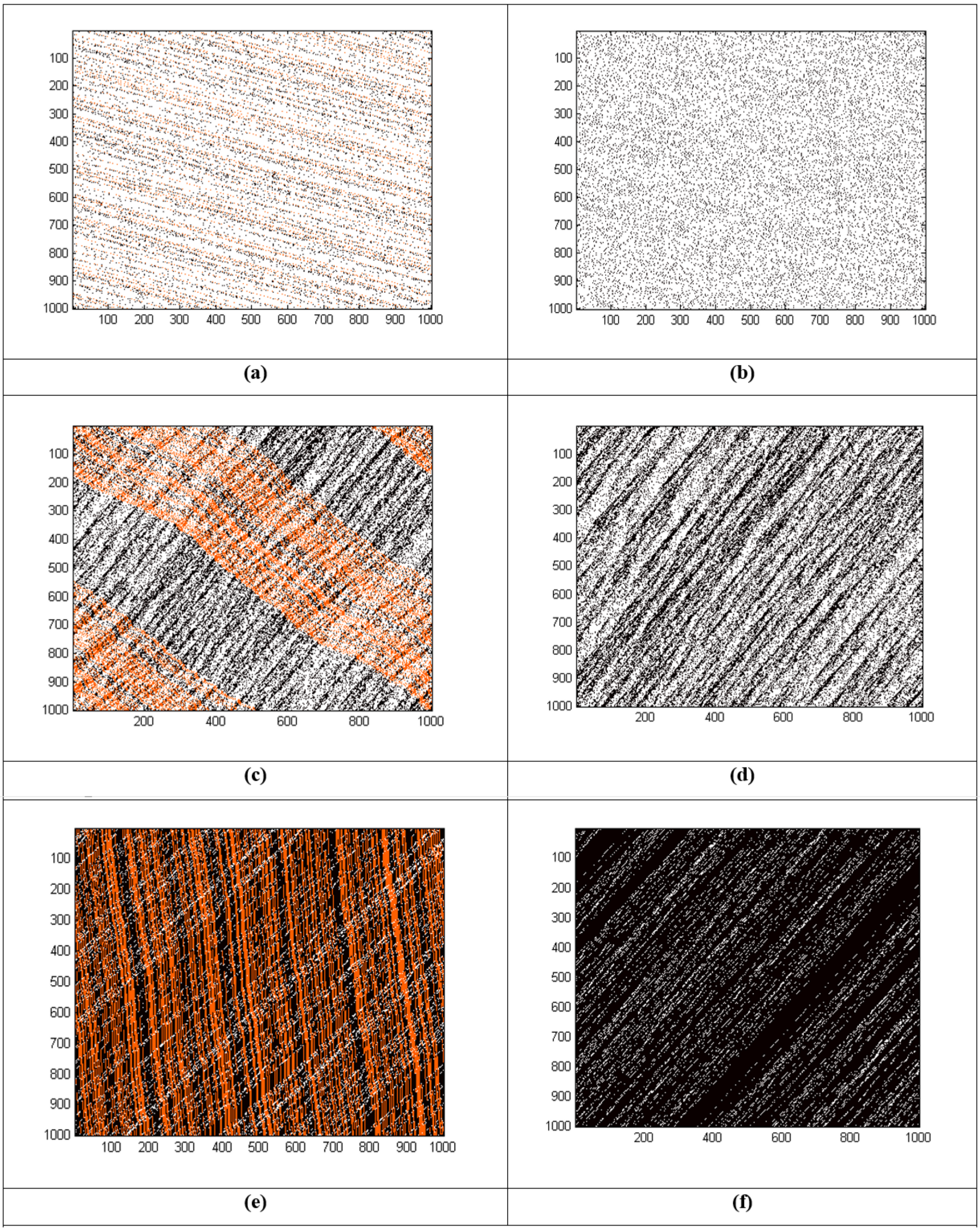

FIGURE IV.10: Space time diagram for inhomogeneous configuration in two-lane traffic model. For $ch^{s}_{lane1} = 0$. Lane 1: (a) $\rho = 0.1$ (c) $\rho = 0.4$ (e) $\rho = 0.9$. Lane 2: (b) $\rho = 0.1$ (d) $\rho = 0.4$ (f) $\rho = 0.9$. Where the white color is the free-space and the black color corresponds to fast vehicles, red color corresponds to slow vehicles.

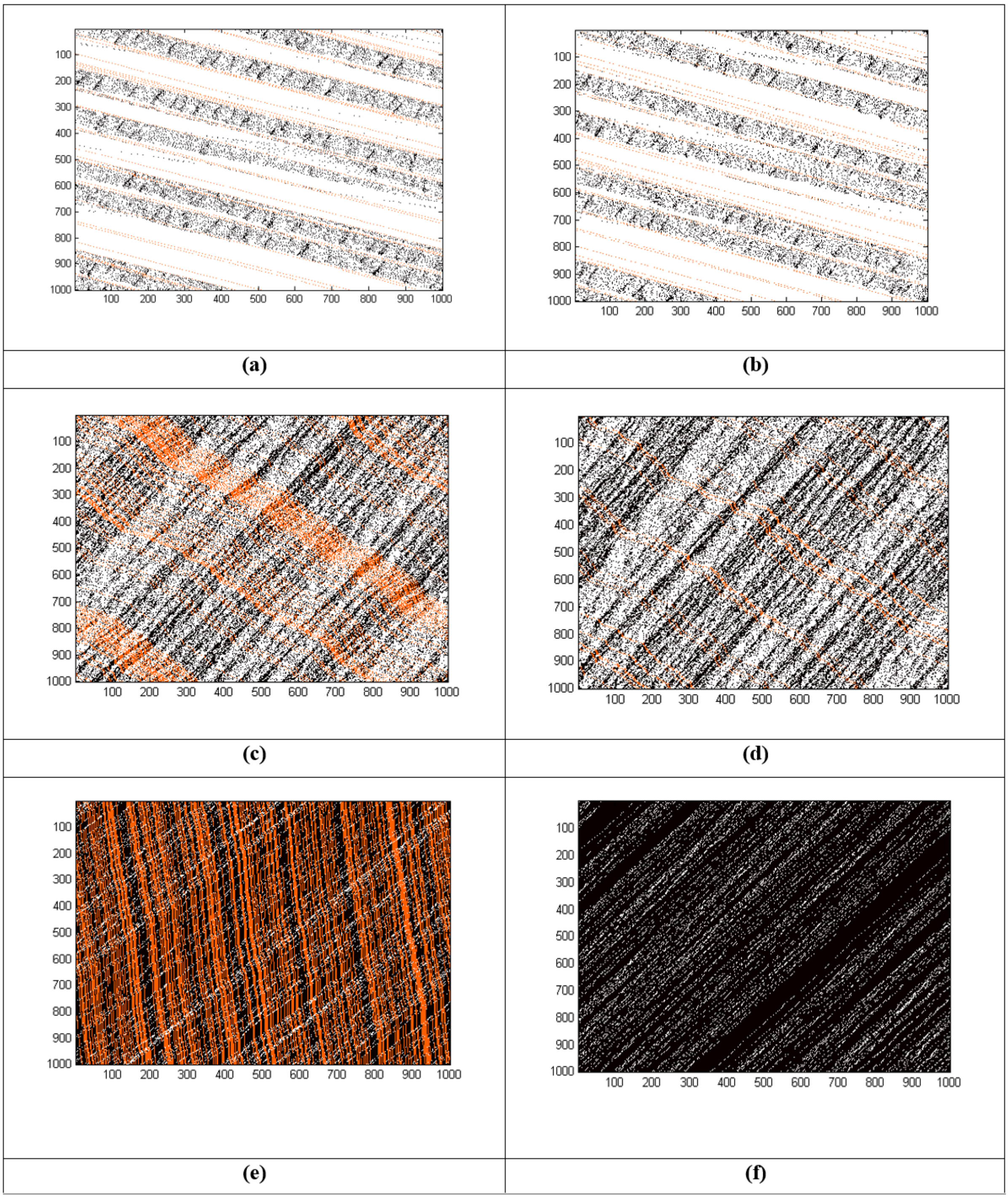

FIGURE IV.11: Space time diagram for inhomogeneous configuration in two-lane traffic model. For $ch^{s}_{lane1} = 0.1$. Lane 1: (a) $\rho = 0.1$ (c) $\rho = 0.4$ (e) $\rho = 0.9$. Lane 2: (b) $\rho = 0.1$ (d) $\rho = 0.4$ (f) $\rho = 0.9$. Where the white color is the free-space and the black color corresponds to fast vehicles, red color corresponds to slow vehicles.

of CO_2 especially in intermediates density. This fact is due to the drastic effect of the slow vehicles on the fast ones.

Chapter V

Traffic flow in two-lane cellular automaton model with two types of Bottlenecks

V.1 Introduction

Nowadays, traffic congestion has become a major problem in many countries around the world. Due to its negative consequences on individuals and society, traffic congestion attracted the attention of scientists from different backgrounds [143–148]. Traffic congestion can be provoked when the demand exceeds the road capacity because of the increase in the density of vehicles. One of the main reasons for the density increase is the bottleneck where it can be a result of a lane drops, accidents area, off-ramp, on-ramp, etc. The name bottleneck means the narrowest point, which is in real traffic can be produced when the density of vehicles in the upstream is higher than that in the downstream. The effect of bottleneck has been studied by researchers to reveals the causality relation between it and the traffic congestion. Implicitly researchers investigated the bottleneck types (i.e., moving and fixed). Chowdhury et al.[149] studied the effect of the slow-moving vehicles (which can be considered as a moving bottleneck) in a two lanes cellular automaton (CA) model. They found that the higher contribution of the fast vehicles to the throughput is observed when the asymmetric lane-changing rules model is adopted (here the asymmetric lane changing rules refers to the case when the fast vehicles have priority over the slow one in a lane, the slow ones have to shift to the slow lane). Knospe et al.[150] discussed the effect of slow vehicles in a two-lane CA model. They observed that even a small number of slow vehicles can induce the formation of platoons at low densities. Juran et al.[151] developed a dynamic traffic assignment model which could determine the impact of moving bottleneck. They found that the moving bottleneck can provoke an increase in travel times and it affects the distribution of traffic among available traveling paths in the network. Using the optimal velocity model [152, 153], Fang et al.[154] showed that the effect of moving bottleneck augments with the increase of traffic density, and their effect becomes lower when the maximum speed of slow-moving vehicles increases. Lakouari et al.[155] studied the interactions between vehicles in bidirectional traffic CA model with two types of vehicles (slow, fast). They found that when the density of one lane increases the slow-moving vehicles control the other lane by imposing their speed over the fast vehicles. Ou and Tang [156] proposed an extended macro traffic flow with a moving bottleneck model in order to study the effects of a moving bottleneck on the evolution and propagation of traffic flow under uniform flow and a small perturbation. They found that the influences of moving bottleneck depend strongly on the initial traffic density.

On the other hand, the effect of the fixed bottleneck was also investigated. Zhu et al. [157] analyzed the effect of speed bottleneck on the spatial-temporal evolution characteristics of traffic and the influence of the position and length of bottleneck on the traffic flow state. They suggested that the use of the feedback signal can improve the traffic situation. Hanaura et al.[158] derived the fundamental diagrams of a two-lane highway with a few slowdown sections. They found the dependence of jam lengths on density numerically and analytically. Zeng et al.[159] proposed a CA model to simulate the traffic flow characteristics under the combined bottleneck of accidents and on-ramp. They observed that the congestion caused by the accident will propagate to the upstream under the saturated flow. Chau et al.[160] investigated the effect of tollbooths on the traffic flow in a single lane CA model based on Fukui and Ishibashi [161] as well as the green wave model proposed by Torok and Kertesz [162].

Furthermore, On-ramps and off-ramps have been studied using CA models in Refs [163–167]. As the bottleneck can provokes jams in the real traffic it can also induce accidents. Marzoug et al. [168] investigated the conflict caused by two vehicles simultaneously entering a bottleneck, this conflict can induce an accident if the vehicles do not pay attention to each other.

In this chapter, we propose a two lanes CA model, where the two types of bottlenecks were considered (i.e., moving and fixed), where the initial configuration of the both types of vehicles is homogenous (i.e., the slow and fast vehicles occupy the both lanes with the same probability which means that we do not consider a lane as a fast or slow). The fixed bottleneck is sited in one lane, vehicles that impeded by the fixed bottleneck can change their lanes in order to increase their speed. This study can also be considered as an attempt to find out the relationship between the length of the bottleneck and the traffic proprieties in a two-lane CA model. The effect of the bottleneck on the vehicle's collision probability was also investigated. The rest of the chapter is organized as follow, in section V.2 we will present the methodology of this investigation, hence for the section V.3 we will discuss the results, the conclusion is given in section V.4.

V.2 Methodology

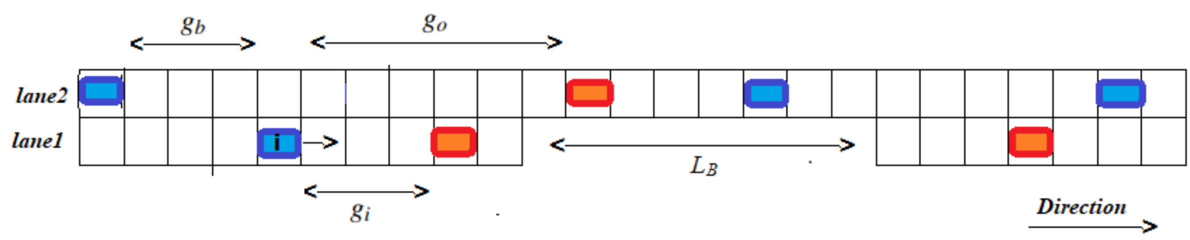

FIGURE V.1: Sketch of the model the blue color represents the fast vehicles while the red color denotes the slow vehicles.

The two-lane CA model mimics a two adjacent unidirectional road, here each lane in the model is composed of L cells. Each cell can be either empty or occupied by only one vehicle. The accumulation in our model is forbidden it means that it is not allowed that one cell can be occupied by two vehicles. The vehicles are characterized by their speed (v_i) and position (x_i). The vehicles differ according to their maximum allowed speed, where the maximum speed of the slow (fast) vehicles is v^s_{max} (v^f_{max}). The vehicles are uniformly distributed all over the two lanes according to the fraction of fast (f_f) and slow vehicles (f_s). The longitudinal motion of vehicles is described by the Nagel and Schreckenberg model (NaSch) according to the rules seen in II.3.2.3.
g_i denote the number of free cells in front of the vehicle i, where $g_i = x_{i+1} - x_i - 1$. The interaction between the two lanes is introduced by the lane-changing rules. The movement of vehicles is divided in two sub-steps. In the first sub-step: vehicles change lanes in parallel according to lane-changing criteria. In the second sub-step: the both lanes are treated as a separate single-lane where the NaSch model is applied. We considered the model proposed by Rickert et al (see II.3.6.3). where the rules of lane-changing taking into account two criteria.

- Incentive criterion:
  - $R'_1 : g_i(t) < v_d = Min(v_{i+1}, v^{(fors)}_{max})$.
- Safety criteria:
  - $R'_2 : g_o(t) > g_i(t)$.
  - $R'_3 : g_b(t) \geq v^{(fors)}_{max}$.

Here, $g_{back}(t)$ ($g_{other}(t)$) denote number of free cells behind (in front) of the vehicle i in the other lane (see Fig.V.1), Here, g_{back} ($g_{other}(t)$) denote number of free cells behind (in front)

of the vehicle i in the other lane (see Fig.V.1), while v_d is the desired speed of the vehicle i at instant t.
Here, the lane-changing probability is defined according to the type of the vehicle (slow or fast) and to the lane (lane 1 or lane 2). In this chapter, only the symmetric case is adopted which means that there is no preference in a lane over another lane or the fast vehicle has a higher probability of lane-changing. The ch is the probability of lane-changing for both types of vehicles from lane 1 (lane 2) to lane 2 (lane 1).
In real traffic, the bottleneck affects strongly the quality of traffic flow nearby it. In our model we considered two types of bottlenecks namely; moving and fixed. The slow-moving vehicles are considered as a moving bottleneck. Hence, in order to mimic the fixed bottlenecks in our model, we consider a L_B sites in the lattices that present an obstacle where, the both lanes are reduced to a single one as shown in Fig V.1.
We use the model proposed by Boccara et al, that take into account the probability of the rear-end collision in a single lane CA model (See II.8.1). These dangerous situations are computed and considered as the signal of the occurrence of a rear-end collision with a probability p'.
On the other side, in the two lanes traffic the collision can be induced by the unsafe lane-changing of the vehicles (i.e., when the vehicles do not respect the safety criteria of the lane-changing). In this propose our investigation takes into account this type of collision. Therefore, we will consider two types of collision namely; rear-end and lane-changing collision. We should note that the accident does not occur really in our system instead of that we have just calculated the probability of an accident to occur. The probability of the lane-changing collision to occur is computed if the following rules are fulfilled:

- Incentive criterion
    - $g_o(t) > g_i(t)$.
    - $g_b(t) < v_e(t+1)$.

Here v_e is the expected speed of the coming vehicle of the destinated lane (i.e the hoping lane for the vehicle that want to improve it speed by lane-changing, here this vehicle can collide with the coming vehicle in the hopping lane).
If the above conditions are achieved, a vehicle will cause an accident with a probability p''. Here, the probability of accident is defined as in II.8.1.

V.3 Results and discussion

In this section we will study the effect of the bottleneck on the traffic flow and the probability of car accidents in both lanes. We consider a two-lane road each is composed of 1000 sites.

The braking probability for all vehicles is $p = 0.2$ and the lane-changing probability is $ch = 1$. The probability for a dangerous situation (a dangerous situation means that the all condition of an accident to occur are met) can cause a rear-end collision (lane-changing collision) is sited as $p' = 0.01$ ($p'' = 0.01$). The traffic is heterogenous that means the existence of two kinds of vehicles that are distinguished by their maximum speed; $v^f_{max} = 5$ for fast vehicles and $v^s_{max} = 3$ for slow ones. The fraction of slow (fast) vehicles is considered as $f_s = 0.2$ ($f_f = 1 - f_s = 0.8$). The systems run for 60000 time-steps. The calculation is done for the last 10000-time steps with 100 independent simulations.

V.3.1 Fundamental diagrams for several length of the bottleneck

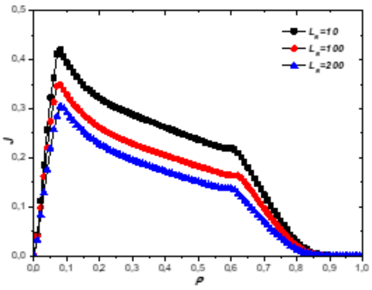

(a)

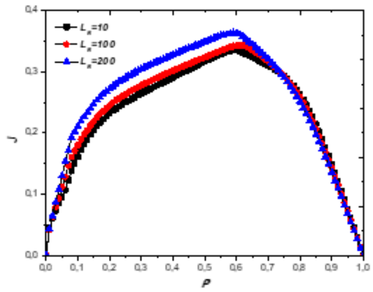

(b)

FIGURE V.2: Fundamental diagrams for several length of the bottleneck where (a): lane 1, (b): lane 2

Traffic flow can be affected by two types of defects, slow moving vehicles that are considered as moving defect and the bottleneck zone which is considered as the static defect. As we know bottlenecks increase the slow platoons and condense free space in front of them likewise the Bose-Einstein condensation in the low temperature [171]. The static defect could induce an emergent phenomenon which is the jam caused by the deceleration of vehicles that reduce the traffic flow locally. During the rest of this chapter and for simplification we refer to the moving bottleneck (fixed bottleneck) by the slow vehicles (bottleneck).

Subsequently, in our computational study, the mixture of both defects is considered (slow vehicles and bottleneck) in the same system. As a first step let us see the throughput in both lanes with the presence of bottleneck and slow vehicles. Fig. V.2 shows the fundamental diagram for different values of bottleneck length L_B. For the lane 1, where the bottleneck is sited, the current J increases rapidly as the density ρ increases until it reaches a maximum value, then it starts decreasing slightly. For high density, the current starts decreasing rapidly until its value becomes zero. For lane 2, the current augments with the density until a maximum value then it drops. Here, the increase of L_B reduces (increase) the current in lane 1 (lane 2).

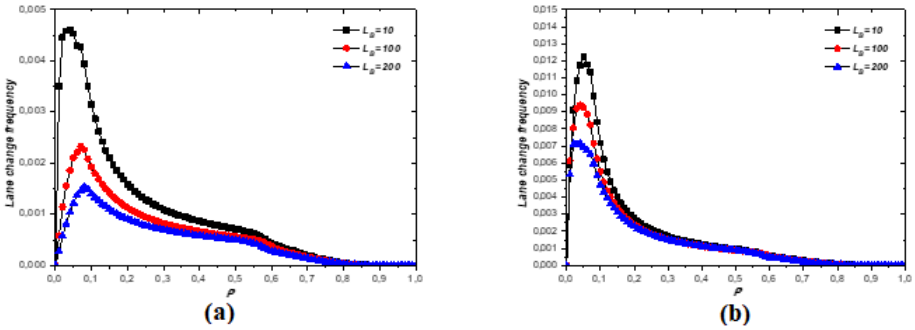

FIGURE V.3: Lane change frequency against the total density of vehicles, where (a): from lane 1 to lane 2, (b): from lane 2 to lane 1.

As we know the interaction between the two lanes is induced by the lane changing of vehicles. Therefore, to understand the variation of the throughput in both lanes it is better to illustrate the lane-changing frequency. Fig. V.3 depicts the lane-changing frequency as a function of the density for different values of L_B. The curves of lane-changing frequency show similar features, it reveals that there is a rapid increase in the lane-changing frequency until its maximum value then starts decreasing gradually, beyond $\rho = 0.75$ it becomes zero. The effect of lane-changing is only presented in the density range 0 to 0.75, another important observation is that the lane changing frequency for the case of short length L_B is the highest. We can explain that by the decrease of the distance between vehicles when the length of the bottleneck is increased, therefore the task of finding an adequate gap to change the lane becomes not obvious which reduces the lane-changing frequency. For the case of $\rho > 0.75$, the lane-changing becomes impossible, therefore, the current is determined only by the longitudinal interaction. In this case, for lane 1 the value of the current becomes zero because of the obstruction of the bottleneck; the vehicles get trapped in this lane. However, for lane 2, lane-changing is not possible for all vehicles, therefore the order of vehicles reminds the same, and for those range of densities, the slow and fast vehicles were forced to reduce their speed. The value of the current remains the same for lane 2 even if the size of the bottleneck in the other lane is reduced.

To get a better insight into the effect of the bottleneck on the traffic characteristics, we present the space-time configuration in Fig. V.4, The white color represents the free space while the black color denotes the fast vehicles and the red color represents the slow vehicles, hence, the yellow color denotes the bottleneck. The horizontal axis represents the space where the evolution of space is from left to the right, while the perpendicular axis represents time, where the evolution of time is from up to down. For low densities, lane 1 where the bottleneck is sited the traffic flow is controlled by the fast vehicles. However, the slow vehicles can be seen only in lane 2. The vehicles try to move with their desired speed as the

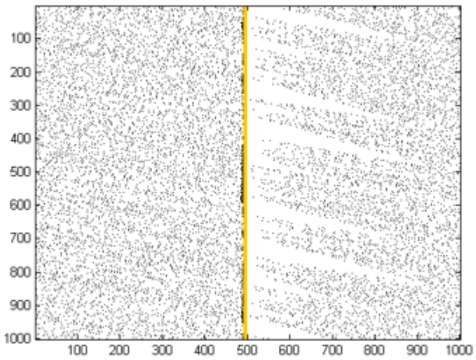

Lane 1

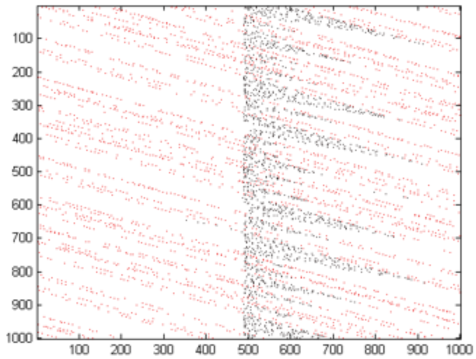

Lane 2

(a)

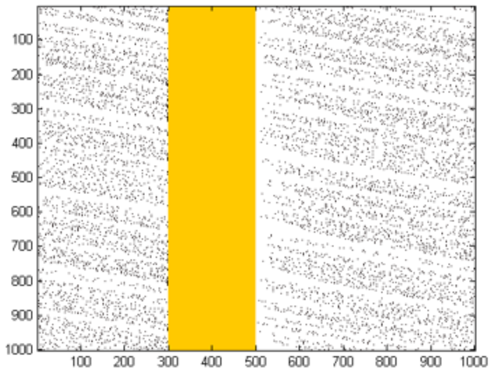

Lane 1

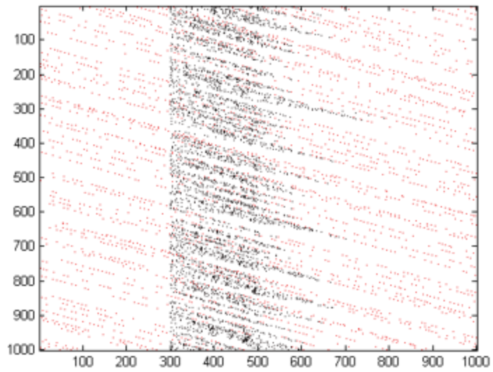

Lane 2

(b)

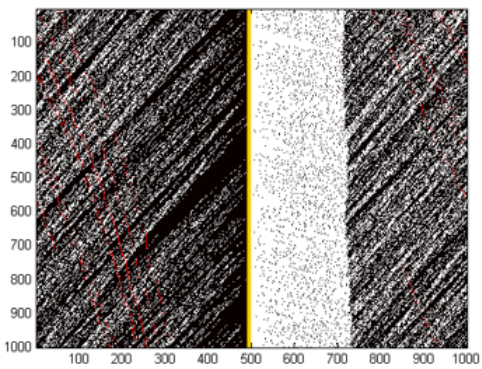

Lane 1

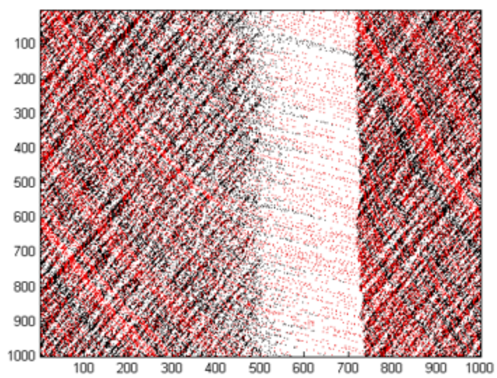

Lane 2

(c)

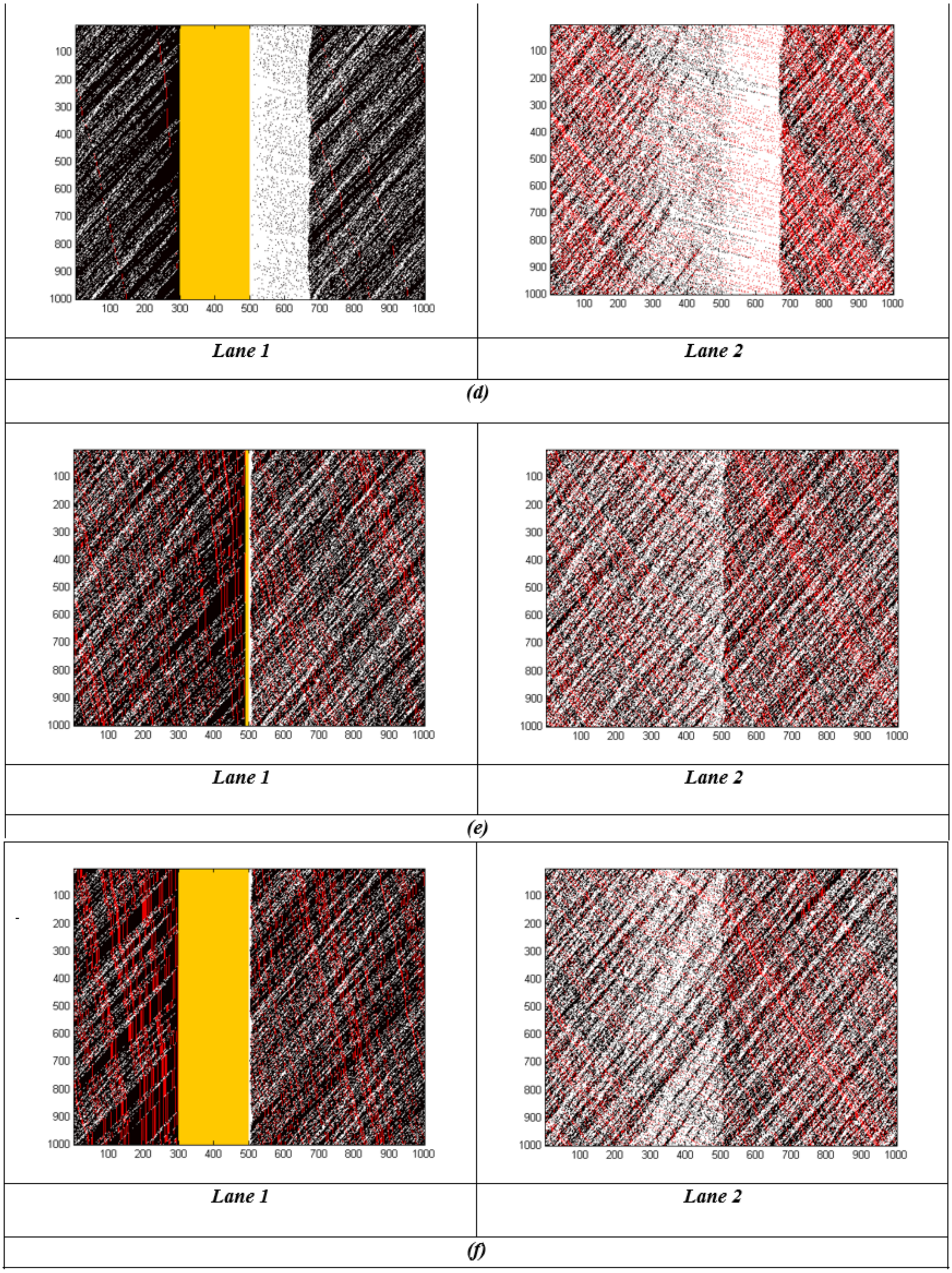

FIGURE V.4: Spacetime configuration for several values of L_B a) $L_B = 10$, $\rho = 0.05$ b) $L_B = 200$, $\rho = 0.05$, c) $L_B = 10$, $\rho = 0.5$ d) $L_B = 200$, $\rho = 0.5$, e) $L_B = 10$, $\rho = 0.65$, f) $L_B = 200$, $\rho = 0.65$

vehicles approach the bottleneck, they change the lane. In this case, for the low densities the number of free spaces is large, this makes the slow vehicles satisfied and confined in this lane. Nevertheless, for the fast vehicles, the situation is different they change the lane in order to increase their speed because of the bottleneck and the slow vehicles. At first, they are obligated to change the lane 1 to skep from the hindrance caused by the bottleneck, after passing the sites of the bottleneck fast vehicles return to lane 1 because of the slow-moving vehicles that control lane 2.
As the density increase, the queue of stopped vehicles increases and the situation in both lanes is worsen. The jam formed behind the bottleneck in lane 1 increase and spread over all this lane. In this case, the lane-changing from lane 1 to lane 2 is reduced because the safety criterion is never fulfilled. On the other hand, the bottleneck blocks the vehicles in lane 1 thus increase the free space upstream of the bottleneck in the same lane. In this case, if the length of the bottleneck L_B increases, the density of vehicles is reduced locally as corresponding to lane 2. This can be explained by the impossibility of lane-changing in the region of the bottleneck (i.e., vehicles in lane 2 cannot move to lane 1 because of the bottleneck), vehicles in lane 2 moves as a cluster with the same speed and when they reach the last sites of the bottleneck vehicles can move to the lane 1 where the free space exists (because of the condensation of the free space caused by the bottleneck) which improve the traffic situation in lane 2 even for high densities.
As we saw from the spacetime configuration the bottleneck plays an important role to defines the traffic flow in both lanes. On one hand, the bottleneck condenses the free space in front of it in both lanes because the hindrance of traffic in lane 1 increases the free space which is useful for lane-changing for vehicles of lane 2 which reduces the number of vehicles in lane 2 as seen. On the other hand, the queue of stopped vehicles increases as the density increases. The bottleneck is considered as a local defect in the two-lane model, the distribution of both defects (bottleneck and slow vehicles) on road can also cause serious problem in traffic, such as the accident.
Hereafter, the vehicle accident was studied, both types of accidents were considered (rear-end collision and the collision due to unsafe lane-changing).

V.3.2 Rear end collision

Let's investigated the rear-end collision probability (see Fig. V.5). For extremely low densities, P^R_{acc} equals zero for both lanes, because all vehicles can move with their desired speeds even with the existence of the bottleneck. However, as the density increase, small perturbations in both lanes induced by the bottleneck appears which reduce the speed of vehicles, as a result, the stopped vehicles emerge which increase the probability of rear-end collision. The graphs of the car accident probability reach a maximum then start decalin, in that case,

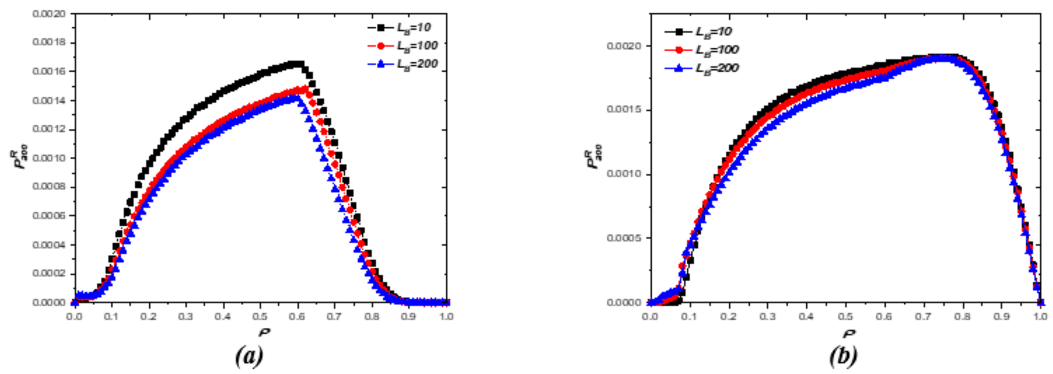

FIGURE V.5: Rear end collision probability for a) lane 1, b) lane 2.

the number of stopped vehicles in both lanes become higher. In lane 1, for high density, the rear-end collision probability becomes zero because of the deadlock situation caused by the bottleneck and the impossibility of lane changing. In lane 2, for low and high density the probability of vehicles rear-end collision is independent of the bottleneck length here the longitudinal interaction between vehicles controls the traffic situation. For the intermediate densities, car accident probability decreases as the length of the bottleneck increase. In order to understand this feature, let's see the frequency of speed in both lanes for $L_B = 10$ and $L_B = 200$ (see Fig. V.6). For the lane 1, the range of the specter of speed is wide for the case of $L_B = 10$ which means that even the presence of stopped vehicles they don't control the system. In this case, the heterogeneities of speed in lane 1 for $L_B = 10$ increase the rear-end collision. On the other hand, for $L_B = 200$ even the probability of stopped vehicles is higher than that in the case of $L_B = 10$ (see Fig. V.7), however, the length of the bottleneck reduces the fluctuation of speed vehicles which reduces the probability of rear-end collision. For lane 2, the situation is slightly different in both terms (qualitatively and quantitatively), here, the specter of speed is heterogeny for both cases, and the bottleneck is not presented in this lane, the increase of the stopped vehicles increases the probability of vehicles accident.

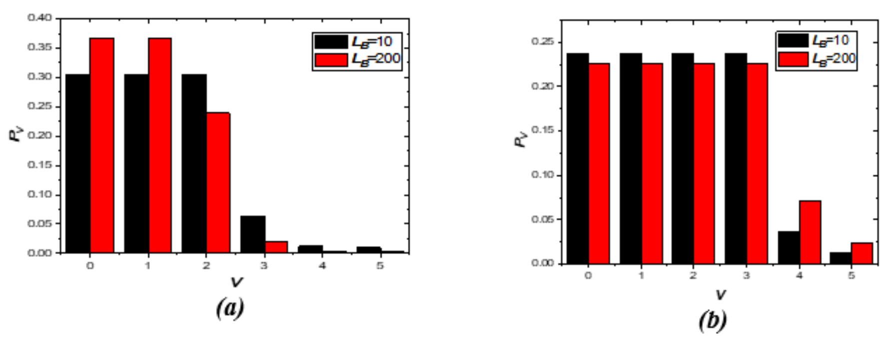

FIGURE V.6: Speed frequency for $\rho = 0.6$ a) lane 1, b) lane 2.

In order to get better insight into the microscopic probability of vehicles accident over the lane, let see the probability of vehicles accidents as a function of the lattice site (see Fig. V.8).

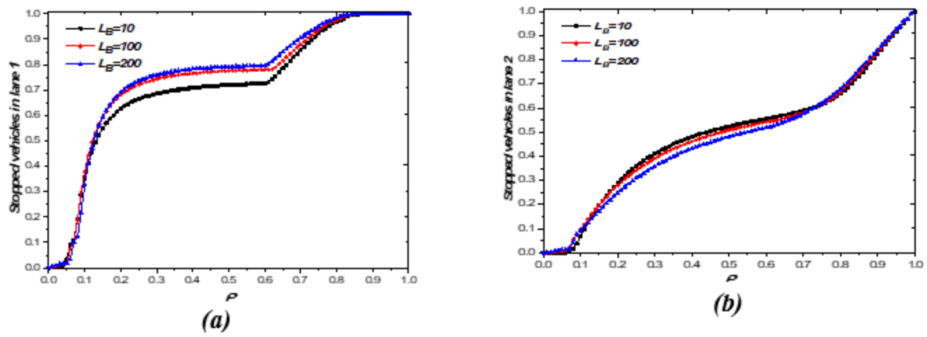

FIGURE V.7: Probability of stopped vehicles for several lengths of bottlneck and for a) lane 1 , b) lane 2.

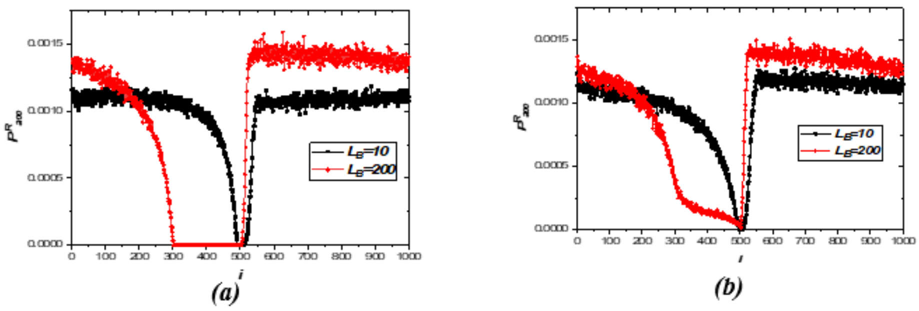

FIGURE V.8: Profile of rear-end collision probability for $\rho = 0.6$ a) lane 1, b) lane 2.

For lane 1, the probability of vehicles accident decreases as we approach the bottleneck, this means that as one approach to the bottleneck the queue of stopped vehicles become stable (see Fig.V.9). The disturbance of the bottleneck cause stops and go far from it as seen in the spacetime configuration and increase the probability to find a stopped vehicle near of it (see Fig. V.9(a)), thus reduce the vehicles accident as we approach the bottleneck. For lane 2, as one approach to the bottleneck the lane-changing frequency decreases which reduces the density and the probability to find a stopped vehicle (see Fig.V.9(b)) in the adjacent sites of the bottleneck, which reduce the vehicle accident probability as we approach to the bottleneck.

V.3.3 Lane-changing collision

As we saw, the bottleneck affects the vehicle's accident in both lanes, the rear-end collisions depend strongly on the bottleneck length. Now let's study the collision due to the unsafe

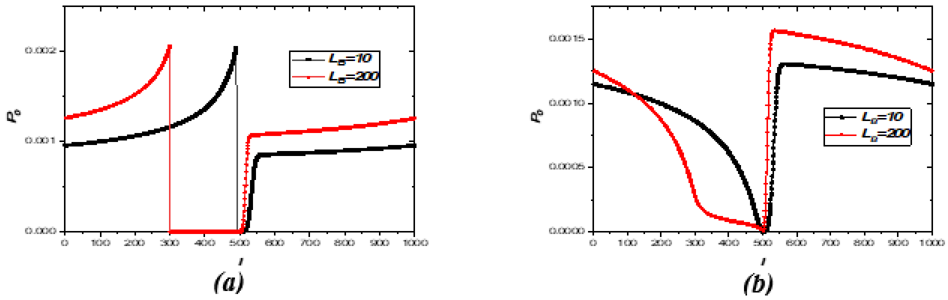

FIGURE V.9: Pofile of stopped vehicles for $\rho = 0.6$ a) lane 1, b) lane 2.

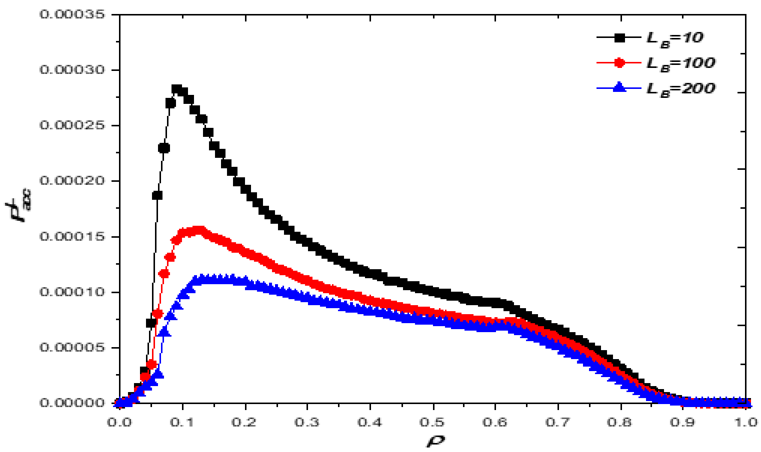

FIGURE V.10: Probability of vehicles collision due to unsafe lane-changing for several length of the bottleneck.

lane-changing. Fig. V.10 shows the probability of vehicles accident due to the unsafe lane changing. As we can see the probability of vehicles collision increases as the density increase reaching a maximum then start to decrease until reaching zero, here, the graphs of the probability of vehicles collision show similar features like the lane-changing frequency. The flexibility of the vehicles for changing lanes is affected by the length of the bottleneck. For a short length $L_B = 10$, the vehicles change the lane more often because the probability to find an adequate space is higher than the case of the large bottleneck length, thus, increase the number of critical cases that can induce the vehicles collision.

V.4 Conclusion

In this chapter, the bottleneck in a two lanes system was investigated. A heterogeneous system was considered (i.e., two types of vehicles slow and fast). The bottleneck was considered as a local defect in the two-lane model, the distribution of both defects (moving and fixed) on traffic can also cause a serious problem in traffic, such as the accident. The maximum current region was observed in extremely low densities for the home lane of the fixed bottleneck, while for the other lane it was observed beyond the density $\rho = 0.5$. The spacetime diagram helped us to understand the interaction between vehicles where we observed that for extremely low densities, vehicles order themselves as one lane is considered as a fast lane and the other lane was controlled by the slow vehicles. Furthermore, the rear-end and lane-changing collisions were investigated. We found that as the length of the fixed bottlenecks increase the probability of both types of collision increase.

General conclusion

The rapid growth of population and urbanization has led to an increase in the demand for transportation, resulting in more vehicles on the road and increased emissions from vehicles. This contributes to air pollution and greenhouse gas emissions particularly carbon dioxide (CO2), which have negative impacts on the environment and public health. The increase in vehicle traffic also leads to energy dissipation, as vehicles consume more fuel when they are stuck in congestion. To address these challenges, researchers have developed various traffic flow models. These models simulate the behavior of vehicles on the road, taking into account factors such as traffic volume, road network design, and driving behavior. There are various types of traffic flow models, including macroscopic models, mesoscopic models, and microscopic models. Each model provides a different level of detail and accuracy, and can be used to study different aspects of traffic, such as emissions, energy dissipation and accidents.
However, microscopic models have become increasingly popular in transportation research. These models are gaining traction because of their capability to simulate individual vehicle behavior, allowing for a detailed analysis of various traffic phenomena such as flow, congestion, and emissions. Additionally, they can show the parameters that can affect in the interactions between vehicles. The complexity of these interactions is explored in different types of road facilities, including access-controlled roads like two-lane highways or expressways.
In this sense, chapter 1 and 2 presented the field of road traffic and the importance of simulation. This presentation allows underlining some empirical and finding results, the traffic variables and the traffic models are also introduced. The asymmetric simple exclusion process (ASEP) can be extended to include two lanes, where particles can move in either direction on each lane. In this extension, two methods of changing-lanes are described (i.e., symmetric and asymmetric).

Chapter 3 considers a mixture of fast and slow vehicles with different lengths and maximum allowed speeds, and evaluated two kinds of the initial configuration (i.e., homogeneous and inhomogeneous), also, addressed the challenges posed by heterogeneity in traffic and the phenomenon of lane changing on energy dissipation and satisfaction rate. We found that slow vehicles hindered the fast ones, which can significantly affect traffic flow, especially if they are confined to one lane, leading to a lot of dissatisfied vehicles that drive at speeds below their maximal speed. Furthermore, we concluded that the distribution of the slow vehicles over the two lanes becomes homogenous, which decreases the flow in both lanes.

Chapter 4 is an extension of the third chapter in which we suggest a cellular automata model that studied the effect of slow-moving vehicles on carbon dioxide emissions for the case of closed boundary conditions with a mixture of types of vehicles. The asymmetric scenario, in which slow vehicles have various probabilities of changing lanes, is assessed. This scenario closely resembles the actual situation when slow-moving vehicles are not allowed to move continuously in the fast lane. Since both fast and slow vehicles can be changed over the two lanes, this initial setup is referred to a homogeneous case. The slow vehicles can therefore only begin in the slow lane in the inhomogeneous design, yet, in both scenarios, the fast vehicles are disrupted randomly in both lanes. We discovered that fast vehicles generate more pollution than slow ones, particularly in intermediate densities. Additionally, in both initial configurations, slow Vehicles affect on the carbon dioxide emissions.

The last chapter examines a two-lane traffic cellular automaton model to understand the effects of static (e.g., lane reductions) and dynamic (e.g., slow-moving vehicles) bottlenecks on traffic flow and road safety. We found that at low vehicle densities, slow vehicles gravitate towards the open lane, while faster vehicles switch lanes to overtake, returning to their original lane post-bottleneck. At high densities, traffic flow near static bottlenecks ceases, independent of bottleneck length. Safety analysis shows that extended static bottlenecks reduce rear-end collision risk due to fewer lane changes and increased vehicle stationarity. At maximum density, gridlock nullifies the chance of such collisions.

For the complement of the works mentioned above, it is recommended to include autonomous vehicles on two-lane roads.

- One of the primary motivations behind autonomous vehicles is to improve road safety. Autonomous vehicles use advanced sensors and artificial intelligence to detect and respond to their surroundings, reducing the likelihood of accidents caused by human error. According to the World Health Organization, over 1.3 million people die each year due to road accidents, and autonomous vehicles have the potential to significantly reduce this number.

- Another motivation for autonomous vehicles is to reduce traffic congestion. Autonomous vehicles can communicate with each other and optimize their routes to avoid congestion, reducing travel time and improving efficiency. This would result in more efficient use of road infrastructure and potentially reduce the need for new road construction.

- Autonomous vehicles can also help reduce carbon emissions and improve air quality by optimizing their routes and reducing the number of vehicles on the road. This would result in less traffic congestion and reduced fuel consumption, which would contribute to a more sustainable transportation system.

- Finally, autonomous vehicles can also increase mobility for people who are unable to drive, such as the elderly or people with disabilities. This would improve their quality of life and allow them to access opportunities that may have been previously inaccessible.

List of publication

1. A. Laarej, A. Karakhi, A. Khallouk, N. Lakouari and H. Ez-Zahraouy. Dissipation energy and satisfaction rate for a two-lane traffic model with two types of vehicles. Chinese Journal of Physics 71, 62-71(2021).

2. A. Karakhi, A. Laarej, A. Khallouk, N. Lakouari and H. Ez-Zahraouy. Car accident in synchronized traffic flow: A stochastic cellular automaton model. International Journal of Modern Physics C 32(01), 2150011(2021).

3. A. Laarej, A. Karakhi, A. Khallouk, N. Lakouari and H. Ez-Zahraouy. Effect slow vehicles on carbon dioxide emission in two-lane cellular automata model, Advanced Intelligent Systems for Sustainable Development.Lecture Notes in Networks and Systems 714, 70–86(2022).

4. A. Laarej, N. Lakouari, A. Karakhi and H. Ez-Zahraouy, Analyzing the effect of fixed and moving bottlenecks on traffic flow and car accidents in a two-lane cellular automaton model. Journal of Applied Engineering Science 24(04), 1179-1191(2023).

Articles in process

1. A. Laarej, A. Karakhi, A. Khallouk, N. Lakouari and H. Ez-Zahraouy. Analyzing Energy Dissipation and Satisfaction Rates in Mixed Traffic Flow With Lights: A Two-Lane Cellular Automaton Approach.

2. A. Laarej, A. Karakhi, A. Khallouk, N. Lakouari and H. Ez-Zahraouy. The impact of speed limit zone on carbon dioxide emission in a modified cellular automata model under an open boundary condition.

Bibliography

[1] Greenshields, B. D. A Study in Highway Capacity. Highway Research Board, Proceedings, Vol.14, p. 458 (1935).

[2] J.G. Wardrop, Proceedings of the Institution of Civil Engineers, Part II, 1 (2) 325 (1952).

[3] M.H. Lighthill, G.B. Whitham, Proceedings of the Royal Society, London Series A 229, 317 (1955).

[4] P.I. Richards, Operations Research 4 (1) 42 (1956).

[5] R. Herman, Editor. Theory of Traffic Flow, Proceedings of Symposium on the Theory of Traffic Flow, Elsevier Science Publishers, New York, page 175 (1961).

[6] H.J. Payne, Math. Models Publ. Sys 28, 51 (1971).

[7] G.B. Whitham, Linear and Nonlinear Waves, Wiley, New York, page 124 (1974).

[8] M. Cremer and J. Ludwig, Math. Comput. Simul. 28, 297 (1986).

[9] K. Nagel and M. Schreckenberg, J. Phys.I (France) 2, 2221 (1992).

[10] S. Espié, J. M. Auberle, MY. Zhang, Inproceeding of driving simulation, conférence (DSC'02), Paris, France, 175, septembre (2002).

[11] Cohen, S. (1993). Ingénierie du Trafic Routier. Eléments de théorie du trafic et applications, Presses de l'Ecole National des Ponts et Chaussées.

[12] Kamata, J. et T. Oda, Eds. (1991). Concise encyclopedia of traffic and transportation systems. Detectors for road traffic Pergamon Press.

[13] P. Kachroo, K. Krishen, J. of Integ. Des. and Proc. Sci. 4, 37 (2000).

[14] J.G.Wardrop (1952). "Some theoretical aspects of road traffic research." Proceedings of the Institude of Civil Engineers (ICE) 2(1): 325-378.

[15] WINDOVER, J.R., CASSIDY, M.J., Some observed details of freeway traffic evolution, Transportation Research Part A, 2001, vol. 35, n° 10, pp. 881-894.

[16] HELBING, D., Traffic and related self-driven many-particle systems, Reviews of Modern Physics, 2001, vol. 73, n° 4, pp. 1067-1141.

[17] DAGANZO, C.F., A behavioral theory of multi-lane traffic flow. Part I : Long homogeneous freeway sections, Transportation Research Part B, 2002, vol. 36, n° 2, pp. 131-158.

[18] CASSIDY, M.J., MAUCH M., An observed traffic pattern in long freeway queues, Transportation Research Part A, 2001, vol. 35, n° 2, pp. 149-162.

[19] DIJKER, T., SCHUURMAN, H., The capacity of asymmetrical weaving sections, In : 82nd Transportation Research Board, 12-16 janvier 2003.

[20] HELBING, D., HENNECKE, A., SHVETSOV, V. et al., Micro- and macrosimulation of freeway traffic, Mathematical and Computer Modelling, 2000, vol. 35, n° 5-6, pp. 517- 547.

[21] L.A. Pipes, “Car following models and the fundamental diagram of road traffic”, Transportation Research, Vol. 1.

[22] G.B. Whitham, “Linear and nonlinear waves”, New York: Wiley.

[23] J. Lebacque, “A finite acceleration scheme for first order macroscopic traffic flow models”, Proceedings of the 8th IFAC symposium on transportation systems (editors: M. Papageorgiou, A. Pouliezos).

[24] Crowthorne, Berkshire : Traffic Safety Division, Traffic Group, Transport and Road Research Laboratory, 1989.

[25] M. Ben-Akiva, M. Bierlaire, D. Burton, H.N. Koutsopoulos, R. Mishalani, “Network State Estimation and Prediction for Real-Time Transportation Mangement Applications”, Networks and Spatial Economics, Vol 1, No. 3/4, pp. 293-318.

[26] DYNASMART Professor, Civil and Environmental Engineering, University of California, Irvine, CA, USA.

[27] DYNAMEQ M. Mahut, “A multi-lane extension of the Space-Time Queue Model of Traffic Dynamics”, presented at TRISTAN IV, Azores Islands, 2001.

[28] C. Gawron, “Simulation-Based Traffic Assignment; Computing User Equilibria in Large Street Networks”, PhD thesis, University of Cologne, Cologne, 1998.

[29] S. Wolfram, Theory and Applications of Cellular Automata (World Scientific, Singapore, 1986).

[30] D. Stauffer, J. Phys. A 24 (1991) 909.

[31] T.M. Liggett, Interacting Particle Systems (Springer, Berlin, 1985).

[32] H. Spohn, Large scale dynamics ofinteracting particles (Springer, Berlin, 1991) and references therein.

[33] D. Chowdhury, L. Santen, and A. Schadschneider. Statistical physics of vehicular traffic and some related systems. Phys. Reports, 329:199, (2000).

[34] C.T. MacDonald, J.H. Gibbs, A.C. Pipkin, Biopolymers 6, 1 (1968).

[35] H. Spohn, Large Scale Dynamics of Interacting Particles, Springer, Heidelberg (1991).

[36] G.M. Schütz, Exactly solvable models for many-body systems far from equilibrium, in: C. Domb and J.L. Lebowitz (Eds.), Phase Transitions and Critical Phenomena, Academic Press, London, vol. 19 (2001).

[37] T. Nagatani, in Ref. I-41 and references therein.

[38] J. Krug and P. Ferrari, J. Phys. A (1996); M. Evans, Europhys. Lett. (1996).

[39] K. Nagel and M. Schreckenberg. A cellular automaton model for free-way traffic. J. Phys. I,2:2221–2229, (1992).

[40] R. Barlovic, L. Santen, A. Schadschneider, M. Schreckenberg, Eur. Phys. J. B 5, 793 (1998).

[41] B.S. Kerner, S.L. Klenov, D.E. Wolf, J. Phys. A 35, 9971 (2002).

[42] M. Takayasu, H. Takayasu, Fractals 1, 860(1993).

[43] S.C. Benjamin, N.F. Johnson, J. Phys. A 29, 3119 (1996).

[44] W. Knospe, L. Santen, A. Schadschneider, M. Schreckenberg, J. Phys. A 33, L477 (2000).

[45] Kerner, S. Boris, PHYS REV LETT. 81, 3797(1998).

[46] J.F. Tian, M. Treiber, S.F. Ma, B. Jia, W.Y. Zhang, Transp. Res. Part B 71, 138(2015).

[47] J.F. Tian, R. Jiang, B. Jia, M.B. Hu, W. Zhang, N. Jia, S.F. Ma, Transp. Res. Part B 93, 338 (2016).

[48] T. Chmura, B. Herz, F. Knorr, T. Pitz, M. Schreckenberg, Phys. A 405, 332(2014).

[49] R.Jiang, Q.S.Wu, J.Phys.A 37, 8197 (2004).

[50] H.K.Lee, R.Barlovic, M.Schreckenberg, D.Kim, Phys. Rev. Lett. 92, 238702 (2004).

[51] K.Gao, R.Jiang, S.X.Hu, B.H.Wang, Q.S.Wu, Phys. Rev. E 76, 026105 (2007).

[52] M.E. Lárraga, L. Alvarez-Icaza, Physica A 389, 5425 (2010).

[53] J.F. Tian, Z.Z. Yuan, M. Treiber, B. Jia, W.Y. Zhang, Physica A 391, 3129 (2012).

[54] H.Yang, J. Lu, X. Hu, J. Jiang, Physica A 392, 4009 (2013).

[55] T. Chmura, B. Herz, F. Knorr, T. Pitz, M. Schreckenberg, Physica A 405, 332 (2014).

[56] Y. Xue, L. Dong, L. Li, S. Dai, Phys. Rev. E 71, 026123 (2005).

[57] M. Fukui, Y .Ishibashi, J. Phys. Soc. Japan 65, 1868 (1996).

[58] Kincaid, Peter (December 1986). The Rule of the Road: An International Guide to History and Practice. Greenwood Press. pp. 50, 86–88, 99–100, 121–122, 198–202. ISBN 978-0-313-25249-5.

[59] "Worldwide Driving Orientation by Country". Retrieved 13 December 2016.

[60] Barta, Patrick. "Shifting the Right of Way to the Left Leaves Some Samoans Feeling Wronged". The Wall Street Journal. Retrieved 4 December 2016.

[61] Watson, Ian. "The rule of the road, 1919–1986: A case study of standards change" (PDF). Retrieved 30 November 2016.

[62] T. Nagatani , Phys. Rev. E, 48 (1993) 3290.

[63] M. Rickert, K. Nagel, M. Schreckenberg, A. Latour, Two lane traffic simulations using cellular automata, Physica A: Statistical Mechanics and its Applications 231 (1996) 534–550.

[64] P. Wagner, K. Nagel and D. E. Wolf, Physica A 234, 687 (1997).

[65] R. Rhodes. Dark Sun: The Making of the Hydrogen Bomb. Simon and Schuster Paperbacks, (1995).

[66] D. Helbing, Phys. Rev. E 55 (1997) 3735.

[67] A. Nakayama, Y. Sugiyama, K. Hasebe, Phys. Rev. E 65 (2002) 016112.

[68] T Wang, Z.-Y Gao, X.-M. Zhao, Acta Phys. Sinica 55 (2006) 634.

[69] W Shi, Y Xue, Physica A 381 (2007) 399.

[70] B.A. Toledo, E. Cerda, J. Rogan, V. Munoz, C. Tenreiro, R. Zarama, J.A. Valdivia, Phys. Rev. E 75 (2007) 026108

[71] J. Krug and P. A. Ferrari, J. Phys. A 29, L465 (1996).

[72] T. Toledo, H. N. Koutsopoulos, and K. I. Ahmed, Transp. Res. Rec. 161 (2007).

[73] T. Toledo, H. N. Koutsopoulos, and M. Ben-Akiva, Transp.Res., Part C: Emerg. Technol. 15, 96(2007).

[74] M. Treiber and D. Helbing, Eur. Phys. J. B 68, 607 (2009).

[75] D. Helbing, Phys. Rev. E 55, 3735 (1997).

[76] A. Lipshtat, PHYSICAL REVIEW E 79, 066110 (2009).

[77] N. Boccara, H. Fuks and Q. Zeng, J. Phys A 30, 3329(1997).

[78] D. Mohan, C.J. Romer, Accidents in childhood and adolescence. The role of research, Geneva: World Health Organization, 31-38 (1991).

[79] D. Huang, J. Phys. A: Math. Gen. 31,6167 (1998).

[80] X. Yang, Y. Ma, J. Phys. A: Math. Gen. 35,10539 (2002).

[81] X. Yang, Y. Ma, Mod. Phys. Lett. B 16, 333 (2002).

[82] X. Yang, Y. Ma, Y. Zhao. J. Phys. A: Math. Gen. 37, 4743 (2004).

[83] N. Moussa. Int. J. Mod. Phys. C 21(12), 1501(2010).

[84] W. Zhang, W. Zhang, X. Yang, Phys. A: Stat. Mech. Appl 387, 4657-4664(2008).

[85] W.W. Zhang, W. Zhang, Eur. Phys. J. B 87, 4(2014).

[86] W.-X. Zhu, L.-D. Zhang, Int. J. Mod. Phys. C 25, 1450018(2014).

[87] N. Lakouari, K. Bentaleb, H. Ez-Zahraouy, A. Benyoussef, Phys. A: Stat. Mech. Appl. 439, 132-141(2015).

[88] A. Khallouk, H. Binoua, N. Lakouari, H. Echab, R. Marzoug, H. Ez-Zahraouy, Int. J. Mod. Phys. B 33, 1950007(2019).

[89] A. K. Daoudia, N. Moussa, Chin. J. Phys 41, 671-681 (2003).

[90] Y. Regragui, N. Moussa, Chin. J. Phys 56, 1273–1285 (2018).

[91] B.Jia, R. Jiang, Q.-S. Wu, Int. J. Mod. Phys. C 15, 381–392(2004).

[92] P. M. Simon, H.A. Gutowitz,, Phys. Rev. E 57, 2441–2444(1998).

[93] K.Nagel, D.E.Wolf, P.Wagner, P.Simon, Phys. Rev. E 58, 1425–1437(1998).

[94] T. Nagatani, J. Phys. A: Math. Gen.26 L781(1993).

[95] T. Nagatani, Phys. A: Stat. Mech. Appl 202, 449-458(1994).

[96] M.Rickert, K.Nagel, M.Schreckenberg, A.Latour, Phys. A: Stat. Mech. Appl 231, 534–550(1996).

[97] K.Nagel, M.Schreckenberg, J. Phys. I 2221, (1992) 2229.

[98] H.Ou, T.-Q. Tang, Phys. A: Stat. Mech. Appl 495, 260–268(2018).

[99] H.B.Zhu, L.Lei, S.Q.Dai, Phys. A: Stat. Mech. Appl 388, 2903–2910 (2009).

[100] D.Chowdhury, D.E.Wolf, M. Schreckenberg, Phys. A: Stat. Mech. Appl 235, 417–439 (1997).

[101] W.Knospe, L.Santen, A.Schadschneider, M.Schreckenberg, Phys. A: Stat. Mech. Appl 20, 614-633(1999).

[102] B.Jia, R.Jian, Q.-S.Wu, M.Hu, Phys. A: Stat. Mech. Appl 348, 544–552 (2005).

[103] Y.S.Qian, J.B. Luo, J.W. Zeng, X.M. Shao, W.B. Guo, meas. 46, 2035-2042 (2013).

[104] X-G. Li, B. Jia, Z.Y. Gao, R. Jiang, Phys. A: Stat. Mech. Appl 367, 479-486(2006).

[105] K. Nagel, D.E. Wolf, P. Wagner, P. Simon, Phys. Rev. E 58 (1998) 1425.

[106] J. Krug, J.A. Ferrari, J. Phys. A 29 (1996) 465.

[107] J. Krug, in: M. Schreckenberg, D.E. Wolf (Eds.), Traffic and Granular Flow 97, Springer, Singapore,1998.

[108] M.R. Evans, Europhys. Lett. 36 (1996) 13.

[109] M.R. Evans, J. Phys. A 30 (1997) 5669.

[110] D.V. Ktitarev, D. Chowdhury, D.E. Wolf, J. Phys. A 30 (1997) L221.

[111] D. Helbing, B. Huberman, Nature 396 (1998) 738 cond-mat=9805025

[112] K. Zhang, S. Batterman, Sci. Total Environ. 450, 307 (2013).

[113] A. Hagenbjörk, E. Malmqvist, K. Mattisson, N.J. Sommar, L. Modig, Monit. Assess. 189, 161(2017).

[114] S. Han, H. Bian, Y. Feng, A. Liu, X. Li, F. Zeng, X. Zhang, Aerosol Air Qual. Res. 11, 128 (2011).

[115] R.M. Harrison, J. Yin, Sci. Total Environ. 249, 85(2000).

[116] C.D. Novi, J. Socio-Econ. 44, 27(2013).

[117] S. Pandian, S. Gokhale, A. K. Ghoshal, Transp. Res. D: Transp. Environ. 14, 180(2009).

[118] S. Hallmark, B. Wang, A. Mudgal, H. Isebrands, Transp. Res. Rec: J. Transp. Res. Board. 2265, 226 (2011).

[119] X. Wang, Y. Xue, B.l.Cen, P. Zhang, H.d. He, Phys. A. 537, 122686(2020).

[120] N. Vandaele, T. Van Woensel, A. Verbruggen, Transp. Res. D. 5, 121(2000).

[121] D. Heidemann, Transp. Sci. 35, 405 (2001).

[122] D. Helbing, J. Phys. A. 36, L593 (2003).

[123] G.F. Newell, Transp. Res. B. 27, 289(1993).

[124] M. Brackstone, M. McDonald, Transp. Res. F: Traffic Psychol. Behav.2, 181 (1999).

[125] K. Nagel et M. Schreckenberg, J. Phys. I. 2, 2221 (1992).

[126] G.L. Chang and Y.M. Kao, Trans. Res. A 25, 375 (1991).

[127] F.L. Hall, T.N. Lam, Trans. Res. A 22, 45(1988).

[128] M. Rickert, K. Nagel, M. Schreckenberg, A. Latour, Phys. A. 231, 534 (1996).

[129] T. Nagatani, J. Phys. A : Math. Gen. 29, 6531(1996).

[130] K. Zhang, S. Batterman, Sci. Total Environ. 450, 307(2013).

[131] C.D. Novi, J. Socio-Econ. 44, 27(2013).

[132] R.M. Harrison, J. Yin, Sci. Total Environ 249, 85(2000).

[133] M.Stafoggia, A.Faustini, M.Rognoni, et al., Epidemiol Prev. 33, 65(2009).

[134] Y.F. Qiao, Y. Xue, X. Wang, B.L. Cen, Y. Wang, W. Pan, Y.X. Zhang, Phys. A 574, 125996(2021).

[135] R. Barlovic, L. Santen, A. Schadschneider, M. Schreckenberg, Eur. Phys. J. B, 5, 793 (1998).

[136] M. Takayasu, H. Takayasu, Fractals. 01, 860(1993).

[137] T. M. L. Wigley, P. D. Jones, Nature 292, 205(1981).

[138] H. Binoua, H. Ez-Zahraouy, A. Khallouk, N. Lakouari, Int. J. Mod. Phys. C. 31 2050154 (2020).

[139] J. C. Pérez-Sansalvador, N. Lakouari, J. Garcia-Diaz, S.E. P. Hernández, Appl. Sci.10, 1592 (2020).

[140] W. Xue, X. Yu, C. Bing-ling, Z. Peng, H. Hong-di, Phys. A. 537, 122686(2020).

[141] L.-D. Zhang, W.-X. Zhu, Phys. A. 428, 481(2015).

[142] Panis, L.I., Broekx, S., Liu, R.: Sci. Total Environ. 371, 270 (2006)

[143] F. Armah, D.Yawson, Alex A. N. M. Pappoe, Sustainability. 2, 252 (2010).

[144] J. Wang, L. Chi, X. Hu and H. Zhou, Sustainability. 6, 676 (2014).

[145] Y. Liu, X Yan, Y. Wang, Z. Yang and J. Wu, Sustainability. 9, 533(2017).

[146] T. Nagatani, Rep. Prog. In Phys. 65, 1331 (2002).

[147] X. Feng, M. Saito and Y. Liu, Int. J. Prod. Res. 54, 3465 (2016).

[148] F. He, X. Yan, Y. Liu and L. Ma, Procedia Eng. 137, 425 (2016).

[149] D. Chowdhury, D.E. Wolf, M. Schreckenberg, Physica A. 235, 417 (1997).

[150] W. Knospe, L. Santen, A. Schadschneider, M. Schreckenberg, Phys. A. 20, 614 (1999).

[151] I. Juran, J. N. Prashker, S. Bekhor and Il. Ishai, Transportation Research Part C: Emerging Technologies. 17, 240 (2009).

[152] M. Bando, K. Hasebe, A. Nakayama, A. Shibata, and Y. Sugiyama, Jpn. J. Ind. Appl. Math. 11, 203 (1994).

[153] M. Bando, K. Hasebe, A. Nakayama, A. Shibata, and Y. Sugiyama, Phys. Rev. E. 51, 1035 (1995).

[154] Y. Fang, J.-Z. Chen and Z.-Y. Peng, Chin. Phys. B. 22, 108902 (2013).

[155] N. Lakouari, K. Bentaleb, H. Ez-Zahraouy, A. Benyoussef, Physica A. 439, 132 (2015).

[156] H. Ou, T.Q. Tang, Physica A. 500, 131 (2018).

[157] K. Zhu, J. Bi, J. Wu, S. Li, Mod. Phys. Lett. B. 30, 1650323 (2016).

[158] H. Hanaura, S. Masukura and T. Nagatani, Physica A. 388, 1196 (2009).

[159] J. Zeng, Y. Qian, Z. Lv, F. Yin, L. Zhu, Y. Zhang, D. Xu. Physica A. 574, 125918 (2021).

[160] H.F. Chau, X. Hao, L.G. Liu, Physica A. 303, 534 (2002).

[161] M. Fukui, Y. Ishibashi, J. Phys. Soc. Jpn. 65, 1868 (1996).

[162] J. Torok, J. Kertesz, Physica A. 231, 515 (1996).

[163] H. Ez-Zahraouy, Z. Benrihane and A. Benyoussef, Int. J. Mod. Phys. B. 18, 2347 (2004).

[164] B. Jia, R. Jiang and Q.S. Wu, Phys. Rev. E. 69, 056105 (2004).

[165] B. Jia, R. Jiang and Q.S. Wu, Physica A. 345, 218 (2005).

[166] F. Li, X.Y. Zhang and Z.Y. Gao, Physica A. 374, 827 (2007).

[167] Y.K. Song and X. M. Zhao, Chin. Phys. B. 18, 5242 (2009).

[168] R. Marzoug, H. Echab, H. Ez-Zahraouy, Eur. Phys. J. B. 90, 240 (2017).

[169] K. Nagel et M. Schreckenberg, J. Phys. I. 2, 2221 (1992).

[170] M. Rickert, K. Nagel, M. Schreckenberg, A. Latour, Physica A. 231, 534 (1996).

[171] M.R. Evans, Europhys. Lett. 36, 13 (1996).